

**SOLUBLE E-CADHERIN AS A MICROENVIRONMENTAL FACTOR
WHICH ENHANCES TUMOR PROGRESSION**

by

Pratima U. Patil

A dissertation submitted to the Faculty of the University of Delaware in partial fulfillment of the requirements for the degree of Doctor of Philosophy in Biological Sciences

Summer 2015

© 2015 Pratima U. Patil
All Rights Reserved

ProQuest Number: 3730276

All rights reserved

INFORMATION TO ALL USERS

The quality of this reproduction is dependent upon the quality of the copy submitted.

In the unlikely event that the author did not send a complete manuscript and there are missing pages, these will be noted. Also, if material had to be removed, a note will indicate the deletion.



ProQuest 3730276

Published by ProQuest LLC (2015). Copyright of the Dissertation is held by the Author.

All rights reserved.

This work is protected against unauthorized copying under Title 17, United States Code
Microform Edition © ProQuest LLC.

ProQuest LLC.
789 East Eisenhower Parkway
P.O. Box 1346
Ann Arbor, MI 48106 - 1346

**SOLUBLE E-CADHERIN AS A MICROENVIRONMENTAL FACTOR
WHICH ENHANCES TUMOR PROGRESSION**

by

Pratima U. Patil

Approved: _____
Robin W. Morgan, Ph.D.
Chair of the Department of Biological Sciences

Approved: _____
George H. Watson, Ph.D.
Dean of the College of Arts and Sciences

Approved: _____
James G. Richards, Ph.D.
Vice Provost for Graduate and Professional Education

I certify that I have read this dissertation and that in my opinion it meets the academic and professional standard required by the University as a dissertation for the degree of Doctor of Philosophy.

Signed:

Robert W. Mason, Ph.D.
Professor in charge of dissertation

I certify that I have read this dissertation and that in my opinion it meets the academic and professional standard required by the University as a dissertation for the degree of Doctor of Philosophy.

Signed:

Ayyappan K. Rajasekaran, Ph.D.
Professor in charge of dissertation

I certify that I have read this dissertation and that in my opinion it meets the academic and professional standard required by the University as a dissertation for the degree of Doctor of Philosophy.

Signed:

Ulhas P. Naik, Ph.D.
Member of dissertation committee

I certify that I have read this dissertation and that in my opinion it meets the academic and professional standard required by the University as a dissertation for the degree of Doctor of Philosophy.

Signed:

Gary H. Lavery, Ph.D.
Member of dissertation committee

I certify that I have read this dissertation and that in my opinion it meets the academic and professional standard required by the University as a dissertation for the degree of Doctor of Philosophy.

Signed:

Donna Woulfe, Ph.D.
Member of dissertation committee

I certify that I have read this dissertation and that in my opinion it meets the academic and professional standard required by the University as a dissertation for the degree of Doctor of Philosophy.

Signed:

Kelvin H. Lee, Ph.D.
Member of dissertation committee

ACKNOWLEDGMENTS

I would like to sincerely thank my advisor Dr. Ayyappan K. Rajasekaran for giving me this incredible project and for always having my back over the last five years. His enthusiasm and passion for science is infectious and has always inspired me to work harder and do better. Raj has always found time and made himself available and never let his personal slumps hamper the progress of this project. I am truly indebted for all the one on one brainstorming sessions with him and the grueling lab meetings as they have honed my scientific reasoning skills and helped me become a better researcher and a confident speaker. I will always remember the random espresso outings he took us to which helped us come back rejuvenated to the lab. He is truly an inspiration and brings out the very best of you scientifically.

I am extremely thankful to Dr. Robert W. Mason, who has been my advisor for the last two years and has greatly facilitated completion of this dissertation work. Dr. Mason made a great deal of effort to quickly learn about my project and come on board. I am grateful for his insightful suggestions and reviews regarding the impact of tumor cells on normal epithelial cells which has helped me rethink some of my experiments and ask the right questions. He has always been supportive of me and solved all the department and administration related issues I faced during my graduate school. I really enjoyed my conversations with him and his ability to put things in perspective and make light of things motivated me on days when I felt dejected. I am truly indebted to him for his constant support and guidance and I am fortunate to have had this interaction with him.

I would like to thank my committee members Dr. Ulhas P. Naik, Dr. Donna Woulfe, Dr. Gary Lavery and Dr. Kelvin Lee for their constant guidance and valuable inputs in all the committee meetings. I am thankful to Dr. Ulhas Naik for his constructive ideas, insights and suggestions which have helped in shaping of this dissertation work. His suggestions have helped me think and design some key experiments for this work and I am extremely grateful to him for his valuable inputs. I would like to thank Dr. Donna Woulfe for her encouragement and support. I learnt a lot from her Pharmacology class which helped in better analysis of my data. She was always very enthusiastic about my progress and was a great support in all the committee meetings. I would also like to thank Dr. Gary Lavery for his constant support and taking the time to keep up with the progress of my work in all the committee meetings. My initial interactions with him helped me understand the requirements of graduate school and what was expected of me. I am grateful to Dr. Kelvin Lee for his constant encouragement and guidance during the course of this dissertation work. He always promptly responded to my numerous emails and I am thankful for his patience and support over the years. I would also like to acknowledge Dr. Melinda Duncan, the graduate school program coordinator for understanding my special situation and accepting me into graduate school in the spring semester. Conversations with her greatly helped me find the right lab and manage graduate school curriculum.

I would also like to extend my gratitude to Dr. Valerie Sampson for her unconditional support and guidance during the tough times in the graduate school. She has been a great friend and a source of strength for me and I have learnt a lot from her over the years. I am grateful to her for her scientific inputs, critical analysis of my data, troubleshooting of my experiments and teaching me real time qPCR.

I would also like to thank all my previous lab members Dr. Vinu Krishnan, Dr. Justin David, Tori Owens and Dr. Selva Kumar and the current Mason Lab member Guizhen Lu, Lisa Glazewski who easily accommodated me and helped me out in the lab. I am grateful to Justin for teaching all the laboratory techniques during the initial grad school years. His critical analysis and inputs during lab meetings helped a great deal in shaping my project. His generous car rides during the initial days were absolutely indispensable. I am also thankful to Vinu for being a great friend and the only constant lab companion over the years. He has always assisted me with anything I needed and together we sorted several issues.

I would like to acknowledge Dr. Sonali Barwe and Dr. Seung Joon Lee. They trained me early on and their technical expertise and assistance has helped me plan and conduct experiments. I would also like to thank Dr. Sigrid Langhans for training me with the confocal microscopy which I used for majority of my dissertation work.

I am extremely fortunate to have shared this challenging graduate school journey with my roommate and labmate Dr. Sona Lakshme Balasubramaniam. We went through each phase of graduate school together and Sona has always been a constant support both inside and outside of the laboratory. It is extremely satisfying to see all the hardwork we put in over the years has finally taken us to the finish line.

I would also like to acknowledge Suzanne Purfield for all of her administrative support at Nemours. She was always helpful and took care of all the complex paperwork at Nemours and helped with the ordering reagents. Suzanne always remembered everyone's birthdays and graciously baked a cake for every birthday. I also want to thank Betty Cowgill for helping out with the paperwork at UD, assisting with registering for classes and keep a track of my academic progress over the years. I would also like

to thank Brenda Radziewicz for assisting with processing of travel awards and reimbursements.

I am blessed to have shared the graduate school life with a wonderful group of graduate students. I would like to thank all my friends Anindita, Aasma, Soma, Sona, Vimal, Vignesh, Praveen, Sai Sidharth, Adithya, Hemanth, Miho, Vinu, Priyanka, Avinash, Anitha, Divya, Kaushiki, Shirin for all of the fun times, get togethers, road trips and parties. They truly are my home away from home and made graduate experience memorable and worthwhile.

Finally, I am fortunate to have an exceptionally supportive family who have always stood by me; my parents Group Captain Uttamrao B. Patil (Retd.) and Mrs. Nanda Patil, my brother Suraj Patil and his wife Prashanthi. I couldn't have made it through this journey without their unconditional love and encouragement at every step of grad school. I would also like to thank my extended family, all my aunts, uncles and cousins who have been loving, encouraging and proud of me. And I am certain the completion of this dissertation brings them as much joy, sense of pride and accomplishment as it brings to me.

TABLE OF CONTENTS

LIST OF TABLES	xiii
LIST OF FIGURES	xiv
ABSTRACT	xvii

Chapter

1 INTRODUCTION	1
1.1 E-cadherin: Structure and Function	1
1.2 E-cadherin Mediated Cell Signaling	6
1.3 E-cadherin as a Tumor Suppressor Gene & Its Role in Epithelial Cancers: Mechanisms by which E-cadherin is down regulated	9
1.4 Over-expression of E-cadherin in tumors	12
1.5 Proteolytic Shedding of E-cadherin: Generation of sE-cad	14
1.6 Elevated sE-cad Levels in Pathological Conditions	19
1.6.1 Cancers	19
1.6.2 Other Non-cancer conditions	20
1.7 Consequences of Elevated sE-cad	22
1.7.1 Loss of Cell Adhesion	22
1.7.2 Increased Cell Migration and Invasion	22
1.7.3 Increased Cell Proliferation and Survival	23
1.7.4 sE-cad Mediated Signaling	24
1.8 Cytoplasmic fragment of E-cadherin (CTF2)	26
1.9 Tumor Microenvironment	27
1.9.1 Cancer Associated Fibroblasts	29
1.9.2 Infiltrating Immune Cells	30
1.9.3 Normal Epithelial Cells	31
1.10 Epithelial to mesenchymal Transition (EMT)	33
1.11 2D vs 3D culture System	35

2	SOLUBLE E-CADHERIN GENERATED BY CARCINOMA CELLS INDUCE LUMEN FILLING IN NORMAL EPITHELIAL CELLS.....	39
2.1	Introduction	39
2.2	Materials and methods.....	44
2.2.1	Cell lines	44
2.2.2	Antibodies and Reagents	45
2.2.3	Three-dimensional (3-D) Matrigel cultures.....	45
2.2.4	Immunofluorescence of 3-D Matrigel cultures	46
2.2.5	Confocal microscopy and quantitation of 3D cysts.....	47
2.2.6	Generating 3D cell lysates and conditioned media from 3D cultures	47
2.2.7	Protein Estimation using Bio-Rad DC Protein Assay	48
2.2.8	Immunoblot analysis	49
2.2.9	Gelatin Zymography.....	49
2.2.10	Transwell Co-culture Assay	50
2.2.11	Purification of sE-cad	50
2.2.12	Immunodepletion Assay	51
2.2.13	qRT-PCR analysis	51
2.2.14	Reversibility Assay.....	52
2.3	Results	52
2.3.1	Co-culture of carcinoma cells with MDCK cysts disrupt luminal architecture	52
2.3.2	MMP-9 present in the conditioned medium is involved in lumen filling	54
2.3.3	MSV-MDCK cells induce shedding of sE-cad from MDCK cysts in MMP-9-dependent manner.....	56
2.3.4	sE-cad is necessary and sufficient for inducing lumen filling in MDCK cysts	58
2.3.5	sE-cad increases MMP-9 levels.....	61
2.3.6	Reversibility Assay.....	65
2.4	Discussion.....	67
3	SOLUBLE E-CADHERIN AND CARCINOMA CELL CONDITIONED MEDIA INDUCE EPITHELIAL TO MESENCYMAL TRANSITION IN NORMAL EPITHELIAL CYSTS.	72
3.1	Introduction	72
3.1.1	EMT and Stemness.....	74

3.1.2	TME and EMT	75
3.2	Materials and Methods	76
3.2.1	Cell lines	76
3.2.2	Antibodies and Reagents	76
3.2.3	Immunofluorescence of 3D Matrigel™ cultures.....	77
3.2.4	Confocal microscopy and quantitation of 3D cysts.....	77
3.2.5	Immunoblotting	78
3.3	Results	78
3.3.1	Long term (96 h) sE-cad and CM treatment induces an EMT- like phenotype in MDCK cysts	78
3.3.2	sE-cad and CM treatment induce actin stress fiber formation	79
3.3.3	sE-cad and CM treatments upregulate expression of N- cadherin and Fibronectin	80
3.3.4	Z-stacks showing EMT Markers in Lumen Filled Cysts.....	82
3.3.5	MSV-MDCK cells and MDCK cysts interact via Fibronectin fibrils.....	83
3.3.6	sE-cad increases $\alpha 1$ integrin levels.....	85
3.3.7	Upregulation of the stem cell marker Oct4 in CM treated lumen filled cysts.....	86
3.3.8	Epithelial Markers Retained in Lumen Filled Cysts Undergoing EMT.....	87
3.4	Discussion.....	88
4	ANALYSIS OF SIGNALLING PATHWAYS ACTIVATED DURING SOLUBLE E-CADHERIN INDUCED LUMEN FILLING AND EPITHELIAL TO MESENCHYMAL TRANSITION IN NORMAL EPITHELIAL CYSTS.....	93
4.1	Introduction	93
4.2	Materials and Methods	99
4.2.1	Cell lines	99
4.2.2	Antibodies and Reagents	100
4.2.3	Immunofluorescence of 3D Matrigel™ cultures.....	101
4.2.4	Confocal microscopy and quantitation of 3D cysts.....	101
4.2.5	Generating 3D cell lysates and conditioned media from 3D cultures	102
4.2.6	Immunoblotting	102
4.2.7	Co-Immunoprecipitation and Immunodepletion	103

4.3	Results	103
4.3.1	sE-cad and MSV-MDCK cells mediate lumen filling by activation of EGFR	103
4.3.2	Increased binding of Grb2 to pEGFR(Tyr-1068) with sE-cad Treatment.....	106
4.3.3	Activation of the downstream ERK1/2 and AKT pathways during Lumen Filling.....	107
4.3.4	Mechanism of EGFR activation in CM treated cysts.....	108
4.3.5	Lumen filling is a consequence of increased survival and proliferation mediated by the MEK/ERK pathway	109
4.3.6	ERK1/2 is the primary pathway involved in lumen filling in MDCK cysts	111
4.3.7	AKT is involved in the induction EMT in MDCK cysts.....	114
4.3.8	Proposed Model for MSV-MDCK induced Lumen Filling and EMT in MDCK cysts.....	120
4.4	Discussion.....	122
5	PERSPECTIVES AND FUTURE DIRECTIONS	125
5.1	Future Directions	129
5.1.1	Does sE-cad binds to cellular E-cadherin as a monomer or an oligomer?.....	129
5.1.2	Where does sE-cad bind cellular E-cadherin in polarized epithelial cells?	130
5.1.3	What is the mechanism of activation of EGFR leading to lumen filling and EMT?	131
5.1.4	Does sE-cad induces lumen filling and EMT in vivo preclinical models?.....	132
5.1.5	Utilizing the 3D culture system and lumen filling: Novel Assay Platform	132
5.1.6	Investigating other possible pathological roles of sE-cad	133
5.1.7	What is the impact of this study on cancer patients?.....	134
	REFERENCES	135
	Appendix	
A	IMAGE REPRINT APPROVALS	157

LIST OF TABLES

Table 1.1: List of E-cadherin Sheddases (Modified from Grabowska et al., 2012)	18
Table 1.2: Table showing sE-cad Levels in various cancers and its prognostic utility (Modified from De Wever et al., 2007 and Grabowska et al., 2012).....	21

LIST OF FIGURES

Figure 1.1:	Schematic representation of the E-cadherin structure.	2
Figure 1.2:	Model showing calcium dependent E-cadherin cis dimers, tryptophan dependent Trans dimers and lateral clustering of E-cadherin	4
Figure 1.3:	Signaling pathways regulated by E-cadherin	8
Figure 1.4:	E-cadherin Ectodomain Shedding.	15
Figure 1.5:	Oncogenic Effects of sE-cad.	25
Figure 1.6:	Figure showing the different components of the tumor microenvironment	28
Figure 1.7:	Schematic of cells undergoing EMT	34
Figure 1.8:	Cells in 2D monolayer vs. in 3D culture system.	36
Figure 1.9:	Pictorial representation of cancer cells in 3D culture system.....	37
Figure 2.1:	Lumen filling with progressive stages of epithelial cancers	41
Figure 2.3:	Experimental Model showing 3-D culture system	46
Figure 2.4:	Co-culture of carcinoma cells with MDCK cysts disrupt luminal architecture.	54
Figure 2.5:	Conditioned medium from co-culture contains high levels of active MMP-9 which is crucial for lumen filling.....	56
Figure 2.6:	MSV-MDCK cells induce MMP-9 mediated shedding of sE-cad from MDCK cysts.	58
Figure 2.7:	sE-cad induces lumen filling in MDCK cysts.	59
Figure 2.8:	sE-cad is necessary for induction of lumen filling in MDCK cysts.	60
Figure 2.9:	sE-cad induces MMP-9 in MDCK cysts.	62
Figure 2.10:	High E-cadherin expression in SUM149 cells.	64
Figure 2.11:	MMP-9 and sE-cad expression are correlated.....	64

Figure 2.12:	Lumen filled cysts form polarized cysts when replated.	66
Figure 2.13:	Proposed Model for MSV-MDCK induced Lumen Filling in MDCK cysts	71
Figure 3.1:	sE-cad and CM induces EMT like phenotype in MDCK cysts.....	79
Figure 3.2:	Presence of Actin stress fibers in Lumen filled cysts.....	79
Figure 3.3:	Upregulation of EMT markers in sE-cad and CM treated cysts	81
Figure 3.4:	Lumen filling and EMT markers in Z-stacks gallery.	82
Figure 3.5:	Fibrillar Fibronectin Network between MSV-MDCK and Lumen filled cysts.	84
Figure 3.6:	Upregulation of $\alpha 1$ integrin levels in sE-cad treated cysts.	85
Figure 3.7:	Upregulation of the stem cell marker Oct4 in lumen filled cysts.....	87
Figure 3.8:	No change in epithelial protein in lumen filled cysts.	88
Figure 4.1:	Signaling Pathways activated by EGFR.	95
Figure 4.2:	Activation of the downstream Ras-Raf-ERK pathway by EGFR and the downstream targets.	96
Figure 4.3:	Activation of the PI3K/AKT pathway by EGFR and its downstream targets.	97
Figure 4.4:	MSV-MDCK cells and sE-cad induce lumen filling in MDCK cells by EGFR activation.	105
Figure 4.5:	sE-cad induces phosphorylation of Tyr-1068 residue of EGFR resulting in Grb2 binding.....	106
Figure 4.6:	sE-cad and CM induce activation of downstream pERK1/2 and AKT pathways in MDCK cysts.	107
Figure 4.7:	Amphiregulin mRNA levels increased in CM treated cysts.	108
Figure 4.8 A:	Lumen filling is a consequence of reduced apoptosis and increased proliferation.	110

Figure 4.8 B: Lumen filling is a consequence of reduced apoptosis and increased proliferation.	111
Figure 4.9: ERK1/2 is involved in lumen filling in MDCK cysts.	113
Figure 4.10: Immunoblot showing phospho ERK 1/2, phospho AKT and total ERK1/2 and total AKT levels in cysts treated with sE-cad in presence of inhibitors for 96h.	114
Figure 4.11 A: AKT is involved in the induction EMT in MDCK cysts.	116
Figure 4.11 B: AKT is involved in the induction of EMT in MDCK cysts.	117
Figure 4.12: Immunoblot showing pAKT, pERK1/2 and total ERK1/2 in sE-cad treated cysts at 48, 72 and 96 h.	118
Figure 4.13 A: AKT is involved in the induction EMT in CM treated MDCK cysts. Immunofluorescence showing EMT expression in cysts treated CM in presence of inhibitors at 96 h.	119
Figure 4.13 B: AKT is involved in the induction of EMT in CM treated MDCK cysts.	120
Figure 4.14: Proposed Model for sequential lumen filling and EMT induced by carcinoma cells in MDCK cysts.	121
Figure 5.1: Pictorial representation of the overall goal of the dissertation work. .	126
Figure 5.2: Purified sE-cad exists as 160 kDa dimer in the conditioned media .	130
Figure 5.3: -catenin and sE-cad show basolateral staining in MDCK cells.	131

ABSTRACT

This study aims to investigate two questions: How do tumor cells interact and alter the normal epithelial cells and whether elevated soluble E-cadherin (sE-cad) levels in the microenvironment impact normal epithelial cells as well. We use a three-dimensional (3D) cell-culture system comprising non-transformed Madin-Darby canine kidney (MDCK) epithelial cells and invasive cancer cells (MSV-MDCK) to determine the impact of tumor cells on the normal epithelial cells. Using 3D co-culture system we demonstrate that carcinoma cells sequentially induced pre-neoplastic lumen filling and EMT in normal epithelial cysts. We provide evidence that carcinoma cells secrete MMP-9 which cleaves extracellular domain of E-cadherin from normal epithelial cells to generate soluble E-cadherin (sE-cad). Addition of purified sE-cad and by immunodepletion of sE-cad from conditioned medium prevented filling up of the lumen indicating that sE-cad was necessary and sufficient to induce lumen filling. Lumen filling is mediated by the activation of EGFR and its downstream ERK and AKT pathways. Long term (72-96hrs) sE-cad treatment induced EMT in normal epithelial cysts and the AKT pathway was found to be implicated in the induction of EMT. We demonstrate our results using *in vitro* 3D culture system, confocal microscopy and western blotting.

While some aspects of the TME such as ECM remodeling and tumor angiogenesis are well studied, the interaction between tumor cells and the adjacent epithelium is poorly understood and this study demonstrates that cancer cells can utilize the surrounding normal epithelial cells as accessories to produce factors necessary to

maintain and promote tumor growth. This finding may have important clinical correlations, as our results suggest that elevated sE-cad levels observed in cancer patients' sera are derived from both tumor cells as well as adjacent normal epithelial cells. *In vivo*, carcinoma cells induced shedding of cell bound E-cadherin from adjacent normal tissue may result in transdifferentiation of the compact epithelial tissue into disorganized mesenchymal phenotype. Elevated sE-cad levels may also have pro-tumorigenic effects on other components of the TME such as the various stromal cell types. Thus, accumulation of sE-cad in the microenvironment may have additive or synergistic effects on the pro-oncogenic TME since it can possibly alter the different components of the TME. Our results further support the idea that effectively eliminating sE-cad may benefit current EGFR-based therapies against various carcinomas as sE-cad can induce EGFR activation even in normal epithelial cells, and blocking sE-cad reduces the phosphorylated levels of several RTKs, the absence of sE-cad in the sera may be of importance for the efficacy of EGFR inhibitor-based therapeutic intervention.

Chapter 1

INTRODUCTION

1.1 E-cadherin: Structure and Function

Epithelial (E)-cadherin is a Ca^{2+} dependent cell adhesion molecule located in the adherens junction and along the basolateral surface in epithelial cells [1, 2]. It belongs to the type I cadherin family of cell adhesion molecules and plays a crucial role in tissue morphogenesis, providing cell polarity and integrity to epithelial tissues, and is also involved in signal transduction [3-5]. E-cadherin consists of a large extracellular domain, which is divided into five subdomains known as cadherin repeats or the extracellular cadherin domains (EC 1-5), a transmembrane domain and a short cytosolic region at the carboxy terminus[6]. Each EC domain consists of repeating amino acid sequence of about 110 amino acids each and possesses a characteristic immunoglobulin (Ig) like fold and hence these domains are also referred to as Ig domains [6, 7]. The cytoplasmic tail of E-cadherin forms the core cadherin-catenin complex by binding to p120 catenin and β -catenin inside the cell membrane. This catenin-cadherin complex interacts with actin binding proteins such as vinculin, α -actinin and formin-1 to modulate the actin cytoskeleton[1]. E-cadherin ectodomain interactions between apposed cells mediate specific cell–cell contacts, whereas the intracellular region functionally links E-cadherin to the underlying actin cytoskeleton and provides integrity and rigidity to the cells. [8-11] (Figure 1.1).

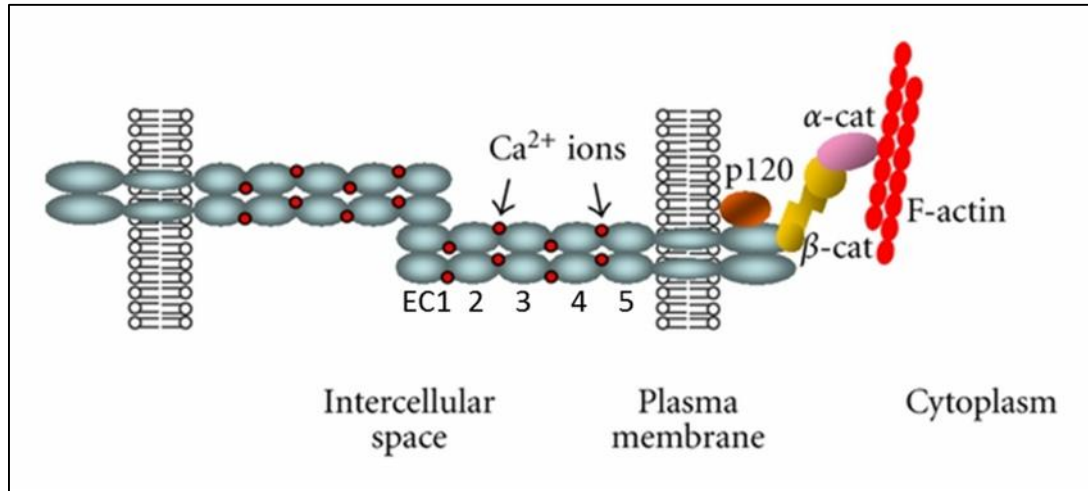


Figure 1.1: Schematic representation of the E-cadherin structure.

Figure reprinted from open access publication **Gama, A. and Schmitt, F.** (2012). Cadherin cell adhesion system in canine mammary cancer: a review. *Vet Med Int* **2012**, 357187.

The EC domains interact with calcium ions, causing a conformational change in the extracellular domain, which results in the formation of adhesive homophilic interactions[12]. Three calcium ions bind between the EC domains and this binding provides a strong curvature to the full length ectodomain. These Ca²⁺ binding sites in the EC domains are among the most conserved sequences across species [13, 14]. Crystallographic studies have shown that E-cadherin monomers within the same cell interact to form ‘cis’ dimers whereas E-cadherin molecules protruding from adjacent cells associate in an antiparallel manner to form ‘trans’ homodimers [7, 15].

There is a lot of discrepancy in the field on the exact mechanism of E-cadherin interactions and how intercellular adhesive binding occurs. However, the majority of reports on E-cadherin binding suggest that the adhesive binding site is localized to the outermost EC1 domain [16, 17]. Chu and colleagues showed that adhesive interaction

is a 2-step model where first the EC1 domain of E-cadherin monomers form weak *trans* dimers. This is followed by lateral clustering of the E-cadherin monomers, which increases the probability of ‘trans’ dimers and strengthens adhesion. Contrary to conclusions from previous crystallographic studies, they demonstrated that the probability of E-cadherin ‘cis’ dimer formation was very low[18]. This is because the ‘cis’ and ‘trans’ interactions shared the same adhesive face [9-11]. The detailed ‘trans’ dimer formation is explained by a strand swap model. The primary feature is the swapping of the ectodomain strands with each other and this occurs by tryptophan (Trp)-2 residue of an EC1 side chain of one E-cadherin monomer intercalating with the hydrophobic core of a neighboring monomer[7, 19]. The Trp-2 hydrophobic interactions are a prerequisite for the stabilization of the adhesive *trans*-homodimers as mutations in this Trp-2 residue or the hydrophobic acceptor pocket result in loss of adhesion function [7]. Additionally, a conserved histidine-alanine-valine (HAV) sequence in the EC1 domain is crucial for E-cadherin interactions [20]. These *trans* dimers and lateral clustering of E-cadherin monomers form a multimeric zipper like structure, which is responsible for interjunctional adhesion [7] [21, 22] (Figure 1.2).

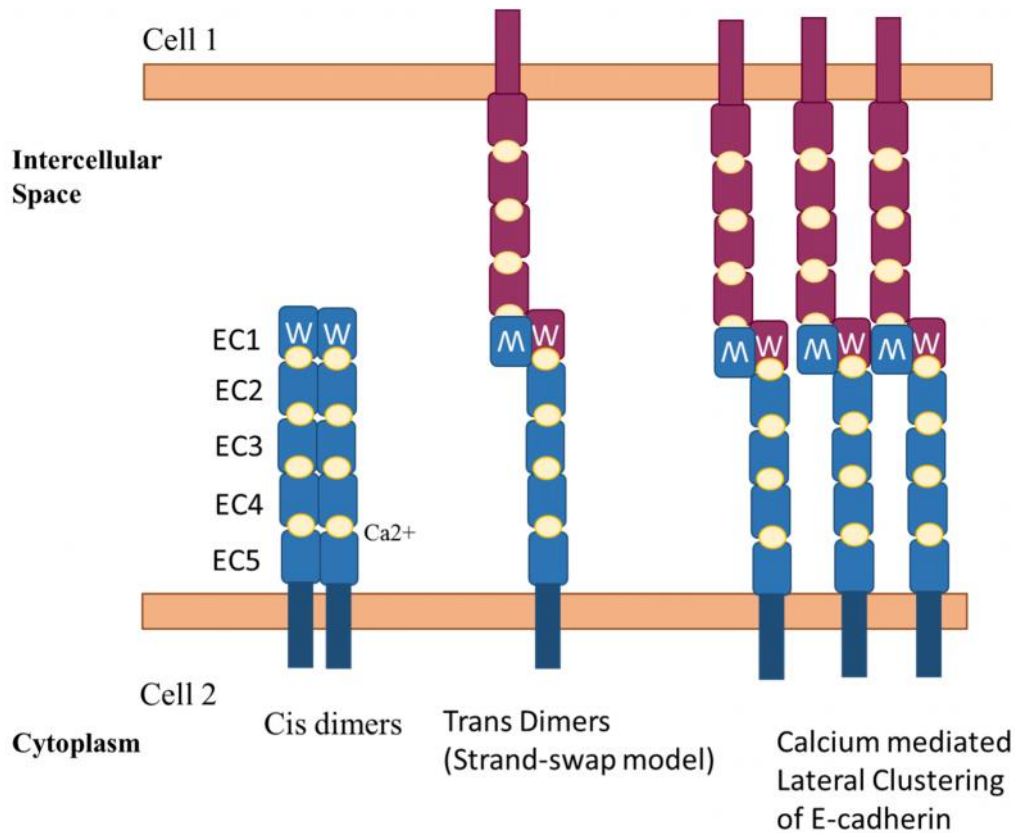


Figure 1.2: Model showing calcium dependent E-cadherin cis dimers, tryptophan dependent Trans dimers and lateral clustering of E-cadherin
 (Adapted from Gumbiner, B. M. (2005). "Regulation of cadherin-mediated adhesion in morphogenesis." *Nat Rev Mol Cell Biol* 6(8): 622-34.)

The adherens junction is a region of cell-cell contact where a gap of 20-25 nm between two adjacent plasma membranes is bridged by the *cis* and *trans* dimers formed by the extracellular domain of the cadherin family molecules [23, 24]. E-cadherin is the central molecule in the formation of adherens junction and facilitates the formation of apical tight junctions and the entire adherens junctional complex. The ECD of E-cadherin is about 20 nm in length. However, the intercellular gap between plasma

membranes at the basolateral regions of two adjacent cells is larger than 25 nm. Therefore, it is likely that the E-cadherin molecules in this region interact only laterally and do not overlap to form the adhesive *trans* dimers [25]. In cancer, E-cadherin is proteolytically cleaved by abnormally expressed proteases in the extracellular environment. However, it is not known whether these proteases cleave E-cadherin from the adherens junction or the basolateral region. This knowledge would also help understand whether the shed E-cadherin is cleaved off as a monomer or a dimer and whether E-cadherin dimers exist in the soluble form.

E-cadherin is an important regulator of epithelial tissue physiology. It is expressed on the epithelial cell surface and it controls adhesion and motility in epithelial cells. When E-cadherin molecules come in contact with each other, they prevent epithelial cells from growing over each other by a phenomenon known as contact inhibition of migration and proliferation. E-cadherin acts as a biochemical velcro which binds epithelial cells together and allows them to form sheets. Epithelial sheets form the epidermis, which acts as an external barrier, and line the internal organs. E-cadherin and the epithelial junctional complex help the epithelial cells form a tight polarized layer and acts as a permeability barrier. It controls the paracellular transport of solutes and water through the cells[1].

E-cadherin also plays a crucial role during early embryonic development in processes such as gastrulation, neurulation and organogenesis[26] and consequently E-cadherin homozygous knockout mutations are lethal and embryos do not develop beyond the blastocyst stage due to severe abnormalities in morula cell adhesion [27]. E-cadherin mediated cell adhesion triggers activation of signaling cascades. Furthermore, this adhesion is a dynamic process that is regulated by several signaling pathways. -

catenin, the primary cytosolic protein that interacts with E-cadherin, also acts as a co-transcriptional activator and activates genes in the wnt signaling pathway. p120 catenin, which binds to the juxtamembrane region of E-cadherin cytoplasmic tail, regulates the actin cytoskeleton organization by influencing RhoA activity. The details of how E-cadherin is actively involved in cell signaling are presented below.

1.2 E-cadherin Mediated Cell Signaling

Not only does the E-cadherin ectodomain region have an adhesive function and play a role in tissue integrity, it is also associated with growth factor receptors, other integrin and cadherins and is an effector of signal transduction pathways via its cytoplasmic tail[28] (Figure 1.3). A wide range of receptor tyrosine kinases and cytoplasmic kinases are found at cell – cell contacts, however the precise relationship between E-cadherin and tyrosine kinase signaling is poorly understood.

Direct cross-talk between E-cadherin and EGF receptors has been reported. The E-cadherin interaction with receptor tyrosine kinase (RTK) is complex. When the EGFR is activated, E-cadherin is downregulated by endocytosis. This destabilizes E-cadherin/catenin adhesive complexes ultimately resulting in disassembly of cell-cell contacts. Contrary to this, when E-cadherin trans dimers form new cell contacts, rapid EGF-independent activation of EGFR activates the downstream mitogen activated protein kinase (MAPK), phosphatidylinositide 3-kinases (PI3k) and Rho GTPase pathways to promote cell proliferation and survival.

In melanoma cell lines, E-cadherin overexpression impairs EGF, hepatocyte growth factor (HGF), and insulin growth factor-1 (IGF-1) mediated receptor signaling[29]. E-cadherin homophilic adhesion is also reported to activate the cytoplasmic tyrosine kinase src. Low levels of src signaling are found to be essential for

the integrity of the cell adhesion junctions. However, src has contrasting effects on E-cadherin and its interaction with E-cadherin is complex. At lower levels of activation, src signaling supports E-cadherin adhesion function, while over-stimulation of src signaling disrupts E-cadherin mediated adhesion [30].

E-cadherin is also a negative regulator of the β -catenin/wnt signaling pathway. When not bound to the cytosolic end of E-cadherin at the surface, β -catenin can translocate to the nucleus and function as a transcriptional cofactor activating wnt signaling genes such as c-myc, cyclin D1 and MMP-7 [31, 32]. E-cadherin recruits β -catenin to the membrane, thereby blocking the nuclear signaling activity of β -catenin. Thus E-cadherin acts as a tumor suppressor protein by suppressing a major proliferation signaling pathway [33, 34].

E-cadherin also contributes to Rho A signaling which plays a crucial role in actin reorganization. Rho A is localized at the E-cadherin rich adherens junction region and there is a co-operative relationship between them. E-cadherin is necessary for junctional Rho A signaling and correspondingly active Rho A signaling stabilizes E-cadherin at the adherens junction and maintains junctional integrity [35]. Moreover, loss of E-cadherin and release of p120-catenin from the cytoplasmic cell adhesion complex activates the Rac1-MAPK signaling pathway and promotes tumor cell growth [36].

Overexpression of E-cadherin in melanoma cells reduces NF- κ B activation, conversely loss of E-cadherin results in an increased activity of NF- κ B transcription factor [37]. In addition, NF- κ B suppression is caused by a physical association of NF- κ B with the E-cadherin/catenin complex [38]. *Helicobacter. pylori* infection causes downregulation of E-cadherin expression that results in activation of the NF- κ B pathway, increasing susceptibility to gastric cancer [39]. Hence, downregulation of E-

cadherin causes activation of NF- B that in turn activates its target genes to increase cell survival; reduce cell apoptosis; and contributes to inflammation associated cancer development.

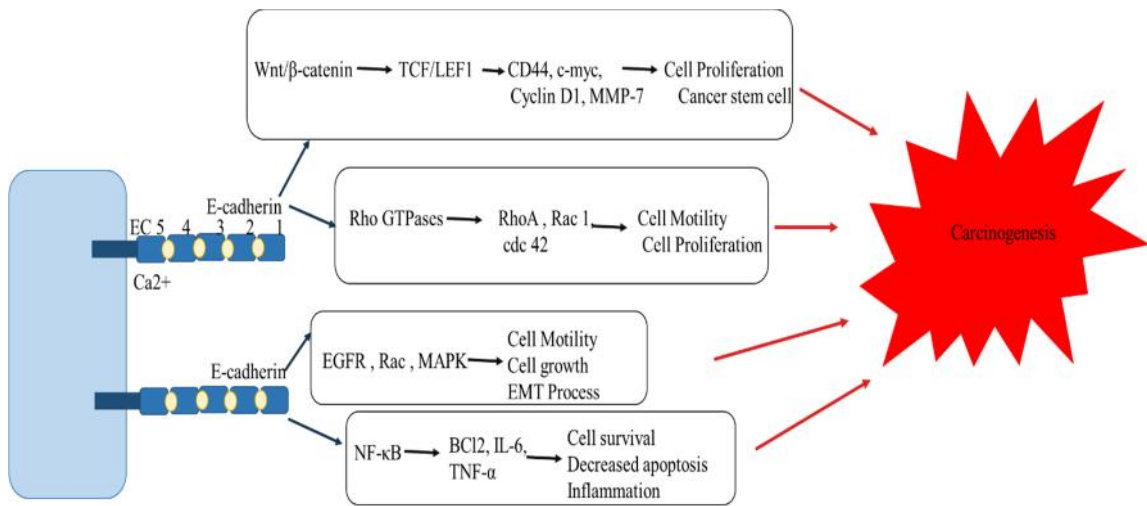


Figure 1.3: Signaling pathways regulated by E-cadherin

Image modified from E-Cadherin and Gastric Cancer: Cause, Consequence, and Applications Rev. Article Xin Liu and Kent-Man Chu

More recently, E-cadherin mediated contact inhibition of proliferation by cells was found to be regulated by Hippo signaling. E-cadherin mediated cell adhesion stimulates the Hippo signaling pathway and restricts the transcriptional activity of YAP protein through its exclusion from the nucleus. Localization of YAP in the cytoplasm allows expression of the growth activating genes. Thus, activation of this pathway by E-cadherin adhesion blocks the translocation of the YAP protein into the nucleus and resulting in proliferation [40].

E-cadherin also exhibits heterophilic interactions with CD103 and killer cell lectin receptor G1 (KLRG1) [41-44]. CD103 ($\alpha_E\beta_7$) is an E-cadherin receptor located on T lymphocytes. The interaction between the extracellular domains EC1 and EC2 of E-cadherin and CD103 helps to target T cells to epithelial cells [43]. KLRG1 is another receptor for E-cadherin which is expressed on T cells and natural killer (NK) cells. The binding of KLRG1 to the EC1 domain of E-cadherin prevents the lysis of epithelial targets [44]. Thus the interaction between monomeric E-cadherin and KLRG1 or CD103 is responsible for regulating the activation threshold of NK and T cells and thereby suppressing immune response [44]. E-cadherin, therefore, not only serves as an adhesion and signaling molecule but is also a crucial targeting molecule for T-cell mediated immune response.

1.3 E-cadherin as a Tumor Suppressor Gene & Its Role in Epithelial Cancers: Mechanisms by which E-cadherin is down regulated

Most human adult cancers arise from epithelial tissues [45]. An important regulator of epithelial cell morphology and physiology is E-cadherin. E-cadherin is a tumor suppressor and an invasion suppressor protein whose expression and function is reduced in most human epithelial cancers including breast, colon, gastric, prostate, endometrial and ovarian cancers [45-50]. Down regulation of E-cadherin brings about fundamental changes in the epithelial phenotype, resulting in reduced polarity, intercellular adhesion and activation of signaling pathways that promote epithelial to mesenchymal transition (EMT) resulting in increased tumor cell migration, invasion and metastatic dissemination. Dysregulation of E-cadherin modulates the cadherin-catenin complex resulting in dysregulation of various signaling pathways in epithelial cells, including Wnt signaling, Rho GTPases, and NF- κ B pathway [34, 37, 38, 51]. Loss

of E-cadherin expression increases NF- κ B activity in melanoma cells and forced expression of E-cadherin inactivates the pathway [37]. E-cadherin sequesters the β -catenin at the membrane preventing its translocation to the nucleus and activating the wnt/ β -catenin signaling pathway [34]. In the wnt/ β -catenin signaling pathway, β -catenin present in the cytoplasm translocates to the nucleus to bind to transcription factors TCF/LEF-1 (Transcription Factor/Lymphoid enhancer-binding factor 1) and activate the wnt target genes including, cyclin D1, MMP-7 and c-myc. Thus, downregulation of E-cadherin results in activation of the wnt signaling pathway. Missense mutations in the E-cadherin gene in gastric carcinomas are associated with increased Rho A activity and migration. E-cadherin expression is found to enhance Rho A activity in non-small cell lung cancer cell lines as well [51, 52]. E-cadherin downregulation results in release of p120 catenin which then activates Rac1-MAPK signaling pathway and promotes transformed cell growth [36]. Thus, E-cadherin down regulation contributes to tumor progression both by altering adhesion status as well as by affecting cell signaling.

Some of the mechanisms by which E-cadherin expression is silenced are genetic mutation, nucleotide deletions, transcriptional repression, epigenetic silencing by hypermethylation, endocytosis, enhanced degradation and proteolytic cleavage [53-56] These mechanisms are discussed in detail in the text below.

Somatic mutations of the *CDH1* gene that encodes for E-cadherin have been found in several carcinomas, including sporadic diffuse gastric cancer [57], colorectal cancer [48], lobular breast cancer [53, 58], and ovarian cancer [59]. Genetic mutations including, insertions, deletions, and non-sense mutations that result in truncated proteins of E-cadherin, loss of E-cadherin's calcium binding sites or increased E-cadherin proteolytic degradation. All these mutations result in reduced adhesive and signaling

functions of E-cadherin, contributing to increased cell proliferation, EMT and cancer progression.

Another mechanism by which E-cadherin is silenced is by **hypermethylation of the *CDH1* promoter**. Typically somatic mutation predispose the *CDH1* gene to epigenetic hypermethylation of the promoter region and it occurs as a second hit in E-cadherin silencing. *Helicobacter pylori* infection is strongly associated with initiation and progression of gastric cancers. One of the early events of *Helicobacter pylori* infection is hypermethylation of many tumor suppressor genes including the *CDH1* gene which is the primary mechanism of silencing E-cadherin and gastric cancer initiation [60].

Transcriptional repression of E-cadherin is another common mechanism by which E-cadherin is downregulated in carcinomas. Several transcription factors such as Snail, E12/E47, ZEB, SIP-1, SLUG and TWIST repress E-cadherin expression at the transcriptional level during embryonic development as well as in several cancer cell lines [48, 61-66]. These transcriptional repressors primarily act by interacting with the proximal E-boxes of the E-cadherin promoter region. Increased expression of transcription factors Snail, Slug and SIP-1 were associated with metastasis and disease aggressiveness in breast and ovarian carcinomas [66].

In other cancers such as prostate and adenocarcinomas, E-cadherin is targeted at the protein level and rendered functionally inactive by calpain to generate a 100kDa E-cadherin fragment [67]. The **proteolytic cleavage** event disrupts the cell adhesion junctional complex. There are several other proteases implicated in the proteolysis of E-cadherin from the cell surface, these include members of the disintegrin family (ADAM10 and 15), bacterial proteases (gingipains and BFT), cathepsins (B, L, S),

matrix metalloproteases (MMP-2, 3, 7, 9, and 14), Kallikrein-7 (KLK7), and plasmin. Proteolytic cleavage of E-cadherin by these proteases result in the generation of an 80 kDa E-cadherin fragment referred as soluble e-cadherin (sE-cad)[68].

Under physiological conditions E-cadherin is turned over by endocytosis and lysosomal degradation. Rapid reductions in levels of E-cadherin at the cell surface and cell junctions occurs by endocytosis during a variety of developmental processes, including, gastrulation, developmental EMT and neuronal patterning. In epithelial cancers, E-cadherin is primarily lost by transcriptional repression and genetic and epigenetic changes, but defects in **E-cadherin internalization** have also been observed. Elevated levels of internalized E-cadherin are observed in nasopharyngeal and oropharyngeal cancers and are associated with poor survival [69, 70]. Elevated src and receptor tyrosine kinase (RTK) oncogenic signaling play a crucial role in abnormal E-cadherin internalization.

1.4 Over-expression of E-cadherin in tumors

E-cadherin does not always function as a tumor suppressor. Several highly aggressive carcinomas such as inflammatory breast cancer (IBC), glioblastomas, and metastatic prostate and ovarian cancers show increased E-cadherin expression [71-74].

In metastatic prostate cancer, exit from EMT and re-expression of E-cadherin is essential for the prostate cancer cells to metastasize to the bone marrow tumor growth sites. In a prostate xenograft model, high levels of the E-cadherin transcriptional repressor ZEB1 were not able to downregulate E-cadherin expression. ZEB1 and E-cadherin are highly co-expressed in the prostate metastatic tumor sites and are associated with disease aggressiveness and drug resistance [73].

IBC is the most aggressive form of breast cancer and E-cadherin is highly expressed in 100% of IBC cases, suggesting a strong connection between E-cadherin overexpression and IBC pathogenesis [71]. In some high grade adult glioblastoma tumors, E-cadherin expression is crucial for cell migration and growth and correlated with poor prognosis in patients [72]. Also in ovarian carcinomas, E-cadherin expression is associated with early events of tumor progression as it is found to be uniformly expressed in benign, borderline as well as all stages of metastatic ovarian cancers. In several such carcinomas, pseudo-epithelial morphology and retained E-cadherin expression is associated with increased tumorigenesis and worsening prognosis. Additionally, E-cadherin is found to be re-expressed in metastatic foci of several carcinomas displaying a well differentiated epithelial morphology similar to the normal epithelial cells [75-77].

This raises the question of how does E-cadherin expressed in the tumor cells does not behave as cell adhesion molecule to form cellular junctions and reduce proliferation and instead acts as pro-tumorigenic protein and facilitates tumor progression in these carcinomas. Multiple reasons have been suggested to explain the tumor promoting role of E-cadherin.

One mechanism is by sustained activation of survival and proliferation pathways in cancer cells that overwhelm the tumor suppressive effects of E-cadherin expression. For instance, in SF67 glioma cell lines, even though E-cadherin is highly expressed, the cells do not have mature cell-cell junctions and thus have a pseudo-epithelial phenotype. Lack of E-cadherin mediated cell junctions may prevent suppression of Rac1 and other signaling pathways normally regulated by the junctional E-cadherin [72]. In the ovarian cancer cell line OVCAR-3, E-cadherin expression is associated with ligand independent

activation of the epidermal growth factor receptor (EGFR) and the downstream mitogen activated protein kinase (MAPK) and AKT pathways.

Another possible explanation is that retained E-cadherin expression permits migration of tumor cells as clusters or multicellular aggregates as observed in ovarian carcinoma and IBC [78, 79]. Circulating IBC cells re-express E-cadherin to form intercellular adhesions and the cohesive tumor emboli [71].

Another explanation for lack of cell contact growth inhibition in cancers that have high E-cadherin expression is that they produce a shorter soluble form of E-cadherin by proteolytically cleaving the E-cadherin ectodomain. The shorter soluble form (80 kDa) of E-cadherin cleaved by proteases is referred to as soluble E-cadherin (sE-cad). Elevated sE-cad levels have been observed in several carcinomas and are correlated with reduced E-cadherin levels in tumors [80]. The focus of this project is to investigate the pro-oncogenic effects of sE-cad and whether tumor cells can induce sE-cad shedding in normal epithelial cells as a mechanism promoting tumor growth.

1.5 Proteolytic Shedding of E-cadherin: Generation of sE-cad

E-cadherin can be lost from the cell surface by proteolytic cleavage to generate extracellular and cytosolic E-cadherin fragments that drive tumor growth, survival, and motility [81]. Several proteases present in the extracellular environment of tumors, such as matrix metalloproteinases (MMP-3,7,9,14 and MT1-MMP), members of a disintegrin and metalloproteinase family (ADAM 10, ADAM15), bacterial proteases (gingipains and BFT), cathepsins (B,L,S), plasmin, and kallikrein 7 are all implicated in the cleavage of E-cadherin[68, 82, 83]. These extracellular proteases can cleave the cell bound E-cadherin (120 kDa) to generate an 80 kDa N-terminal extracellular fragment and a smaller (38 kDa) membrane-bound intracellular C-terminal fragment. Following

the cleavage by extracellular proteases, the membrane bound fragment is susceptible to further processing by presenilin-1/ gamma-secretase complex to release a 33 kDa C-terminal fragment 2 (E-cad/CTF2) into the cytosol resulting in the disruption of adherens junction complex [81]. The larger ectodomain fragment contains the five extracellular domains of E-cadherin and is referred to as soluble E-cadherin (sE-cad) since it is shed from the plasma membrane and diffuses into the extracellular space (Figure 1.4). Proteolytic processing of E-cadherin substantially changes its functional properties, transforming it from a tumor suppressor to a tumor promoting protein. The cleaved E-cad fragments possess distinct oncogenic properties.

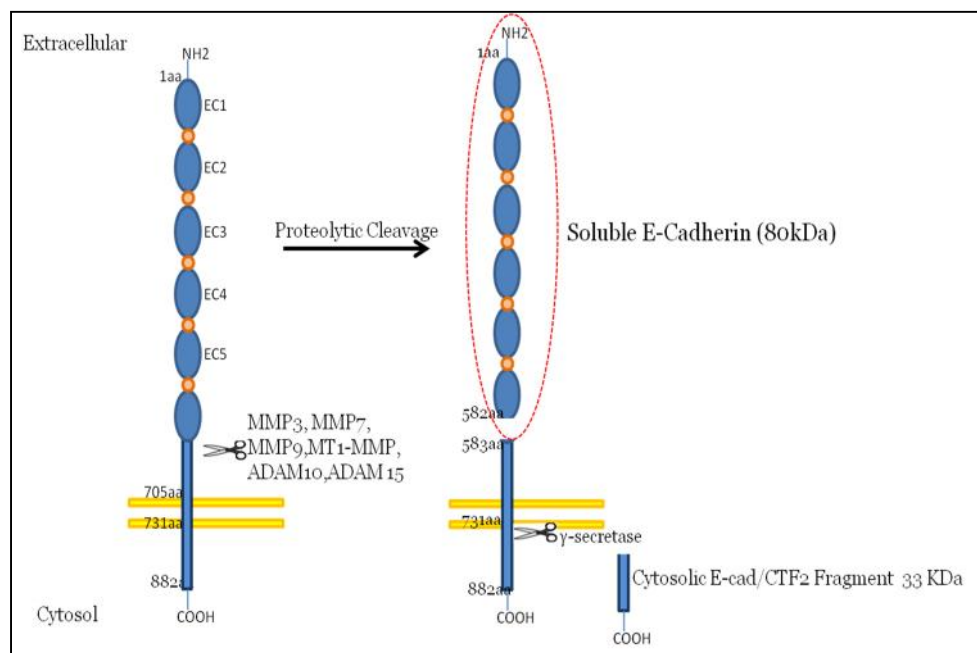


Figure 1.4: E-cadherin Ectodomain Shedding.

The MMP cleavage point for E-cadherin is between amino acids Leucine 581 and Serine 582 or between Serine 582 and Aspartic acid 583. This cleavage generates a ~582 aa long, 80 kDa soluble E-cadherin fragment and a shorter 296 aa long membrane-tethered fragment.

Under physiological conditions such as during apoptosis, the full length E-cadherin is downregulated by different mechanism. It involves caspase and metalloproteinase activity resulting in three detectable fragments, a 29kDa cytoplasmic fragment (fragment 1), an 84kDa extracellular fragment (fragment 3), and a 24kDa transmembrane domain fused to the cytoplasmic domain (fragment 2). Caspase 3 belongs to the cysteine-aspartic acid protease (caspase) family and is involved in cellular apoptosis. Its activity is crucial for cytoplasmic cleavage and the cleavage point is mapped at Asp⁷⁵². Metalloproteinase activity drives the extracellular proteolysis at the cleavage site Leu⁵⁸¹-Ser⁵⁸². This cleavage disrupts the cadherin interactions resulting in loss of cell adhesion [84]. *In vitro*, sE-cad shedding occurs in response to serum withdrawal or to growth factor and pro-inflammatory cytokine stimulation.

sE-cad was first detected in the conditioned medium of the breast cancer cells, MCF-7 and then in the body fluids of patients diagnosed with a variety of cancers [85]. However, it is now reported in a variety of diseases, including, bacterial and viral infections (HIV), autoimmune diseases and organ failure [68]. Though there are no protease which exclusively cleaves only E-cadherin, Table 1.1 describes all the different sheddases which are misregulated or overexpressed in diseases and reported to cleave E-cadherin in response to different stimuli [68]. These proteases are identified in different cancer cell lines and knock out mouse models using specific inhibitors and siRNA techniques.

sE-cad has a highly conserved histidine-alanine-valine (HAV) amino acid sequence in first extra cellular repeat (EC1) at its N-terminal end [20]. The HAV sequence is crucial for homophilic binding and adhesive activity of cadherins[6].

Purified sE-cad disrupts cell-cell adhesion in cultured epithelial cells, and this adhesive activity was dependent on the conserved HAV sequence in its N terminal region.

Table 1.1: List of E-cadherin Sheddases (Modified from Grabowska et al., 2012)

Sheddases	Stimulus	System
ADAM 10	IL-1 , TNF- , IFN- , TGF- , Lipopolysaccharide (LPS) Growing cultures Helicobacter pylori infection EGF	Normal keratinocytes Melanoma cell line Gastric carcinoma cell line Benign prostatic hyperplasia cell line
ADAM 15	Serum withdrawal	Breast cancer cell line Prostate cancer cell line Bladder cancer cell line
BFT, Fragilysin	B. fragilis infection	Colorectal cancer cell line
Cathepsins (B,L,S)	Mislocalized and upregulated cathepsins	Mouse pancreatic cancer model
Gingipains	P. gingivalis infection	Canine kidney cell line
KLK7	Overexpressed in pancreatic cancer	Pancreatic cancer cell line
MMP-2	Protein Kinase D1 (PKD1)	Prostate cancer cell line
MMP-3, Stromelysin	(Activated mutant)	Breast cancer cell line Ms mammary cell line
MMP-7, Matrilysin	HGF HGF Lung injury (bleomycin)	Gastric cancer cell line Prostate cancer cell line Lung cancer cell line, mouse lung injury Breast cancer cell line
MMP-9	Interaction with collagen binding integrins ($\alpha 2 \beta 1$, $\alpha 3 \beta 1$) EGF PKD1	Ovarian carcinoma cell line Head and neck cancer cell line Prostate cancer cell line

Table 1.1 (Continued)

Sheddases	Stimulus	System
MT1-MMP MMP-14	Ischemia	Normal rat kidney cell line
Plasmin	LPA None (growing cultures)	Ovarian carcinoma cell line Canine kidney cell line
Ionomycin	Calcium influx,	Lung tumor cell line
	Ischemia (lung transplant)	Rat lung transplantation
TIMP-2 sensitive TAPIE- sensitive	Phorbol ester (PMA) Serum withdrawal Apoptosis (staurosporine,camptothecin)	Breast cancer cell line Breast cancer cell line Canine kidney cell line

1.6 Elevated sE-cad Levels in Pathological Conditions

1.6.1 Cancers

Increased levels of sE-cad has been observed in the sera and urine of cancer patients diagnosed with a variety of cancers, including breast, bladder, skin, ovarian, colorectal and lung cancers. Elevated sE-cad levels are indicative of disease progression, patient survival and poor prognosis [82]. Depending on the type of cancer, elevated sE-cad levels are correlate with different aspects of disease. For instance, in bladder cancer the levels correlate with the tumor grade and two fold higher sE-cad levels in urine are detected across all stages and grades of bladder cancers [86-88]. In colorectal, non-small cell lung carcinoma and esophageal squamous cell carcinomas, sE-cad levels not only correlate with metastasis but also are a marker for treatment success as sE-cad levels decrease with chemotherapy treatment [89-91]. Similarly,

increased sE-cad levels in gastric cancer are indicative of patient survival and recurrence and thus help diagnose early failed therapy and appropriate treatment plan in gastric cancer patients [92]. In liver carcinoma, patients with sE-cad levels higher than 8,000ng/ml are at a high risk for metastasis and relapse [93]. In ovarian cancer, the serum sE-cad levels do not vary significantly however, sE-cad levels are significantly higher in the local cystic fluid of ovarian ascites from malignant ovarian cancer in comparison to the benign patients [94]. In prostate cancer and skin carcinoma, sE-cad levels are useful as a marker for disease progression and high levels can categorize patients as high-risk for recurrence [95, 96].

High sE-cad levels are also observed in patients with non-epithelial cancers such as leukemia, multiple myeloma and leiomyosarcoma. In multiple myeloma sE-cad levels are five times higher than the control samples and consequently can be used as a biomarker [97].

1.6.2 Other Non-cancer conditions

Although initially sE-cad was extensively studied as a biomarker in various types of cancer, it is also detected in several non-cancer conditions such as benign prostatic hyperplasia (BPH), dermatitis, psoriasis, acute pancreatitis, diabetes, and diabetic nephropathy [68]. sE-cad levels correlate with the severity of the disease. For instance, in BPH patients, the levels of sE-cad are significantly higher than in normal control patients but not as high as in prostate cancer patients [95, 98]. Similarly, sE-cad levels in the sera are elevated in patients suffering from acute psoriasis and dermatitis, but are not as high as in patients with skin cancer where high sE-cad levels are an indicator of invasion [95, 98]. sE-cad levels are also elevated in pancreatitis and can help to differentiate between mild acute and severe acute pancreatitis and distinguish

pancreatitis from other abdominal inflammatory pathologies [99]. In diabetic patients, sE-cad levels in the urine may be an indicator of diabetic nephropathy [100]. In HIV infections, high sE-cad serum levels correlate with high HIV viral titers and are a marker for the severity of the infection [101]. sE-cad levels in patient serum increase with the amount of sepsis and organ dysfunction and are a biomarker for tissue injury and systemic inflammatory responses after surgery [102, 103].

Table 1.2: Table showing sE-cad Levels in various cancers and its prognostic utility (Modified from De Wever et al., 2007 and Grabowska et al., 2012)

Biological Fluid	Cancer	sE-cad Levels ($\mu\text{g/ml}$)		Characteristics
		Cancer Patients	Normal	
Serum	Gastric	3 -15	2-5	Predicts long term survival, recurrence
Serum Urine	Bladder	3- 15 1.2 - 1.6	1- 3 0.5 -0.9	Correlates with tumor grade, tumor number and recurrence
Serum	Prostate	~27	6	Associated with biochemical failure, metastasis
Serum	Ovarian	7	5.5	Correlates with tumor grade
Serum	Colorectal	5.5	3	Correlates with cancer progression
Serum	Melanoma	1.5	0.8	Correlates with advanced disease
Serum	Non small lung	3.4	1	Correlates with distant metastasis
Serum	Liver	6-10 Above 8	2-5	Correlates with cancer progression Correlates with recurrence
Cyst Fluid	Ovarian	12	2	Facilitate distinction between benign and malignant
Serum	Non-Epithelial Leimyosarcoma Leukemia Multiple Myeloma	3.2 2.5 \pm 1 Above 3	2 2 0.6	Correlates with Cancer Correlates with Cancer Survival

E-cadherin cleavage also occurs during infection by bacteria such as *Bacteroides fragilis* and *Porphyromonas gingivalis* [104, 105]. sE-cad shed by *P. gingivalis* results in disruption of cell adhesion and suppressing innate immune response and thereby contributing to periodontitis [104, 106]. MMP-7 and sE-cad levels are upregulated in pulmonary fibrosis patients and play a role in disease progression [107].

1.7 Consequences of Elevated sE-cad

sE-cad released from cell surfaces enters the bloodstream and acts as an autocrine/paracrine signaling molecule. In the recent past, several reports have demonstrated pathophysiological effects of sE-cad. In several cancer cells, sE-cad has tumor-promoting effects as it enhances tumor cell proliferation, migration and invasion, and activates various oncogenic signaling pathways. The pro-oncogenic effects of sE-cad are shown in Figure 1.5.

1.7.1 Loss of Cell Adhesion

Recombinant sE-cad added exogenously to epithelial cells destabilizes adherens junctions, thereby facilitating tumor cell proliferation, migration and invasion [108, 109]. In pancreatic cancer cells and in epithelial MDCK cells, sE-cad interferes with cell aggregation assays, and immunodepletion of sE-cad from conditioned media results in the re-aggregation of cells (20, 31). Thus sE-cad can disrupt epithelial adherens junctions and hinder cell aggregation.

1.7.2 Increased Cell Migration and Invasion

As sE-cad disrupts cell junctions it promotes increase in cell motility and invasion *in vitro* [110]. Another mechanism by which sE-cad facilitates invasion is by inducing upregulation of MMPs in the cells [111]. sE-cad treatment induced

upregulation of MMP-2, MMP-9, and MT1-MMP at the mRNA and protein levels in lung tumor cells [111]. Synthetic peptides containing only the HAV sequence of E-cadherin were also sufficient to promote invasion of cells into the chick heart and collagen type I gels by MMP overexpression. sE-cad does not alter the expression of tissue inhibitor of metalloproteinase (TIMP) thereby creating an imbalance in the levels of MMPs and their regulator TIMPs facilitating tumor promotion [111]. The addition of the zinc-dependent disintegrin metalloproteinase, ADAM -10, to mouse fibroblasts and human keratinocytes mediates sE-cad shedding and leads to reduced cell adhesion and increased migration [83].

1.7.3 Increased Cell Proliferation and Survival

MMP-7 mediated sE-cad shedding enhances RhoA activity and cyclin D1 expression resulting in increased proliferation, migration and loss of contact inhibition in non-transformed epithelial cells [112]. ADAM 10 is involved in the proteolytic processing of E-cadherin under physiological conditions and is critical during embryonic development [83]. It is also upregulated in metastatic melanoma and *Helicobacter pylori* infection of gastric cell lines and is implicated in sE-cad shedding [113, 114]. ADAM-10 overexpression results in translocation of β -catenin to the cytoplasm and activation of the β -catenin mediated signaling pathways. This ultimately results in increased expression of downstream β -catenin regulated genes such as cyclin D1, c-myc leading to increased proliferation in human epithelial keratinocytes and ADAM 10 knockdown mouse models.

The proteolytic processing of E-cad converts the adhesion protein into a soluble growth factor and an anti-apoptotic molecule [115]. In normal Madin-Darby canine kidney cells, recombinant purified sE-cad inhibits apoptosis when cells were subjected

to serum starvation by activating HER1, PI3K, AKT and ERK1/2 signaling pathways [115].

1.7.4 sE-cad Mediated Signaling

The extracellular domain of E-cadherin can interact with and activate the epidermal growth factor receptor (EGFR) [116]. Several reports have now shown that sE-cad also retains the ability to interact with EGFR family of receptors. Zinc-dependent disintegrin metalloproteinase ADAM 15 is upregulated in prostate and breast cancers and is also associated with shedding of sE-cad in these carcinomas [117]. Najj et al., demonstrated that ADAM 15 cleaved sE-cad from breast cancer cells binds and activates the HER2 and HER3 receptors of the EGFR family [117]. sE-cad mediated heterodimerization and activation of the HER2-HER3 receptors further activates the downstream extracellular regulated kinase (ERK) pathway promoting cell migration and proliferation in the breast cancer cells [117]. In human skin squamous carcinoma tissues, decrease in full-length E-cadherin protein levels correlated with an increase in sE-cad levels. sE-cad also contributes to skin carcinogenesis via association with HER1, HER2, and insulin-like growth factor-1 receptor (IGF-1R) in human skin squamous cancer tissues [118]. This same group recently provided *in vivo* and *in vitro* proof of concept of targeting sE-cad using a monoclonal antibody against the ectodomain of E-cadherin (Decma-1) to improve outcomes in breast and skin carcinogenesis. Decma-1 suppressed tumor growth and showed potent anticancer activity by downregulating the HER family members and components of the MAPK-PI3K/Akt/mTOR pathways [119, 120]. Most of the investigations on the pro-oncogenic effects of sE-cad are focused on tumor cells and the influence of elevated sE-cad levels on normal tissue architecture is not well understood.

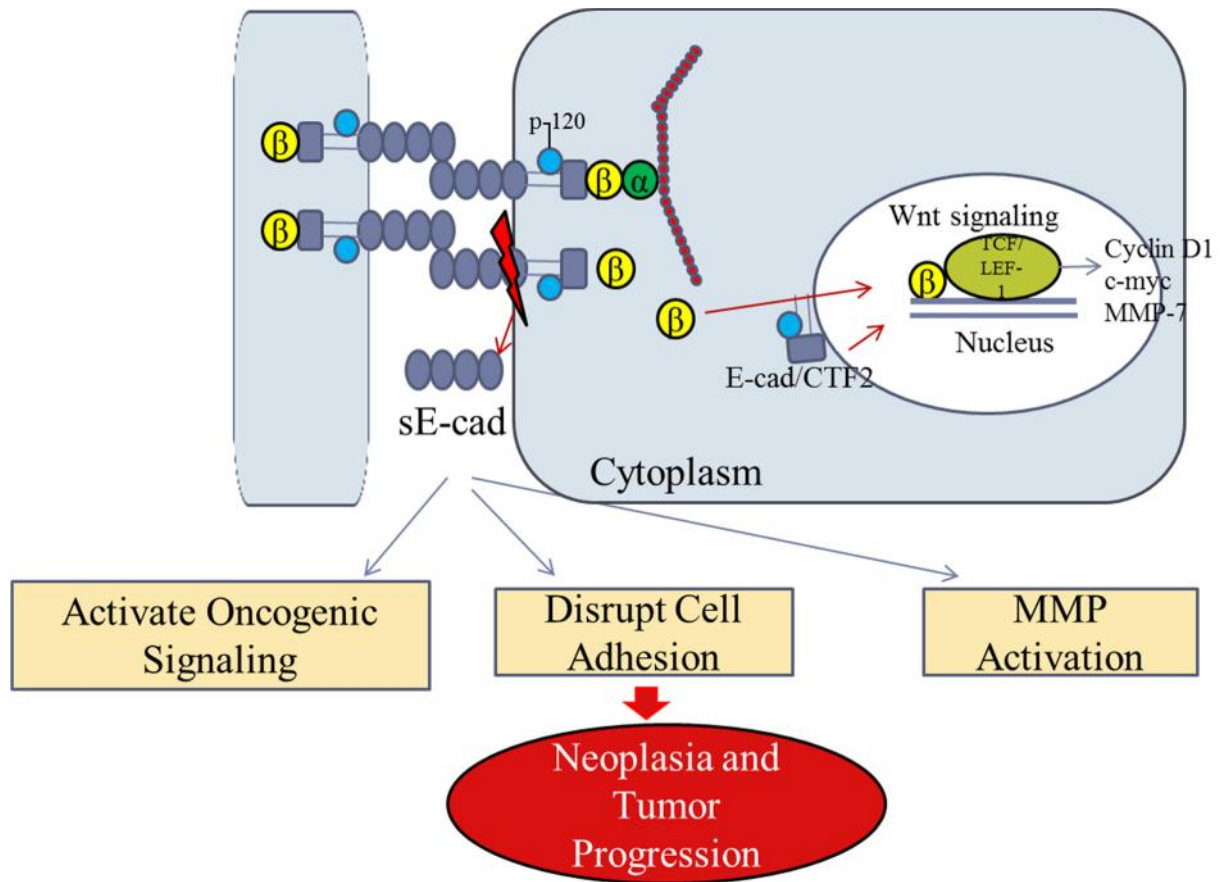


Figure 1.5: Oncogenic Effects of sE-cad.

The figure depicts consequences of sE-cad shedding. Generation of sE-cad by E-cadherin cleavage reduces the amount of full-length E-cadherin on the plasma membrane, disrupts existing adherens junctions, activates the expression of matrix metalloproteinases (MMP) to augment ectodomain shedding, and activates EGFR pathway signaling by different mechanisms. Intracellular cleavage of E-cadherin activates Wnt/ β -catenin pathway signaling (step 5) (Figure modified from David and Rajasekaran, 2012).

Immune Response Suppression: sE-cad can act as a dummy ligand for KLRG1, an E-cadherin receptor present on T-cells and natural killer (NK) cells, and thus interfere with immune cell interactions. In HIV-infected patients, presence of recombinant sE-cad in peripheral blood hampers the ability of T cells to secrete IFN-

gamma and interferes with its anti-viral functions of T-cells in response to HIV treatment [101].

1.8 Cytoplasmic fragment of E-cadherin (CTF2)

Following the extracellular metalloproteinase activity, the shorter membrane bound E-cadherin fragment is cleaved by γ -secretase to release a cytoplasmic fragment of E-cadherin referred as E-cad/CTF2 [121]. This released cytoplasmic E-cad/CTF2 fragment translocates to the nucleus and directly interacts with DNA. p120-catenin was found to be essential for its nuclear localization and the DNA association occurs via p120 catenin [121]. Nuclear localization of E-cad/CTF2 protected cells from apoptosis [121]. Furthermore, p120 catenin binds to the transcriptional repressor Kaiso, which is a negative regulator of the wnt- catenin signaling pathway. p120 catenin-Kaiso binding relieves the Kaiso mediated transcriptional repression. E-cad/CTF2 was demonstrated to enhance this p120 catenin mediated transcriptional regulation by forming a complex with p120 catenin and Kaiso [121].

Release of the E-cad/CTF2 fragment causes disruption of the cadherin-catenin complex resulting in the release of β -catenin. Free β -catenin in the cytoplasm can translocate to the nucleus leading to the activation of the wnt signaling pathway. However, more studies need to be done to evaluate the role of E-cad/CTF2 in β -catenin mediated activation of wnt signaling. Thus, E-cadherin cleavage and the release of its fragments can promote tumor cell proliferation and survival by dual mechanisms both by the sE-cad and CTF2 mediated processes.

In other diseases such as Alzheimer's disease which have increased γ -secretase activity, E-cad/CTF2 is found to be beneficial and protective. E-cad/CTF2 promotes

lysosomal/endosomal degradation of the amyloid precursor protein (APP) cleavage products thereby preventing its accumulation in cells [122]

1.9 Tumor Microenvironment

The present study also addresses the question of, how tumor cells interact with and alter the normal epithelial cells in the vicinity and whether elevated sE-cad in the tumor niche influence the normal epithelial cells along with the tumor cells. Since sE-cad promotes growth, motility and survival of tumor cells, it is crucial to understand the interplay between the different components of tumor microenvironment and how sE-cad influences each of these components.

Tumor tissue comprises of a heterogeneous population of cells consisting of malignant tumor cells and non-malignant host cells. This cellular niche in which the tumor resides is referred to as tumor microenvironment (TME). TME is comprised of a heterogeneous population of cells, including stromal cells, adjacent normal epithelial cells, fibroblasts, infiltrating immune cells, and angiogenic vascular cells; and secretions from these cells such as growth factors, cytokines and extracellular matrix (ECM) as shown in Figure 1.6 [123].

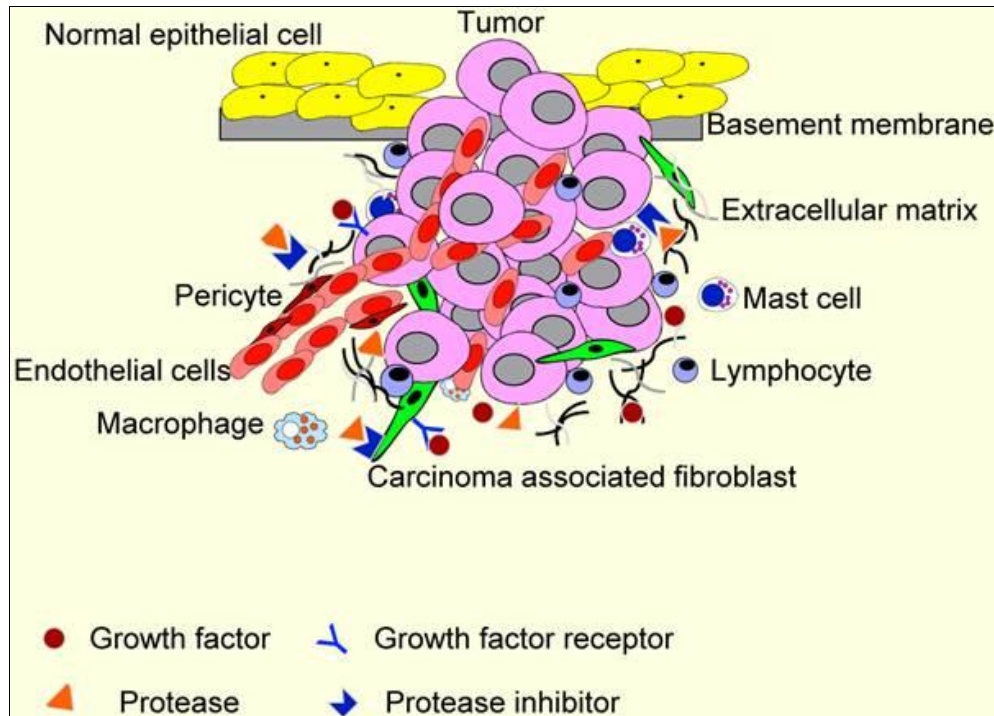


Figure 1.6: Figure showing the different components of the tumor microenvironment. (Reprinted with permission from Koontongkaew et al., J Cancer 4 (2013) 66-83)

Several reports have shown that genetic abnormality in tumor cells alone is not sufficient for cancer progression and tumor development greatly depends on the contributions from the different components of the TME. According to the ‘seed and soil’ hypothesis, proposed by Paget [124] tumor cells are ‘seeds’ that require a congenial microenvironment (the ‘soil’) to grow and metastasize. Cancer cells alter and corrupt the TME components so that they can be exploited for tumor progression [123]. Tumor-host interactions are an important factor in determining how tumor cells behave and respond to therapy. Thus, the TME plays a vital role in development of malignant tumors by contributing to all the six major hallmarks of cancer which are sustained proliferation, evasion of apoptosis, angiogenesis, invasion/metastasis, evasion of

immune destruction, and reprogramming of energy metabolism [125]. Some tumor-host cell interactions and mechanisms by which the TME contributes to carcinogenesis are illustrated below.

1.9.1 Cancer Associated Fibroblasts

Tumor cells can alter the adjacent connective tissue fibroblasts, activate adipocytes or recruit mesenchymal stem cells to differentiate into myofibroblasts or adipocytes. All these cell types are present in the TME and have been collectively referred to as cancer associated fibroblast (CAFs)[123]. CAFs play an important role in all stages of carcinogenesis, promoting tumor proliferation, migration, invasion and angiogenesis. CAFs secrete mitogenic growth factors, including hepatocyte growth factor (HGF), EGF family members, insulin-like growth factor-1 (IGF-1), stromal cell-derived factor-1 (SDF-1/CXCL12), and a variety of FGFs which exert paracrine signaling pathways and stimulate cancer cell proliferation[123] [126]. Tumor cells can also induce CAFs to secrete MMPs which cause ECM-remodeling and formation of neoplastic ECM [123].

Tumor cells also modify CAFs so that they can induce angiogenesis. Depending on the TME, CAFs produce a variety of pro-angiogenic signaling proteins, including, VEGF, FGFs, and IL-8/CXCL8 and PDGF-C. These factors not only stimulate angiogenesis but also provide resistance against anti-VEGF therapy. Additionally, the MMPs secreted by CAFs release angiogenic factors such as bFGF, VEGF and TGF- β from the extracellular matrix and facilitate in recruiting pro-angiogenic macrophages. All these chemoattractants help in recruiting endothelial cells to the tumor tissue and stimulate angiogenesis vital for tumor growth and survival. CAFs are also critical during

invasion and metastasis. They secrete HGF and TGF- ligands which are critical in tumor cell invasiveness by induction of epithelial to mesenchymal transition (EMT).

Cancers disseminate into the circulation along with CAFs thereby transporting parts of the microenvironment to the metastatic site [127]. Pharmacological blockade of CAFs has improved efficacy of cytotoxic drugs in pancreatic cancers. Initiated prostate epithelial cells when injected along with CAFs induced prostate cancer in nude mice model however when injected along with normal prostatic fibroblasts, tumor promoting effects were not reported thereby suggesting that they are directly involved in epithelial tumor progression.

1.9.2 Infiltrating Immune Cells

Infiltrating immune cells (IICs) play a dual role in the TME, they have both immunosuppressive activity that allows tumor progression as well as cytotoxic activity which blocks tumorigenesis [123]. Tumor cells secrete immune suppressive factors (VEGF, IL-10, PGE₂) which exert systemic effects on the immune system. The corrupted immune cells, which include leukocytes, neutrophils, immature monocytes, regulatory T cells (T_{reg}), Tumor associated macrophages (TAMs), mast cells, dendritic cells and T helper cells, have tumor promoting effects and are involved in the chronic inflammatory response[123]. Tumor cells alter host hematopoiesis resulting in production of immature dendritic cells which lack antigen presenting function [128]. This prevents activation of cytotoxic T and B lymphocyte as well as natural killer (NK) cells, resulting in immunosuppression. Also, these altered immune cells abnormally express proteolytic enzymes which modify the ECM matrix and release mitogenic agents to promote tumor growth and invasiveness [129].

Monocytes and macrophages also block apoptotic signals in metastatic cancer cells when they are detached from basement membranes during invasion. For instance, TAMs support anchorage independent survival of metastatic breast cancer cells. The vascular cell adhesion molecule-1 (VCAM-1) present on breast cancer cells binds to the $\alpha 4$ integrin of TAMs. This $\alpha 4$ -integrin/VCAM-1 interaction activates PI3K-AKT signaling and induces anchorage dependent survival in these cells [130].

The different cell types in TME interact not just with the cancer cells but also with each other to promote neoplastic growth. Endothelial cells express a variety of leukocyte adhesion molecules to induce leukocyte recruitment by while IICs produce a diverse assortment of soluble factors such as VEGF, bFGF, TNF- α , TGF- β , platelet-derived growth factor (PDGF), placental growth factor (PIGF), chemokines CXCL12, IL-8/CXCL8, matrix metalloproteinases (MMP-2, -7, -9, -12, and -14) all of which influence endothelial cell survival, proliferation culminating in new blood vessel formation[131]. TAMs also provide resistance against anti-VEGF-A/VEGFR therapies by blocking colony stimulating factor-1 (CSF-1) signaling [132].

1.9.3 Normal Epithelial Cells

Normal epithelial cells adjacent to the tumor tissues react and respond to the repertoire of factors secreted by the cancer cells. These responses may manifest as changes in their transcriptome, proteome, expression of cell surface markers and dysregulation of signaling pathways. Depending on how epithelial cells encounter the adjacent cancer cells, they can resist or promote tumor growth.

Pistone *et al.* demonstrated that conditioned media (CM) collected from human breast tumor tissue explants increased proliferation, migration and MMP-9 expression and reduced cell adhesion and in both non-transformed mammary epithelial cells

(MCF10A) and breast cancer cells (MCF-7 & IBH-7) suggesting tumor tissues secrete soluble factors that can modify microenvironment and promote growth of both normal and tumor tissue [133]. However, Spink et al., demonstrated that MCF-10A breast epithelial cells inhibited the proliferation of MCF-7 breast cancer cells in the MCF-10A/MCF-7-GFP co-culture system [134, 135]. Also EGF and 17beta-estradiol, which stimulate MCF-7 cell proliferation in monocultures did not have any effect in the co-culture system. These results indicate that in the early stages of breast carcinogenesis the normal epithelial cells may have a protective role by inhibiting tumor proliferation [134].

Cancer cells also induce secretion of hyaluronan (HA) in normal epithelial cells [134]. Elevated HA levels disturb the normal cell-cell adhesions and cell-ECM interactions in the epithelial tissue, resulting in disruption of the epithelial barrier. These morphological aberrations ultimately lead to spindle defects, epithelial deregulation, and pre-neoplastic changes in the epithelial tissues.

Interleukin 15 (IL-15) is another soluble factor, produced by several cancer cells, which interacts with several different components of the TME. IL-15 secretion by colon cancer cells is linked to depletion of TAMs [136]. It is also associated with activation of wnt signaling in normal epithelial cells [137]. IL-15 can induce src activity in both cancer and adjacent normal cells. Activated src phosphorylates inducible nitric oxide synthase (iNOS), an enzyme implicated in inflammation and cell mediated immunity. Src mediated phosphorylation of iNOS increases its half-life and thus increases its stability in both normal cells and cancer cells [138].

Soluble factors such as vascular endothelial growth factor (VEGF) and tumor necrosis factor (TNF) produced in the TME can act distantly in secondary organs,

promoting the formation of the premetastatic niche [139, 140]. sE-cad in the TME may also function as a long-range signaling molecule. Elevated circulating levels of sE-cad in the sera might prepare metastatic sites for tumor cells by disrupting epithelial junctions thereby creating a more conducive ‘soil’ for tumor growth. In the tumor niche, elevated sE-cad could also alter the structure and behavior of normal epithelial cells in the TME. The role of sE-cad in remodeling the ECM by induction of MMPs, and in inducing EMT-like changes in the normal epithelial cells is not known.

1.10 Epithelial to mesenchymal Transition (EMT)

In cancer metastasis tumor cells must first detach from the primary tumor site, then invade into a distant secondary sites, and finally proliferate at the secondary sites [141]. A process critical for metastasis is epithelial to mesenchymal transition (EMT), whereby tumor cells downregulate their epithelial features and gain mesenchymal properties (Figure 1.7). Some of the epithelial markers downregulated during EMT are E-cadherin, cytokeratin, mucin 1, ZO-1 and desmoplakin. Downregulation of these epithelial proteins causes a loss of cell polarity and dissolution of epithelial junctions. Some of the mesenchymal proteins that are expressed during this transition are Fibronectin, vimentin filaments, and the non-epithelial N-cadherin. These proteins aid in mesenchymal cell migration and cytoskeletal remodeling [142]. Induction of EMT thus not only modifies adhesive capabilities of tumor cells but also make them more motile and invasive by dramatic reorganization of their actin cytoskeleton [142].

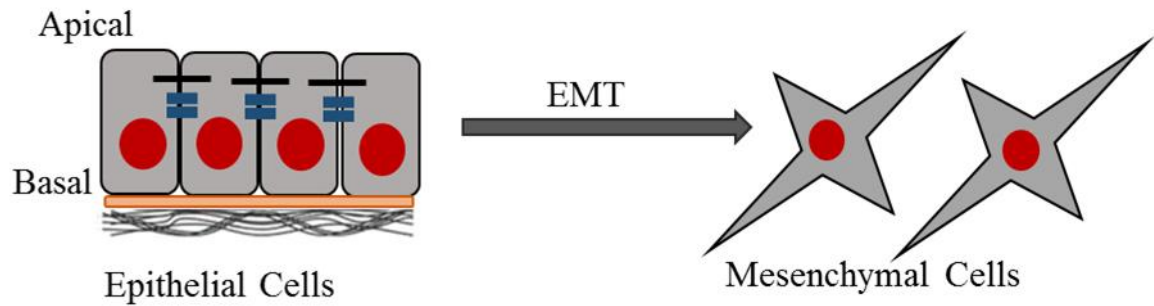


Figure 1.7: Schematic of cells undergoing EMT

(Adapted from Xu J, Lamouille S, Derynck R. (2009). "TGF-beta induced epithelial to mesenchymal transition." *Cell Res.* (2009) 19(2): 156-72.

There are several mechanisms that induce EMT. Several major signaling pathways during development such the TGF- β , Wnt, Notch, and Ras kinase signaling cascades have all been implicated in the induction of EMT [141, 142]. The TGF- β pathway is the major pathway activated during induction of EMT. In the TME, TGF- β is produced by the stromal cells and they induce expression of transcription factors Snail1/2, ZEB1/2 and Twist which repress E-cadherin transcription [125, 143]. Other oncogenic pathways such Src, EGFR, NF- κ B, ETS, integrin are also known to induce EMT[144]. Recent studies have implicated the PI3K/AKT pathway in the induction of EMT in cancer.

The extracellular cues from the TME also play a critical role in induction of EMT in tumor cells. Components of the tumor microenvironment such as cancer associated fibroblasts (CAF), macrophages, inflammatory cytokines, growth factors and hypoxia all contribute to induction of EMT. These factors promote EMT by induction of transcriptional activator ZEB1, TWIST and SNAIL1/2 [141]. Elevated MMP-9 in the TME is also associated with induction of EMT in lung cancer.

Transitioning to the mesenchymal state confers a lot of advantages to tumor cells such as stemness, protection from cell death, immune evasion and resistance to conventional and targeted therapies and therefore EMT is a central process in epithelial cancers.

1.11 2D vs 3D culture System

Most studies used to evaluate the cellular interactions and signaling transduction pathways involved in cell function are performed in two-dimensional (2D) cultures in petri dishes or plates. In 2D cultures, cells adhere to an artificial plastic or glass surface and grow in monolayers that come in contact with other cells only at their periphery. They do not exhibit cell polarity or a structured cell organization as seen *in vivo*. Physiological processes that involve transportation and gradient of soluble factors, oxygen, nutrients and wastes removal, or communication between different types of cells cannot be easily studied in these 2D culture systems.

Three-dimensional (3D) culture systems address some of the limitations of the conventional 2D culture system and are more closely related to *in vivo* systems. Epithelial cells grown in an ECM matrix display apical-basal polarity with a hollow central lumen resembling the epithelial morphology *in vivo* [145]. Due to these changes in cell shape and organization, cells in 3D show difference in behavior such as changes in protein expression, differentiation and function. Unlike on flat monolayers where all cells proliferate at the same rate, growing epithelial cells in 3D culture system exhibit zones of proliferation where cells on the periphery divide more rapidly in comparison to the inner zones which are more quiescent and necrotic zones [146]. These properties make 3D cultures a more relevant system to study changes in epithelial cell morphology and polarity. Furthermore, in the 2D culture system cells only adhere to one flat surface

where as in the 3D culture system the cells adhere to the ECM matrix, have greater intercellular communication and are influenced by extracellular environment and the factors secreted into this environment. Figure 1.8 depicts MDCK cells grown on plastic dish and on matrigel 3D culture system.

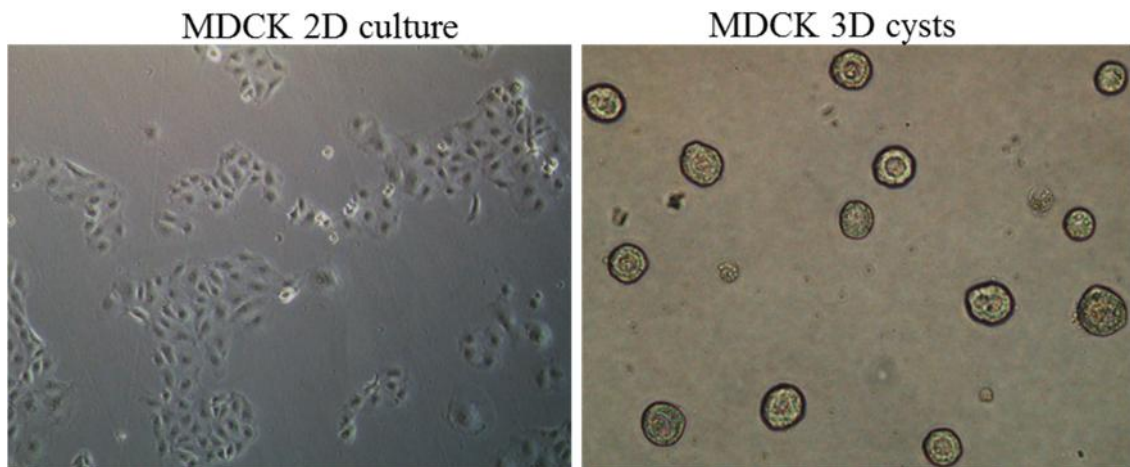


Figure 1.8: Cells in 2D monolayer vs. in 3D culture system.

3D culture system can also be utilized to distinguish between the epithelial cells and some of the carcinoma cell lines. Epithelial cells in 3D culture systems undergo controlled proliferation and differentiation in response to the extracellular microenvironment to form well-organized spherical acinar-like structures with a hollow lumen (Figure 1.8). Cancer cells on the other hand do not respond to cues from the ECM matrix and continue to divide uncontrollably to form spheroids with no lumen [147]. Filling up of the lumen and loss of apico-basal polarity is a salient feature of early epithelial carcinogenesis and the 3D culture system is an ideal system to investigate the signaling changes occurring during these early pre-neoplastic phase [145].

Cancer cells in 3D culture systems with normal connective tissue and epithelial cells mimic the TME. 3D co-culture systems are valuable for investigating the interaction between tumor cells and the other cells in the TME and have a very divergent gene expression pattern which is more faithful representation of the cancer tissue.

Additionally, it is a more relevant system to evaluate chemotherapeutics and investigate drug resistance because unlike in monolayers, there is a gradient of drug penetration in 3D tumor spheroids with reduced drug accessibility in the 3D inner core (Figure 5). Thus 3D tumor spheroids as well as epithelial 3D cultures are more representative system to investigate cell-cell and cell-paracrine interactions.

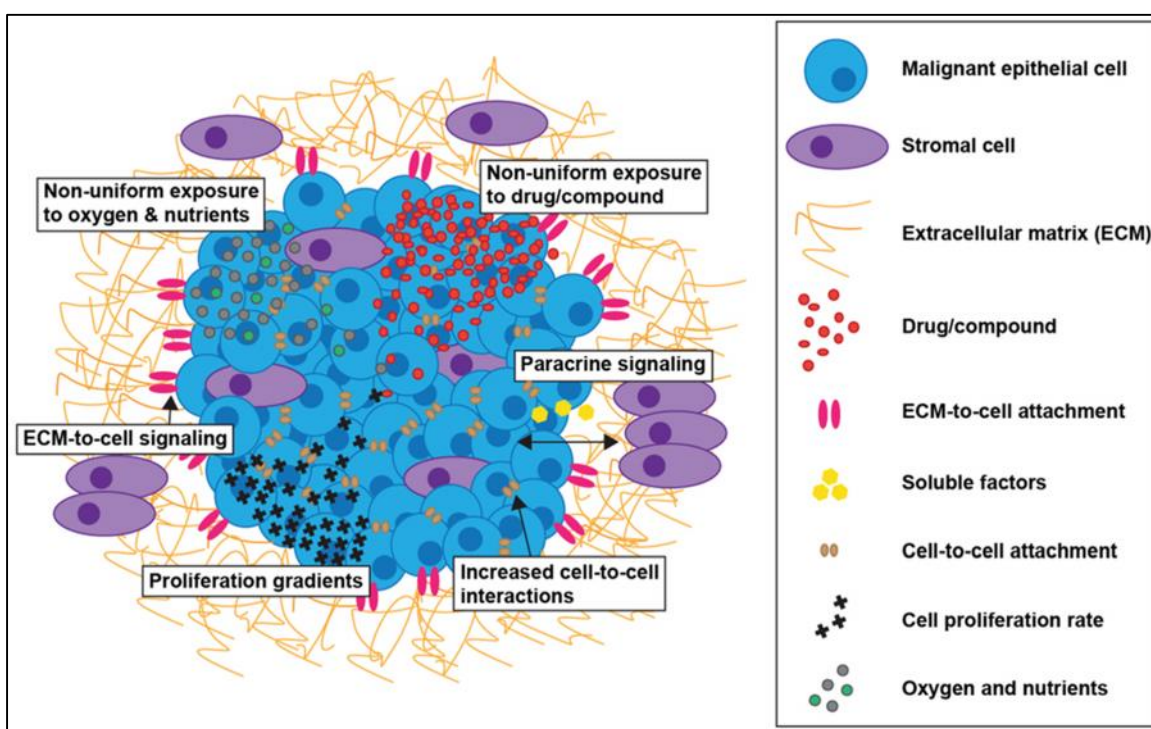


Figure 1.9: Pictorial representation of cancer cells in 3D culture system

(Figure reprinted from open access journal Lovitt CJ, Shelper TB, Avery VM (2014). "Advanced Cell Culture Techniques for Cancer Drug Discovery." *Biology*. 3(2), 345-367.

In this work, we utilize a 3D co-culture system to assay the impact of tumor cells on adjacent normal epithelial cells and investigate EMT pathways on 3D culture system. Chapter 2 focusses on the impact of carcinoma cells on the adjacent normal epithelial cysts, more specifically how sE-cad generated by normal epithelial cysts alter the epithelial cyst morphology. In chapter 3 we examined the impact of long term (96 hr) treatment with CM or sE-cad on MDCK cysts which are lumen filled. Chapter 4 addresses the major oncogenic signaling activated by sE-cad and involved in lumen filling and EMT.

Chapter 2

SOLUBLE E-CADHERIN GENERATED BY CARCINOMA CELLS INDUCE LUMEN FILLING IN NORMAL EPITHELIAL CELLS

2.1 Introduction

Bidirectional communication between tumor cells and the microenvironment plays a crucial role in driving tumor progression. The tumor microenvironment (TME) consists of heterogeneous population of cells that includes stromal cells, adjacent normal cells, fibroblasts, and immune cells, and components of the extracellular matrix (ECM). Transformed tumor cells are capable of initiating crucial changes in the different components of the TME, such as the ECM, fibroblasts, and inflammatory cells, so that they can acquire invasiveness and metastatic properties [123]. During the initial stages of carcinogenesis the surrounding normal epithelial cells and other microenvironment components are anti-tumorigenic as they block proliferation and survival of transformed cells [148-150]. However, once tumor cells multiply and override this self-defense mechanism they modify and modify the non-transformed cell types so that they participate in the process of tumorigenesis[151]. For instance, normal prostate epithelial cells can induce intraepithelial neoplasia in mice when co-injected with carcinoma associated fibroblasts (CAFs) but not when co-injected with normal fibroblasts suggesting that the CAFs have been altered by the tumor cells [152]. Similarly CAFs from breast cancer, induce EMT and enhance metastatic potential of both premalignant and malignant breast epithelial cells, unlike normal fibroblasts which suppress metastasis [153]. While some aspects of the TME such as ECM remodeling

and tumor angiogenesis are well studied, the interaction between tumor cells and the adjacent epithelium is poorly understood.

Epithelial cells form well ordered, multiple layered sheets such as the skin that serve as an external barrier. They also line internal organs and form tubular networks in the major organs such as lung, kidney, liver, pancreas, salivary glands, mammary glands and the reproductive passage [8]. Epithelial cells in these glandular organs are organized in tubules and cyst-like spheroids. These epithelial cysts, which are regarded as the building blocks of glandular organs, are characterized by a hollow lumen and have apico-basal polarity. An intact, hollow lumen is formed by selective apoptosis of centrally located cells [154] [155]. Lumen formation is critical for the well-ordered morphology and proper control and functioning of these organs. However, abnormal pathophysiological conditions can cause lesions in the lumen, resulting in multiple lumen formation and, finally, filling of the luminal space by cells. Filling up of the lumen is a salient feature of early, pre-invasive stages of epithelial cancers [156]. Several carcinomas such as breast, kidney, prostate and others display lumen filling and architectural disorder during their early stages, before they invade the basement membrane and disseminate into surrounding tissues (Figure 2.1) [154]. The molecular mechanisms that occur during the initial lumen filling stage of tumorigenesis are poorly understood.

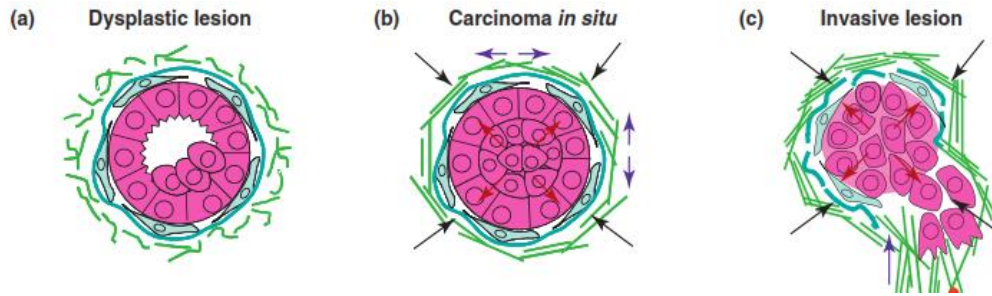


Figure 2.1: Lumen filling with progressive stages of epithelial cancers

Figure reprinted from open access journal, Yu, H., J.K. Mouw, and V.M. Weaver, Forcing form and function: biomechanical regulation of tumor evolution. *Trends Cell Biol*, 2011. 21(1): p. 47-56. Normal breast tissues consists of ducts and lobules with hollow lumen. The tumor cells infiltrate the surrounding fibrous and adipose tissue in invasive carcinomas once the epithelial tissue lumen is completely filled with cells.

Epithelial cells, when grown in a gel of extracellular matrix (ECM), such as collagen I or Matrigel (an extract of the ECM produced by Englebreth–Holm–Swarm tumors), form three-dimensional (3D) structures referred to as cysts which are more ‘*in-vivo-like*’ as they can recapitulate the essential features of the *in vivo* glandular epithelium. These 3D culture systems have helped in identifying factors and regulatory molecules crucial for formation and maintenance of luminal space and apicobasal polarity. 3D culture systems can be utilized to distinguish between normal epithelial cells and transformed tumorigenic cells, as formation of a hollow lumen is characteristic of normal epithelial cells. Carcinoma cells on the other hand develop into unpolarized clusters. In this study, we propose to utilize luminal filling and disruption of the epithelial architecture in 3D cultures as a hallmark of preneoplastic growth.

A key event observed during epithelial derived cancers is the down regulation of E-cadherin, a Ca^{2+} -dependent cell adhesion molecule located in the adherens junction and along the basolateral surface of epithelial cells [2] [157]. One mechanism by which

tumor cells downregulate E-cadherin is by the proteolytic cleavage of its extracellular domain. Several proteases present in the extracellular environment, such as matrix metalloproteinases (MMP-3, MMP-7, MMP-9 and MT1-MMP), ADAM10, ADAM15, plasmin, and kallikrein 7 can cleave the ectodomain region of the membrane-bound E-cadherin to generate an 80 kDa fragment referred to as soluble E-cadherin (sE-cad) [82, 83]. This post translational processing of E-cadherin via ectodomain shedding plays an important role in carcinogenesis.

Matrix metalloproteinase (MMP)-9 levels are elevated in several different cancers, and the enzyme plays a central role in tumor cell initiation/progression, metastatic ability and genetic instability[158]. It is also implicated in shedding of E-cadherin in ovarian, head and neck, and prostate cancer cell lines[68]. MMP-9 is a 92 kDa endopeptidase which cleaves E-cadherin between amino acids Leucine 581 and Serine 582 to generate a 581 aa long soluble E-cadherin fragment. Additional substrates of MMP-9 include Insulin like growth factor -binding protein (IGF-BP), Heparin binding (HB)-EGF and a variety of basement membrane and extracellular matrix components such as collagens type IV,V,1X ,elastin, proteoglycan and gelatin [158-160].

Significantly elevated sE-cad levels have been observed in the sera and urine of cancer patients diagnosed with a variety of cancers. Increased circulating levels of sE-cad are indicative of histopathological grade, metastasis recurrence and poor prognosis [82, 161, 162]. A significant body of research designed to determine the pathophysiological effects of sE-cad has demonstrated its tumor-promoting effects in enhancing tumor cell proliferation, migration and invasion, and activation of various oncogenic signaling pathways. sE-cad promotes cell motility and invasion *in vitro*[110].

Exogenously added recombinant sE-cad destabilizes adherens junctions and enhances tumor cell proliferation, migration and invasion [108, 109]. The extracellular domain of E-cadherin can interact with and activate the epidermal growth factor receptor (EGFR) [116]. The shedding of E-cad converts it into a soluble growth factor and an antiapoptotic molecule. In the MCF-7 breast cancer cell line, sE-cad was shown to complex with HER2 and HER3 receptors and activate downstream signaling, thereby promoting migration and invasion [117]. In our laboratory, we demonstrated that sE-cad acts as a survival factor and prevents apoptosis [115]. Recombinant purified sE-cad inhibited apoptosis of normal Madin-Darby canine kidney (MDCK) cells subjected to serum starvation, via activation of HER1, PI3K, AKT and ERK1/2 signaling pathways [115]. sE-cad also upregulates expression of key MMPs (MMP-2, MMP-7, and MMP-9) via EGFR activation [111]. In human skin squamous carcinoma tissues, a decrease in full-length E-cadherin expression correlated with increasing sE-cad levels. sE-cad also contributes to skin carcinogenesis via association with HER1, HER2 and insulin-like growth factor-1 receptor (IGF-1R) in human skin squamous cancer tissues [119]. The same group recently provided *in vivo* and *in vitro* proof of concept of the role of sE-cad in tumorigenesis by targeting sE-cad using a monoclonal antibody against the ectodomain of E-cadherin (Decma-1) in breast carcinomas. Decma-1 suppressed tumor growth and showed potent anticancer activity by downregulating the HER family members and components of the MAPK-PI3K/AKT/mTOR pathways [118]. All these studies on sE-cad have validated it as an oncogenic target. However, whether elevated sE-cad levels also impact normal epithelial cells and dysregulate cell signaling events in them is yet to be elucidated.

This study aims to investigate two questions: How do tumor cells interact and alter the normal epithelial cells and does elevated sE-cad levels in the microenvironment impact normal epithelial cells. We use a three-dimensional (3D) cell-culture system comprising non-transformed Madin-Darby canine kidney (MDCK) epithelial cells and invasive cancer cells (MSV-MDCK) to determine the impact of tumor cells on normal epithelial cells. MDCK cells, when grown on MatrigelTM, a reconstituted basement membrane matrix derived from Englebreth–Holm–Swarm tumors, formed spherical polarized cysts consisting of a hollow lumen lined by cells reflecting the *in vivo* epithelial organization. In this study, we propose to utilize luminal filling and disruption of the epithelial architecture in 3D epithelial cysts as a marker of preneoplastic growth.

2.2 Materials and methods

2.2.1 Cell lines

Madin-Darby canine kidney cells (MDCK) purchased from American Type Culture Collection (Manassas, VA) were maintained in DMEM with 1 g/L sodium bicarbonate, 10% fetal bovine serum, 1 mM L-glutamine, 100 U/ml penicillin, and 100 µg/ml streptomycin. The Moloney Sarcoma virus-transformed MDCK cell line (MSV-MDCK) has been described previously [163]. Cell lines expressing GFP and RFP were generated by transfection. MDCK epithelial cells stably expressing RFP-actin were used for live microscopy experiments. MDCK-RFP cells were kind gift from Dr. Anne Muesch, Albert Einstein Medical College, NY. MSV-MDCK cells expressing GFP were generated in the laboratory [164].

2.2.2 Antibodies and Reagents

Primary antibodies used in this study for immunoblotting and immunostaining were as follows: E-cadherin antibody Decma-1 (U2354, Sigma-Aldrich), MMP-9 (sc-6840, Santa Cruz Biotechnology). The mouse, rabbit and rat horseradish peroxidase-conjugated secondary antibodies were obtained from Cell Signaling Technology. Anti-Mouse Alexa Fluor-488, Anti-Rabbit Alexa 633, Alexa-Fluor-546-conjugated phalloidin and TOPRO-3 were purchased from Molecular Probes (Eugene, OR). Growth factor-reduced MatrigelTM (BD-Biosciences) was used for three-dimensional culture. Protein-free, serum-free UltraDOMATM media (Lonza) was used for conditioned medium experiments. BD cell recovery solution (BD# 354253) was used to harvest 3D cultures from the MatrigelTM matrix. 1 μ M MMP-9 Inhibitor I (EMD Millipore Chemicals, CAS117749-58-4), and the broad spectrum MMP inhibitor Marimastat (Tocris Biosciences) were used wherever indicated.

2.2.3 Three-dimensional (3-D) Matrigel cultures

MDCK 3D cultures were grown and maintained in MatrigelTM as previously described [165, 166]. Briefly, MDCK cells were trypsinized and suspended at a final concentration of 15,000 cells/ml in 2% growth factor-reduced MatrigelTM (BD Biosciences, Bedford, MA). The cell/ MatrigelTM mixture (4,500 cells per well per 300 μ l) was layered onto MatrigelTM-coated chambers, 3.5 μ L/well, (LAB-TEK II Chambered Coverglass, Nalgene Nunc International) and allowed to culture at 37°C, 5% CO₂ and 95% humidity. Cells were monitored daily for acini formation. Media was replenished every 2 days. MDCK acini grow in about 72-96 hr (Figure 2.3). For sE-cad experiments, acini were cultured with 10 μ g/ml of recombinant purified sE-cad in serum-free medium for the indicated time points. Experiments requiring MSV-MDCK

co-culture, MSV-MDCK cells (3,000 cells per 200 μ l) were overlaid onto acini on day 3 of culture and monitored at indicated time points. Conditioned Media (CM) is obtained from growth media from a 48-hour culture of MSV-MDCK cells collected and spun down to remove floating cells and other debris.

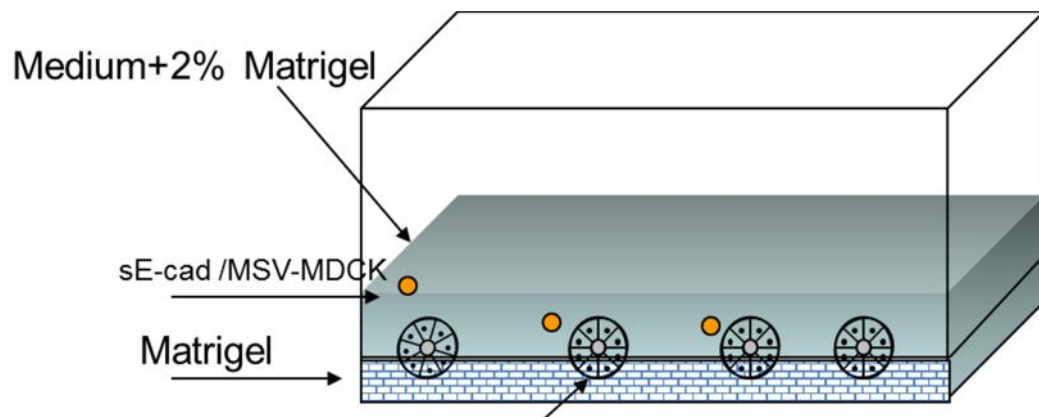


Figure 2.3: Experimental Model showing 3-D culture system

2.2.4 Immunofluorescence of 3-D Matrigel cultures

Cells grown in MatrigelTM were prepared and immunostained as follows: 3D MDCK cultures were fixed with 4% paraformaldehyde for 15 minutes at room temperature, washed three times with phosphate-buffered saline (PBS), then permeabilized and blocked with PBS, 0.7% fish skin gelatin and 10% saponin (PFS) for 30 minutes at room temperature. The fixed and permeabilized acini were stained for the following antibodies: β -catenin, actin, and phospho EGFR, Ki67, Bcl2, N-cadherin and Fibronectin by incubating the antibodies at 1:400 dilution in PFS overnight at 4°C. Staining was detected using Alexa-488, 546- and 633-conjugated secondary antibodies

at 1:400 dilution in PFS and added to cultures for 2 hours at room temperature. TOPRO-3 at 1:1000 dilution was used to stain nuclei. Cells and acini were then washed with PBS three times. For immunofluorescence with MDCK cells grown on filter. Recombinant myc-tagged sE-cad is added to the MDCK cells grown on filters as a polarized monolayer and incubated for 2hr and 4hr to allow binding. Following binding the monolayer is washed and the filters are cut for immunofluorescence processing. An anti-myc antibody is used to label sE-cad and anti β -catenin antibody is used to stain the basolateral membrane. Confocal microscope vertical sections are utilized to visualize both sE-cad and β -catenin co-localization.

2.2.5 Confocal microscopy and quantitation of 3D cysts

Images were captured using a *Leica* TCS SP5 scanning confocal microscope (Leica Microsystems Inc., Buffalo Grove, IL) using a 63X oil objective lens. The cysts were assessed for the presence of cells within the lumen. The number of cysts with clear or filled lumens were counted across at least ten different fields and expressed as a percentage of total number of cysts. All images were captured using the same laser intensity and gain/offset settings.

2.2.6 Generating 3D cell lysates and conditioned media from 3D cultures

3D cyst protein lysates were prepared by recovering cultured cells from the Matrigel™ basement matrix using a cell recovery solution (Corning Life Sciences Product#354253) following the manufacturer's instructions. The harvested cysts were then lysed as described previously [167]. Briefly, chilled RIPA buffer (50 mM Tris-HCl pH 7.4, 1% NP-40, 0.5 % Na-deoxycholate, 0.1% SDS, 150 mM NaCl, 2mM EDTA) supplemented with 1x protease inhibitor cocktail and 1% phenylmethylsulfonyl fluoride

was added to the harvested cyst pellet. The cells in RIPA buffer were incubated on ice for 15 minutes followed by sonication for 15 minutes at 4°C. Lysates were cleared by centrifugation at 14,000 rpm for 15 minutes at 4°C. Supernatants were collected and the protein concentration was measured using Bio-Rad DC reagent (Bio-Rad Hercules, CA) as per manufacturer's instructions. For detection of proteins (shed sE-cad and MMP-9) in the CM, the cysts were grown in UltraDOMA-PF to prevent interference from albumin and other serum proteins present in the complete media. CM was collected and concentrated using Amicon ultracentrifugation filter devices (EMD, Millipore). Equal amounts of concentrated media were then loaded onto SDS-polyacrylamide gels and analyzed by immunoblotting or gelatin zymography.

2.2.7 Protein Estimation using Bio-Rad DC Protein Assay

The DC protein assay is a colorimetric assay based on the principle of Lowry protein estimation. The assay was performed following manufacturer's instructions provided in the kit. The working reagent A' was prepared by adding 20µl of reagent S to 1ml of reagent A. BSA standards were prepared ranging from 1mg/ml to 10 mg/ml. 10µl of the BSA standards and the protein samples was pipetted in triplicates into each well of the microtitre plate. 25 µl of the reagent A' was added to each of the well. Then 200 µl of reagent B is added to all the wells. The plate is mixed by orbital shaking in the Victor X4 multilabel plate reader and incubated in dark for 15 min before reading the absorbance at 750nm. The protein concentration was calculated using the equation of the slope of the standard curve of BSA.

2.2.8 Immunoblot analysis

SDS-containing polyacrylamide gel electrophoresis (SDS-PAGE) was carried out to separate proteins in 3D cyst lysates. Separated proteins were transferred from the gel to a nitrocellulose membrane. For immunoblotting, the membranes were blocked in 5% non-fat milk in TBS/0.1% Tween 20 (TBS-T), following which, the membranes were probed with different primary antibodies at a dilution of 1:1000 and incubated overnight at 4°C. The membranes were further probed with HRP-conjugated anti-rabbit, -mouse and -rat secondary antibodies diluted 1:2000 in 5% non-fat milk/TBS-T and incubated for 1 hour at room temperature. Antibody binding was visualized by Enhanced Chemiluminescence (ECL) and ECL prime (GE Biosciences). The blots were soaked in the ECL solution and sealed. They were then exposed to X-ray film for various incubation times in the developing room and passed through the film developer.

2.2.9 Gelatin Zymography

The gelatinolytic activity of CM was visualized by gelatin zymography. Control MDCK cysts, cysts challenged with MSV-MDCK cells and with different treatments were incubated in protein-free, serum-free UltraDOMA for 24-48 hr. CM from the different cultures was centrifuged at 1000 rpm for 5 minutes to remove cell debris, and concentrated by centrifugation using Centricon-30 microconcentrators (Amicon Inc. Beverly, MA). Equal volumes of the samples were used for gelatin zymography, which was performed as described previously, with modifications [168]. Samples were mixed with zymogram sample buffer (BioRad) and loaded onto 8% SDS-polyacrylamide gels containing 0.1% gelatin. The gels were run in zymogram running buffer without SDS, and then incubated in 1x zymogram renaturation solution (BioRad) for 30 minutes at room temperature, followed by overnight incubation at room

temperature in the zymogram development solution (BioRad). The gels were stained with Coomassie Brilliant Blue R250 for 2 hours at room temperature, and destained until the gelatinolytic activities were detected as clear bands against the blue background.

2.2.10 Transwell Co-culture Assay

MDCK cysts were grown on 0.4 μm pore size Transwell (TW) filters (Corning Life Sciences, Lowell, MA) and cultured in a 6-well plate for 3 days. MSV-MDCK carcinoma cells were seeded at increasing densities ranging from 3000-20000 cells per well on a separate 6-well plate. Fully formed MDCK cysts (96 hours) on TW filters were then transferred onto the MSV-MDCK cells. Gradient co-cultures in the presence and absence of MMP-9 inhibitor were maintained for 48 hours. Conditioned medium from the lower (basolateral side) and upper (apical side) chambers was used for analyzing MMP-9 and sE-cad levels. MMP-9 activity in the conditioned medium was analyzed using gelatin chromatography.

2.2.11 Purification of sE-cad

sE-cad was purified from the sE-cad overexpressing HEK-293T cells using Ni-NTA resin as described previously [115]. Briefly, sE-cad overexpressing HEK-293T cells were generated by stably expressing the pSEC-Tag2-SECAD vector into HEK-293T cells and stable clones were selected with Zeocin (Invitrogen). sE-cad-HEK-293T cells were grown in Ultra-DOMA-PF (Cambrex, Rutherford, NJ) media for 48h. 100 $\mu\text{g}/\text{ml}$ of Zeocin antibiotic was added to induce sE-cad expression into the extracellular media. The media was collected and centrifuged to remove cells and debris. The cell free growth media from 48 h was mixed with Ni-NTA resin overnight in a spinner flask to

allow the His-tag sE-cad to binds to the Ni-NTA resin. Resin was then loaded into a column. The resin was washed with 2x column volumes of phosphate buffer (160 mM phosphate, 4 M NaCl, 5 mM Imidazole, pH 7.4), and 5x column volumes of phosphate buffer containing 10 mM Imidazole to remove any nonspecific protein. sE-cad was eluted with 5x column volumes of phosphate buffer containing 250 mM Imidazole. Fractions (1 ml) were collected and the purity of each fraction was determined by SDS-PAGE. sE-cad containing fractions were pooled, concentrated using centriplus centrifuge filters (Millipore) and dialyzed against sterile PBS at 4 °C. Concentration of the purified sE-cad was determined using a Bio-Rad protein DC kit (Hercules, CA). The purified, concentrated sE-cad was aliquoted and stored at -80°C until further use.

2.2.12 Immunodepletion Assay

To deplete sE-cad from the co-culture CM, the CM was collected and cleared of cells by centrifugation. The CM was then incubated overnight with anti-E-cadherin antibody coupled to Protein A agarose beads. Depletion of sE-cad from CM was confirmed using SDS-PAGE of CM samples and the Protein A agarose beads .The sE-cad depleted CM was then added back to new MDCK cysts to determine its effect on lumen filling.

2.2.13 qRT-PCR analysis

Cells were harvested from Matrigel as described previously. RNA was then extracted from the 3D cyst lysate by Trizol and cDNA was generated by iScript™ cDNA Synthesis Kit (Bio-Rad) as per manufacturer's instructions. Quantitative PCR was performed using the SYBR Green PCR Master Mix (Applied Biosystems) in a 384 well plate on a 7900HT Fast Real-Time PCR system (Applied Biosystems). The

following primers were used: (a) MMP-9 (forward: GAGACTGGAGAGCTGGACAA, reverse: GCAAGTCT TCCGAGTAGTTT), (b) GAPDH (forward: GCTGTCCAACCACA TCTCCTC, reverse: TGGGGCCGAAGATC CTGTT). RNA levels were calculated by relative quantification (RQ) normalized to the endogenous control GAPDH. Samples were assayed in triplicates.

2.2.14 Reversibility Assay

To determine whether the lumen-filled cysts are permanently altered upon long-term treatment with sE-cad and CM, the cysts were harvested from the MatrigelTM matrix using the BD cell dissociation media as described above. The MatrigelTM-free cells were trypsinized and a cell suspension at a final concentration of 15,000 cells/ml in 2% growth factor reduced MatrigelTM was prepared. This cell/ MatrigelTM mixture (4,500 cells per well per 300 μ l) was layered onto MatrigelTM-coated Lab-Tek II chambers as described earlier. Cells were monitored daily for cyst formation, and the percentage of filled cysts was calculated in the control versus sE-cad- and CM-treated cysts.

2.3 Results

2.3.1 Co-culture of carcinoma cells with MDCK cysts disrupt luminal architecture

To investigate how invasive carcinoma cells influence adjacent normal epithelial cells, RFP- tagged-MDCK cysts (Red) were co-cultured with MSV-MDCK cells (Green). In 72 hours RFP- tagged-MDCK cells formed a polarized cyst with a hollow lumen. Co-culture with MSV-MDCK cells disrupted luminal architecture of MDCK cysts (Figure 2.4). At early time points, the cysts revealed multiple lumens (Figure 2.4

B and C) whereas at later time points the lumen was filled with cells (Figure 2.4 D). Quantification revealed that in co-culture 80% of the cysts showed filled lumen (Figure 2.4 G). MSV-MDCK cells made direct contact with MDCK cysts by extending filopodia-like structures (Figure 2.4 D arrow). Interestingly, when MDCK cysts were not in direct contact with MSV-MDCK cells they still showed filled lumen suggesting that some soluble component produced in co-culture is involved in the induction of lumen filling in MDCK cysts. Consistent with this hypothesis, conditioned medium collected from MSV-MDCK cells induced lumen filling in about 80% of MDCK cysts (Figure 2.4 E-F and H). These results indicate that carcinoma cells disrupt epithelial luminal architecture by secreting a soluble factor.

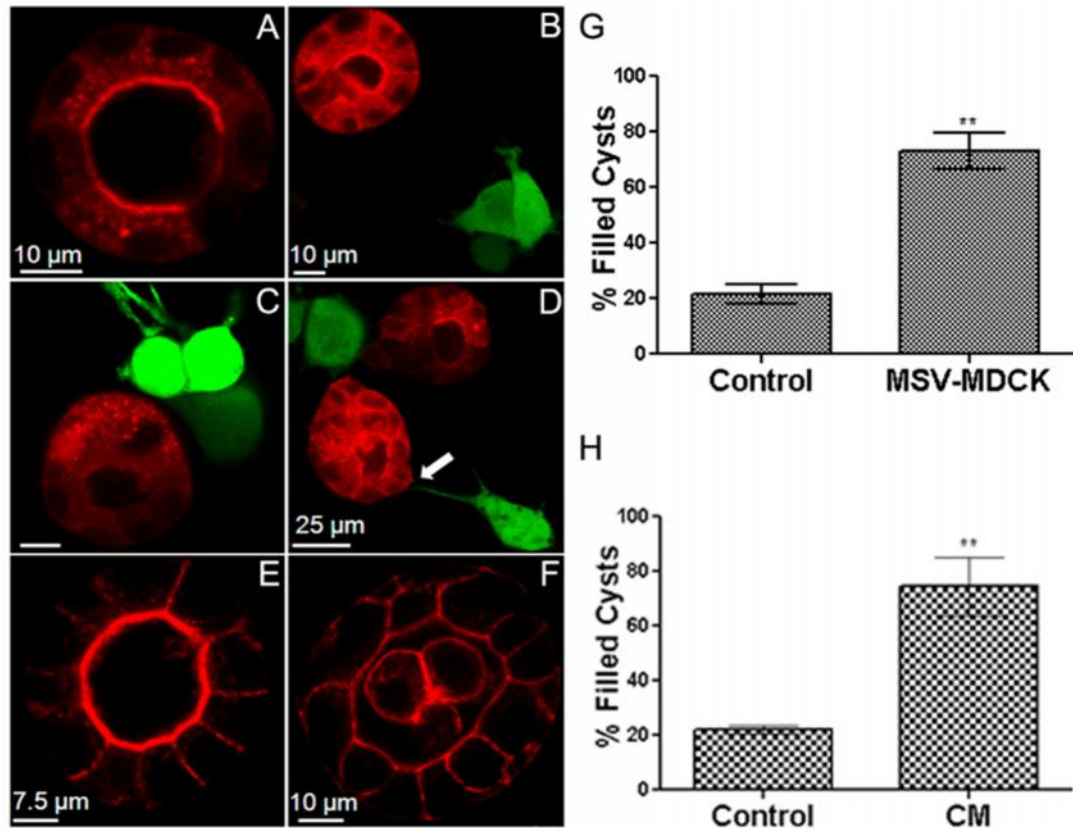


Figure 2.4: Co-culture of carcinoma cells with MDCK cysts disrupt luminal architecture.

MDCK-RFP cysts (red) were formed by culturing the cells for 72 h in Matrigel™ (A). MSV-MDCK-GFP cells (green) were then added in co-cultures and imaged after 4 h (B), 8 h (C) and 24 h (D). Control cysts were cultured alone for an additional 24 h (E). MDCK-RFP cysts were treated with conditioned medium (CM) from MSV-MDCK cells for 24 h (F). Lumen filled cysts in three independent experiments were counted and compared to controls after 24 h in the co-culture (G) and CM (H) experiments.

2.3.2 MMP-9 present in the conditioned medium is involved in lumen filling

MMP-9 secreted by invasive carcinoma cells has been shown to facilitate invasion by modification of the extracellular matrix [158]. Therefore, we sought to investigate the levels of MMPs in conditioned medium derived from co-culture. MDCK

cysts in co-culture showed a 3.7-fold increase in total MMP-9 levels compared to cysts grown alone (Figure 2.5 A). Quantification of active MMP-9 using gelatin zymography revealed a 2.3-fold increase in the co-culture conditioned medium. Addition of CAS-1177749, an MMP-9 inhibitor, significantly reduced the level of active MMP-9 (Figure 2.5 B) but the total MMP-9 protein level was not altered (Figure 2.5A). Pre-treatment of MSV-MDCK cells with MMP-9 inhibitor and subsequent co-culture with MDCK cells failed to induce lumen filling (Figure 2.5 C). Quantification of these results indicated that MMP-9 inhibitor treatment was effective in blocking lumen filling in about 70% of the cysts in co-culture (Figure 2.5 D). These results suggest that co-cultured MSV-MDCK cells produce high levels of active MMP-9, which is involved in inducing lumen filling in MDCK cysts.

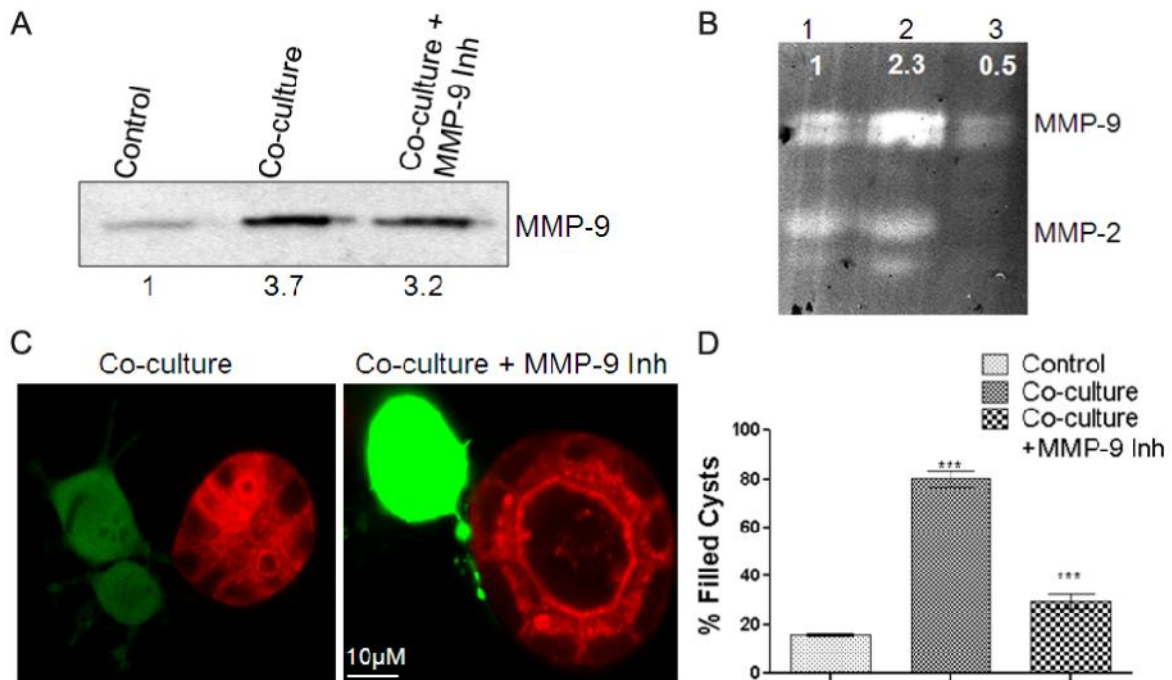


Figure 2.5: Conditioned medium from co-culture contains high levels of active MMP-9 which is crucial for lumen filling.

(A), Immunoblot showing MMP-9 levels in the supernatant from MDCK 3D cultures. (B), Zymogram showing MMP-9 activity Lane 1-MDCK control, 2-Co-culture 3-Co-culture + 10 μM MMP-9 inhibitor. (C), Immunofluorescence showing co-culture in presence and absence of 10 μM MMP-9 Inhibitor after 24hr treatment. Note –The absence of lumen filling with MMP-9 inhibition (Right panel). (D), Quantification of lumen filling in MDCK cysts in presence and absence of MMP-9 Inhibitor from average of three independent experiments.

2.3.3 MSV-MDCK cells induce shedding of sE-cad from MDCK cysts in MMP-9-dependent manner

MMP-9 cleaves the E-cadherin extracellular domain to produce a soluble fragment known as sE-cad [108]. MSV-MDCK cells express very little E-cadherin [169] and, therefore, sE-cad shedding from MSV-MDCK cells is unlikely. This led us

to hypothesize that under co-culture conditions, MMP-9 produced by MSV-MDCK cells cleaves cell surface E-cadherin from MDCK cells to generate sE-cad.

Two independent assays were used to demonstrate that sE-cad is produced from MDCK cells. First, MDCK cells were grown on transwell filters to form polarized monolayers with functional tight junctions ($TER > 250 \text{ ohms/cm}^2$). MSV-MDCK cells were co-cultured in the lower chamber, facing the basolateral side of the polarized MDCK monolayer (Figure 2.6A). Active MMP-9 and sE-cad levels in the media from apical and basolateral chambers were determined using gelatin zymography and immunoblot analyses, respectively. MMP-9 and sE-cad were not detected in the CM collected from the apical chamber. Analysis of the MMP-9 activity in the basolateral chamber by zymography revealed a 6-fold increase in the conditioned medium from co-culture compared to MDCK cells grown alone. There was a dose-dependent increase in MMP-9 levels with increasing number of MSV-MDCK cells in the bottom chamber. In the presence of the inhibitor the MMP-9 activity was substantially reduced (Figure 2.6 B). Immunoblot analysis revealed a 2-fold increase in the sE-cad levels from co-culture conditioned medium (Figure 2.6 B, bottom panel). We then evaluated sE-cad shedding using our 3D-culture system. In this assay, MSV-MDCK cells were co-cultured with MDCK cysts, and the levels of sE-cad in the conditioned medium was compared to MDCK cysts grown alone. There was a 1.9-fold increase in sE-cad levels in the conditioned medium of MDCK cysts challenged with MSV-MDCK cells compared to that of control. MMP-9 inhibition reduced the sE-cad levels by 75% (Figure 2.6 C). Taken together, these results demonstrate that MSV-MDCK cells induce MMP-9-mediated sE-cad shedding from the basolateral surface of MDCK cells.

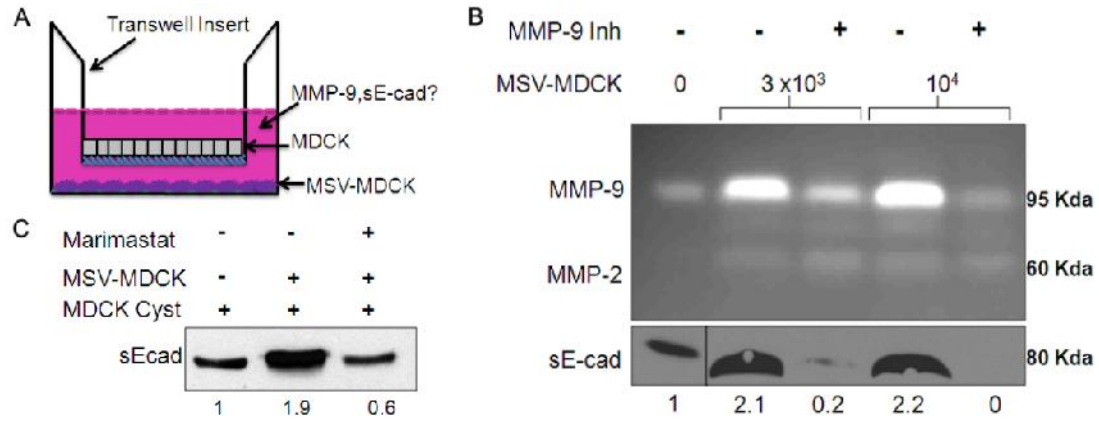


Figure 2.6: MSV-MDCK cells induce MMP-9 mediated shedding of sE-cad from MDCK cysts.

(A), Diagrammatic representation of transwell co-culture system. (B), Top Panel- Zymogram showing MMP-9 activity in the conditioned media from the bottom chamber of the transwell. Dose-dependent increase in MMP-9 levels with increasing number of MSV-MDCK cells in the bottom chamber was observed. 10 μ M of MMP-9 Inhibitor was used to block MMP-9 activity in the bottom chamber. Bottom Panel - Immunoblot showing sE-cad levels in the conditioned medium in the bottom chamber of the transwell. (C), Media from co-cultures as described in Figure 2 were examined for sE-cad. sE-cad levels were increased in the co-culture supernatant. Note: In the presence of MMP-9 inhibitor, sE-cad levels were reduced.

2.3.4 sE-cad is necessary and sufficient for inducing lumen filling in MDCK cysts

Lumen filling might be induced by multiple factors present in the CM. To determine whether sE-cad is exclusively involved and sufficient for lumen filling, two independent assays were performed. First, we tested the effect of purified sE-cad on lumen filling. MDCK-RFP tagged (red) cysts were used for this experiment to investigate the impact of sE-cad on live cells over a period of 24 hr. As shown in figure 2.7 A, 10 μ g/ml purified sE-cad exogenously added to MDCK cysts induced lumen filling and multiple lumen formation in MDCK cysts in a time dependent manner.

Quantification of these results indicated that sE-cad induced lumen filling in 80% of MDCK cysts in 24hr (Figure 2.7 B). At the initial time points (4 & 8 hr) sE-cad disrupted the luminal architecture and induced morphological changes. Cysts treated with sE-cad for longer than 24 hr were lumen filled and larger in size compared to the control cysts.

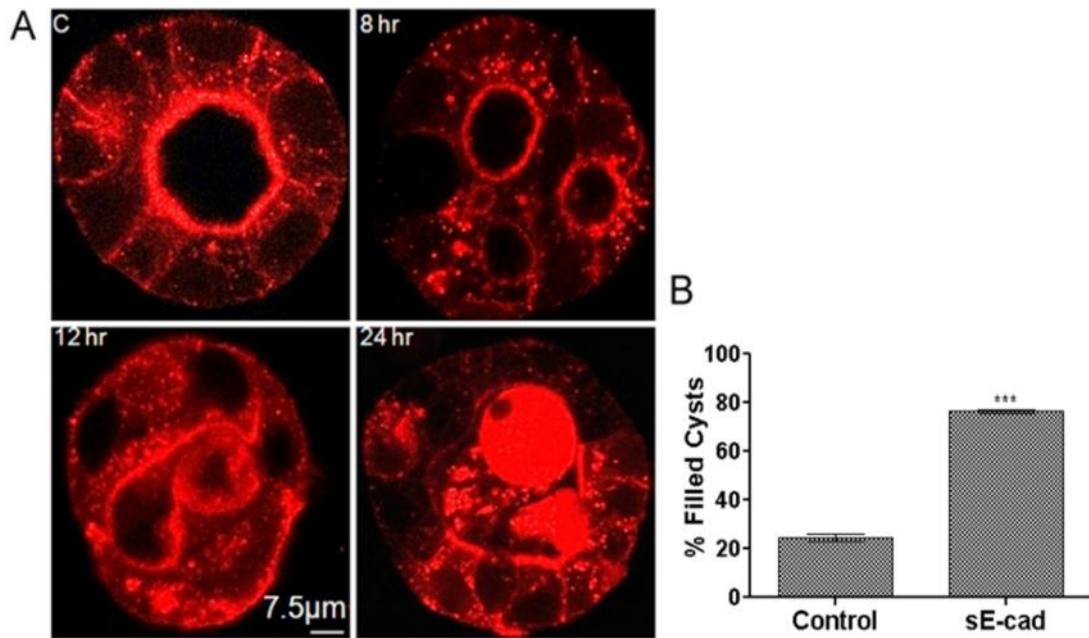


Figure 2.7: sE-cad induces lumen filling in MDCK cysts.

(A), Confocal images showing lumen filling and disrupted epithelial architecture induced by 10 µg/ml purified sE-cad over 24hr. (B), Quantification of lumen filling from 3 independent experiments.

Next, to demonstrate that sE-cad is exclusively involved in the induction of lumen filling, a sE-cad immunodepletion assay was utilized. In this assay, sE-cad was removed from the co-culture CM by immunoprecipitation using an antibody against the extracellular domain of E-cadherin. sE-cad depletion in the CM was confirmed by

immunoblotting (Fig. 2.8 A). sE-cad depleted CM failed to induce lumen filling in the MDCK cysts, whereas untreated CM induced lumen filling in 80% of the cysts (Fig. 2.8 B and C). These results demonstrate that sE-cad is necessary and sufficient for lumen filling in MDCK cysts. It also indicates that lumen filling induced by MSV-MDCK cells is sE-cad-mediated.

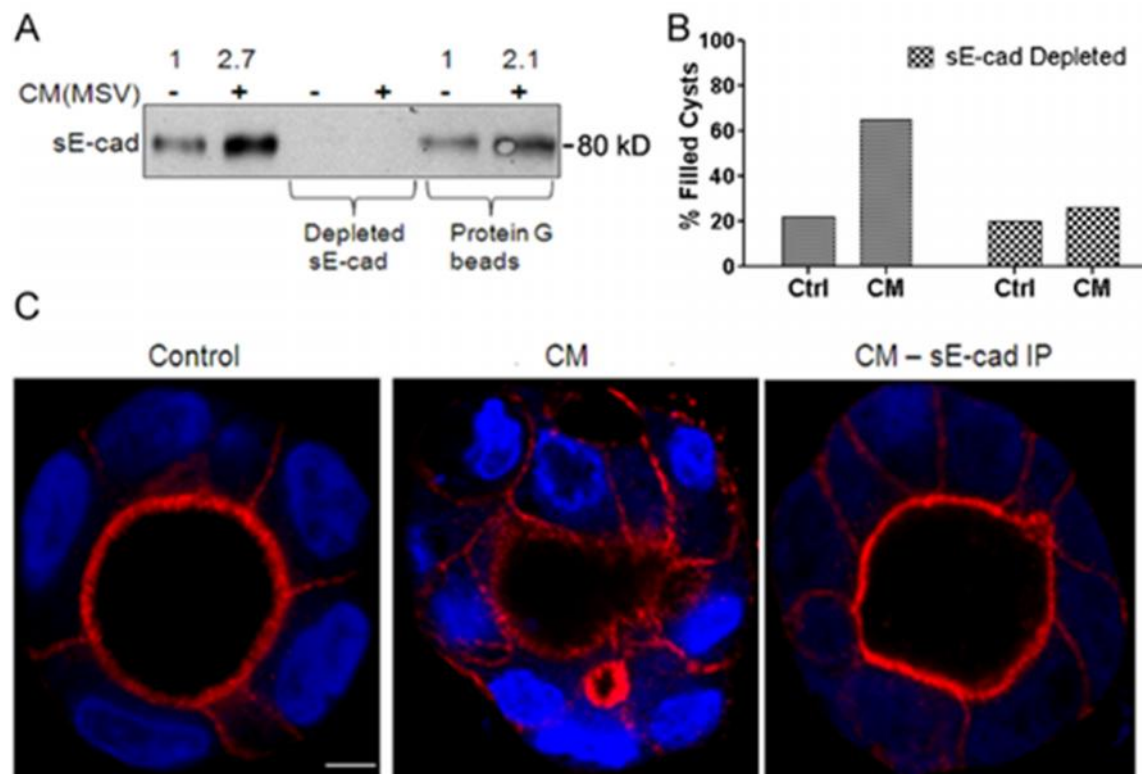


Figure 2.8: sE-cad is necessary for induction of lumen filling in MDCK cysts.

(A), Immunoblot showing sE-cad levels in the conditioned media before and after immunodepletion of sE-cad. Note: The immunodepleted sE-cad is bound to Protein G beads. (B), Quantification of lumen filled cysts in presence of CM and sE-cad depleted CM. (C), Representative confocal images of control cysts, CM treated cysts and cysts treated with sE-cad depleted CM. Cysts were stained for actin (red) and TOPRO-3 (nuclear marker, blue).

2.3.5 sE-cad increases MMP-9 levels

sE-cad is reported to upregulate the expression of MMP-2, MMP-9 and MT1-MMP in lung tumor cells[111]. To investigate whether sE-cad can induce upregulation of MMP-9 in epithelial MDCK cysts in 3D culture as well, MMP-9 levels were determined in sE-cad treated cysts. MDCK cysts showed increased MMP-9 expression with sE-cad treatment as seen in immunofluorescence (Figure 2.9 A). This data is supported by immunoblot results which also show elevated MMP-9 levels with sE-cad treated. An EGFR kinase inhibitor CL-387785, MEK/ERK Inhibitor U0126 and a PI3K/AKT LY294002 inhibitor were used to determine the pathway implicated in sE-cad mediated MMP-9 production. LY294005 completely blocked MMP-9 expression suggesting the PI3K/AKT pathway is implicated in the sE-cad mediated MMP-9 release in MDCK cysts (Figure 2.9 B).

To determine whether sE-cad upregulates MMP-9 expression at the transcriptional level, the mRNA levels of MMP-9 in sE-cad treated and control cysts were quantified. MMP-9 mRNA was 2.2 fold higher in sE-cad treated cysts compared to the control MDCK cysts (Figure 2.9 C). These results demonstrate sE-cad induces upregulation of MMP-9 mRNA as well as protein levels in MDCK cysts. Furthermore, these results also indicate that MMP-9 released from MSV-MDCK can induce MMP-9 production from MDCK cysts in a sE-cad dependent manner.

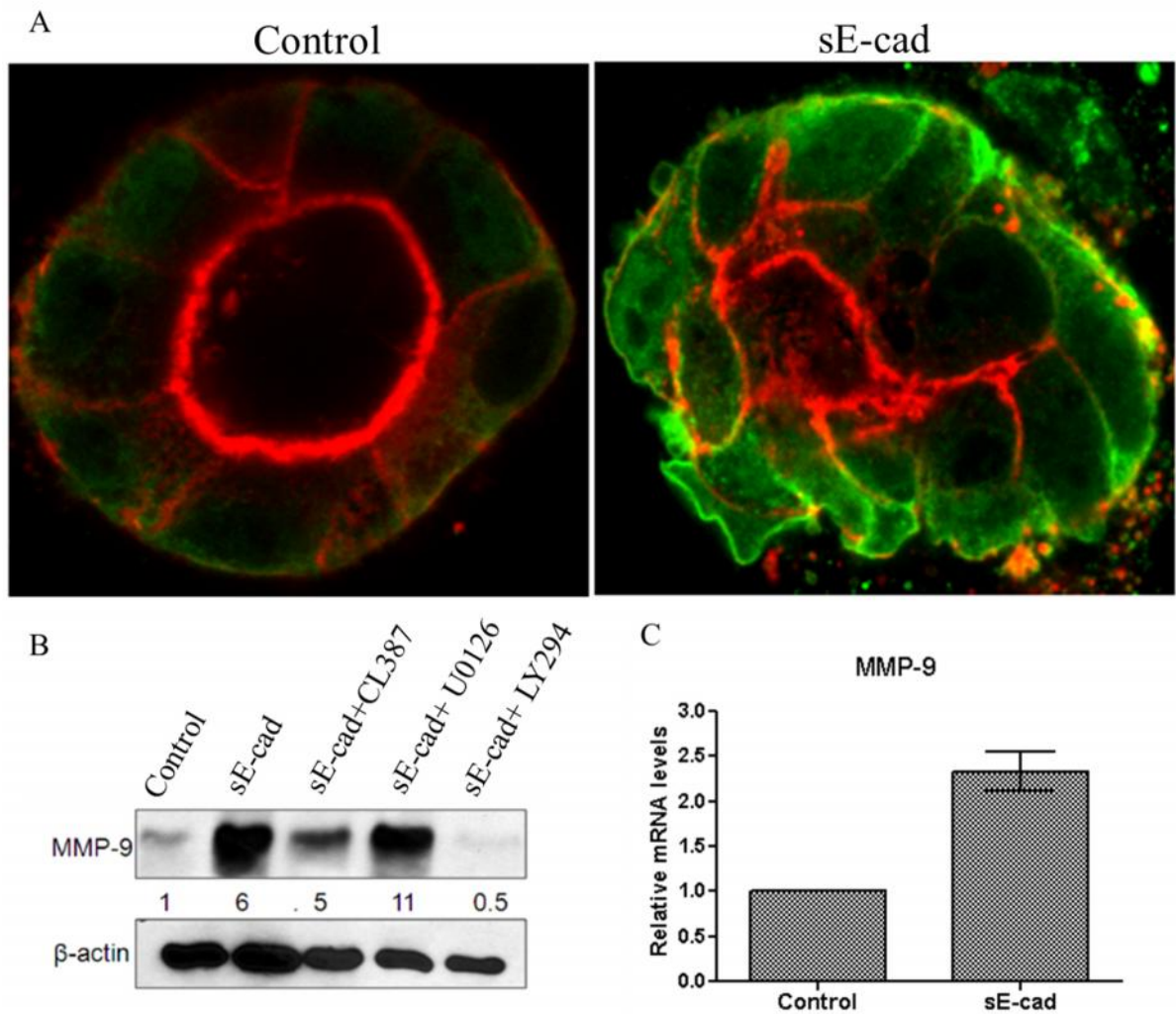


Figure 2.9: sE-cad induces MMP-9 in MDCK cysts.

(A), Representative images showing immunofluorescence staining of MMP-9 (green) and actin (red) in MDCK and sE-cad treated MDCK cysts. (B), Immunoblots showing MMP-9 and β -actin levels in MDCK cysts treated with sE-cad in presence and absence of inhibitors. 10 μ M of CL-387,785, U0126 and LY294002 were used for 24 hr. (C), Graph showing MMP-9 mRNA level in MDCK and sE-cad treated MDCK cysts quantitated by qRT-PCR. Mean values from three independent experiments are plotted. Error bars denote s.e. of the Mean. ($p = 0.249$).

Next, we tested the association between MMP-9 and sE-cad in another cell line. SUM149 is a human inflammatory breast cancer cell line which expresses high levels of E-cadherin. Immunofluorescence analysis of SUM149 cells showed elevated E-cadherin expression (Figure 2.10). Although these cells have high E-cadherin, these cells are not polarized and E-cadherin is expressed all over the cell surface (Figure 2.10). In 3D cultures, SUM149 cells form spherical aggregates but do not have a hollow lumens, a distinguishing feature of cancer cells in 3D culture (Figure 2.10). Immunoblot analysis revealed elevated levels of sE-cad and MMP-9 levels in the SUM149 conditioned media from 2D and 3D cultures (Figure 2,11A). Zymogram analysis demonstrated active MMP-9 levels in the SUM 149 2D and 3D conditioned media (Figure 2.11 B). These results also indicate high MMP-9 acts on cellular E-cadherin to shed sE-cad which then by a positive feedback mechanism induces MMP-9 expression.

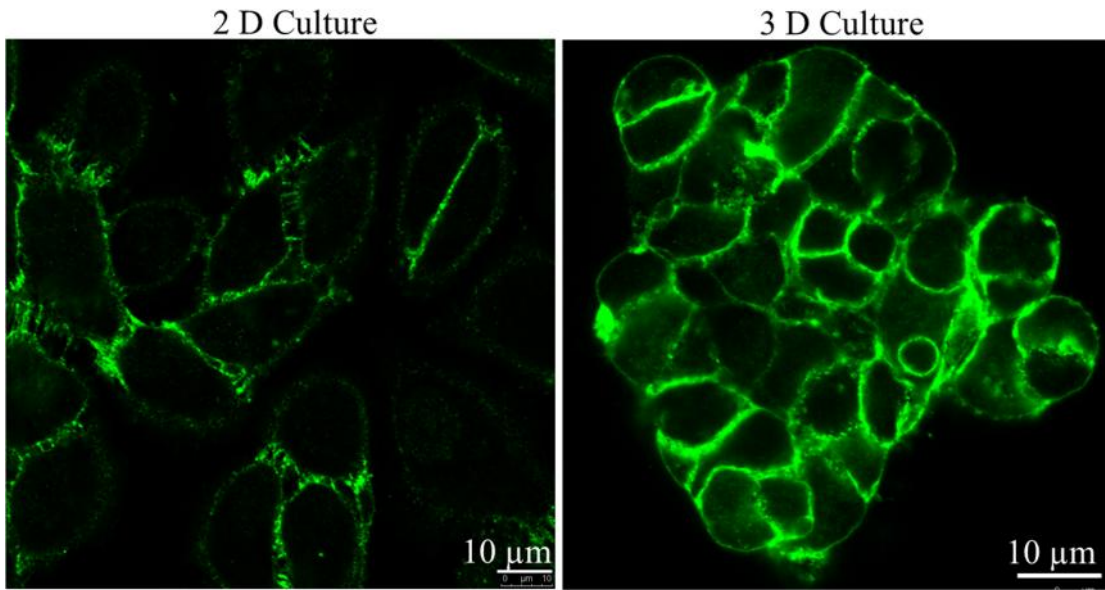


Figure 2.10: High E-cadherin expression in SUM149 cells.
 Representative images showing E-cadherin (green) immunofluorescence staining in SUM 149 cells.

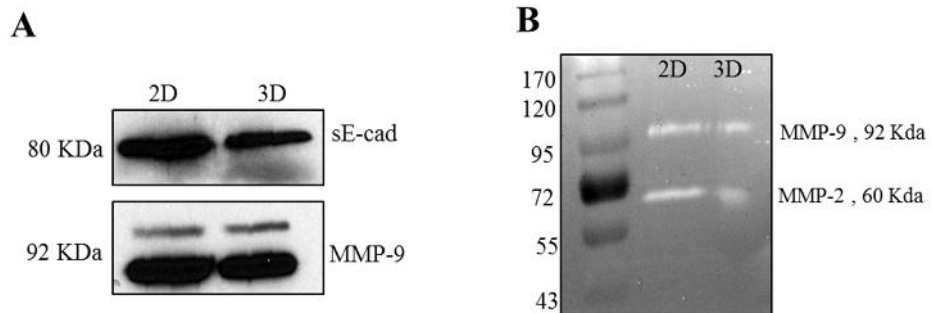


Figure 2.11: MMP-9 and sE-cad expression are correlated.
 (A), Immunoblot showing sE-cad and MMP-9 levels in the conditioned media in SUM149 2D and 3D cultures. (B), Zymogram showing MMP-9 activity from SUM149 conditioned media.

2.3.6 Reversibility Assay

To determine whether long term sE-cad and CM treatment results in permanent morphological and cellular alterations in 3D MDCK cysts, we tested the ability of lumen filled cysts to re-form hollow spherical cysts. In this reversibility assay, lumen filled cysts from Matrigel™ were collected, the cells trypsinized and plated back on Matrigel™ to see whether they were capable of reforming hollow cysts. 80% of the control cysts reformed hollow cysts when re-plated on Matrigel™, whereas MDCK cells collected from CM- or sE-cad-treated lumen filled cysts were also able to form hollow cysts more than 50% of the time (Figure 2.12). Formation of hollow polarized cysts on basement matrix *in vitro* is a hallmark of non-transformed epithelial cells. These results indicate that sE-cad and CM-induced morphological changes and lumen filling effects are reversible and last as long as they are present in the vicinity and do not induce permanent transformations in MDCK cysts.

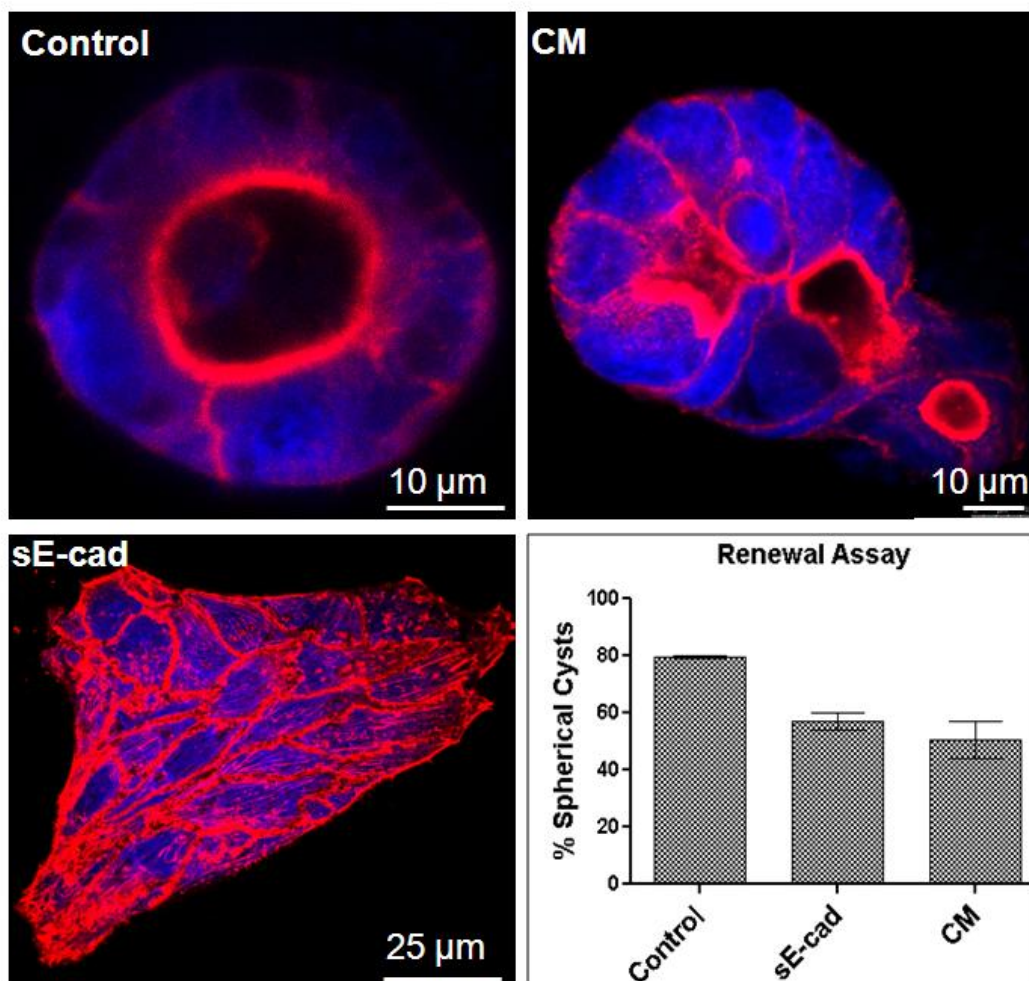


Figure 2.12: Lumen filled cysts form polarized cysts when replated.

Control MDCK cysts and CM and sE-cad treated lumen filled cysts were harvested and replated on Matrigel™ matrix to form polarized hollow cysts. Representative confocal images of cysts formed from control cysts, CM treated cysts and sE-cad treated cysts. Cysts were stained for actin (red) and TOPRO-3 (nuclear marker, blue). Bottom right panel, Quantification of % hollow cysts formed from three independent experiments.

2.4 Discussion

Carcinoma cells interact with the adjacent normal epithelial cells during carcinoma *in situ* stages as well as during the homing of the metastatic cancer cells into the host epithelium [151]. Tumor cells initiate crucial changes in the different components of the tumor microenvironment (TME) and transform them to support cancer progression. TME influences not only carcinoma cells but also tumor-adjacent normal epithelial cells. While it is well known that the tumor microenvironment contributes to metastatic dormancy and tumor stability, as well as emergence into invasive and metastatic carcinoma [170], the mechanism(s) by which carcinoma cells or the tumor environment influence tumor adjacent normal epithelial cells is not known. In this study, using a 3D co-culture system comprising of normal epithelial cells (MDCK) and carcinoma cells (MSV-MDCK), we demonstrated that carcinoma cells induced structural alterations in normal epithelial cysts, resulting in preneoplastic lumen filling. We showed that carcinoma cells secrete MMP-9 which cleaves cellular E-cadherin from normal epithelial cells to generate sE-cad. We further demonstrated that sE-cad is necessary and sufficient to induce lumen filling. To our knowledge, this is the first demonstration that carcinoma cells present in the vicinity can disrupt the epithelial architecture and induce lumen filling in normal epithelial cysts. Further, these studies demonstrate that sE-cad generated by carcinoma cells can induce upregulation of MMP-9 in normal epithelial cells which can act on MDCK E-cadherin and further enhance sE-cad shedding via a feedback mechanism (Figure 2.13). Clinically, these studies suggest that elevated levels of sE-cad present in cancer patients' sera may have a pathological role in the transdifferentiation of normal epithelial cells thereby facilitating invasion and metastatic potential.

Filling of the luminal space and multiple lumen lesions are distinctive features of early, pre-invasive stages of carcinoma development [156]. A 3D co-culture system comprising of epithelial cysts and carcinoma cells resembles normal epithelial tissue co-existing with tumor cells *in vivo*. This novel 3D assay allowed us demonstrate that carcinoma cells disrupt epithelial architecture by inducing pre-neoplastic lumen filling. Interference with the key regulators of the apico-basal polarity and tight junction assembly such as the Crumbs 3 and PAR complexes, β 1 integrin, RhoA, Na, K generates multiple lumina or no lumen in epithelial cysts [171-176]. However, how these markers are affected during carcinogenesis is not well known. Our results indicate that carcinoma cells in the vicinity of normal tissue may come in direct physical contact with the normal epithelial cells via filopodia like projections or alternatively secrete soluble factors which then disrupts luminal architecture. Data obtained using conditioned media strongly suggest that secretion of soluble factors is the primary mechanism by which carcinoma cells induce normal cell transformation. Recent studies have also demonstrated that carcinoma cells induce oncogenic transformation in the adjacent normal epithelial cells using exosomes to force adjacent normal cells to participate in cancer progression [177].

A key soluble factor identified in our assay is MMP-9. The levels of this protease are elevated in a variety of cancers, and elevated MMP-9 levels play a central role in tumor cell initiation/progression, metastatic ability and genetic instability [158]. While MMP-9 is implicated in the shedding of E-cadherin in several cancer cell lines [68], it is not known how this processing influences normal epithelial cells adjacent to the tumor in the context of tumor microenvironment. Our 3D co-culture system enabled us to identify that MMP-9 released by carcinoma cells acts on the cell bound E-cadherin of

normal epithelial cells to release sE-cad. Inhibition of MMP-9 abolished sE-cad shedding and consequently the lumen filling phenotype. Lack of E-cadherin expression on MSV-MDCK cells confirms that the source of sE-cad present in the CM is primarily from MDCK cells. Although active MMP-2 was also observed in our zymogram, specific inhibition of MMP-9 suggests that MMP-9 plays a prominent role in the production of sE-cad in this co-culture system. Also, we cannot rule out the involvement of other MMPs or soluble factors present in the CM, which may act upstream of MMP-9 and may be involved in the activation of MMP-9 and production of sE-cad. Additionally, our results also demonstrate that sE-cad in the microenvironment alters normal epithelial cells by inducing increased MMP-9 secretion.

Two complementary approaches were utilized to conclude that sE-cad is essential and sufficient for the induction of lumen filling in 3D culture. Exogenously added sE-cad induced lumen filling within 24hrs, whereas, immunodepletion of sE-cad from the CM blocked lumen filling phenotype indicating that sE-cad is critical factor of the CM that is involved in the lumen filling of MDCK cells. sE-cad has been shown to influence tumor cell proliferation, migration and invasion [80, 83, 108-110, 117]. Here, we demonstrate a previously unknown finding that sE-cad disrupted luminal architecture of fully formed cysts. This situation is reminiscent of early tumorigenesis suggesting sE-cad in the tumor microenvironment may induce preneoplastic lumen filling in adjacent normal epithelial cells.

In polarized epithelial cells E-cadherin is localized at the adherens junction and along the basolateral region. Which of these pools of E-cadherin is cleaved by MMP-9 to generate sE-cad is yet to be elucidated. Transwell co-culture assay using MDCK and MSV-MDCK cells revealed that MMP-9 and sE-cad were detected only in the bottom

chamber indicating that the MMP-9 produced by the MSV-MDCK cells cleaved the basolateral pool of E-cadherin from MDCK monolayer. MMP-9 inhibition in the basal chamber abrogated sE-cad shedding further confirming this result. It is known that the space between adjacent epithelial cells at the adherens junction is 10-20nm [23, 24]. However, intercellular space increases below the adherens junction region. Therefore, it is likely that proteases have easy access to the basolaterally localized E-cadherin [81]. Future work is necessary to examine whether adherens junction pool of E-cadherin is involved in the generation of sE-cad.

In summary, results from this chapter demonstrate that carcinoma cells can disrupt the epithelial architecture and induce sE-cad shedding. sE-cad is the soluble factor essential to induce lumen filling in MDCK cells. Furthermore, sE-cad in the microenvironment induced aberrant upregulation of MMP-9 in normal epithelial cells which can further result in alterations in the epithelial architecture and the extracellular matrix. However, these morphological changes and lumen filling effects are observed as long as carcinoma cells and sE-cad are present in the vicinity and these changes can be reversed once the MDCK cysts were removed from the co-culture system.

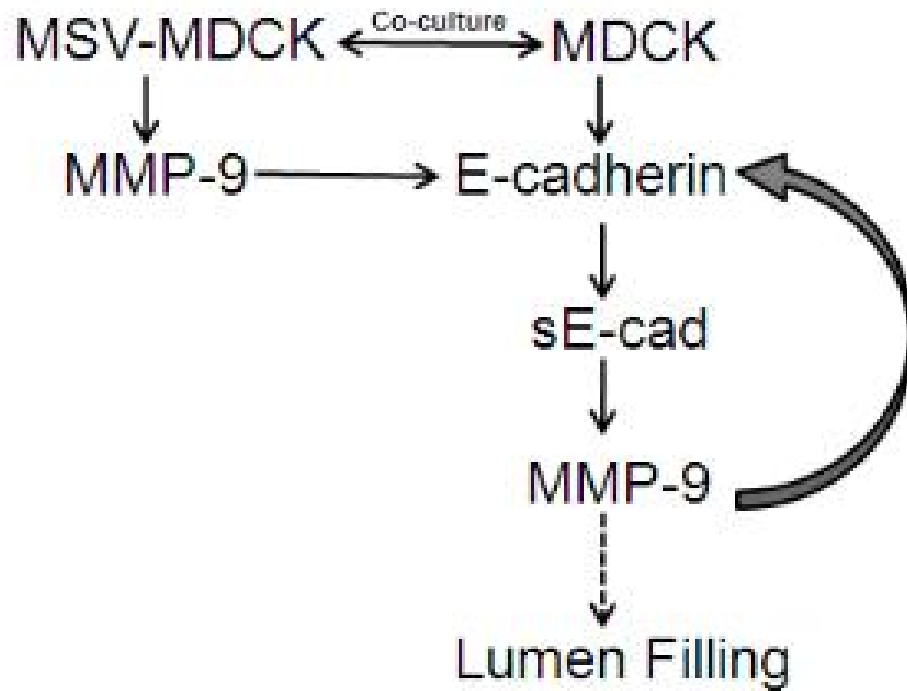


Figure 2.13: Proposed Model for MSV-MDCK induced Lumen Filling in MDCK cysts

Chapter 3

SOLUBLE E-CADHERIN AND CARCINOMA CELL CONDITIONED MEDIA INDUCE EPITHELIAL TO MESENCYMAL TRANSITION IN NORMAL EPITHELIAL CYSTS.

3.1 Introduction

A vast majority of cancers arise from epithelial tissues and a critical process in the evolution of primary tumor into malignant carcinoma and metastasis is epithelial–mesenchymal transition (EMT) [178]. EMT is a cellular process during which differentiated epithelial cells lose their epithelial features such as polarized organization and intercellular junctions, undergo cytoskeletal remodeling, and change in cell shape to acquire a more fibroblast-like cell morphology[179]. Concomitantly, these de-differentiated tumor cells upregulate mesenchymal features to acquire a more migratory and invasive behavior by remodeling cell-cell and cell-matrix interactions. Not only does EMT facilitate dissemination of cancer cells from the primary tumor site, it also protects the cancer cells from apoptosis, anoikis, cellular senescence and anti-tumor immune responses [178].

Gene expression profiling experiments have implicated more than a thousand genes which are altered during EMT[179]. Some of the key epithelial markers lost during EMT include, tight junction proteins claudins and occludins, the proteins in the adherens junction complex E-cadherin, and β -catenin, and cytokeratins [143]. Simultaneously, a variety of mesenchymal markers are expressed during EMT, including neural cadherin (N-cadherin), vimentin, fibronectin, MMPs, integrins α v and

1, and smooth muscle actin [179, 180]. Cancer cells can undergo either complete EMT where expression of several of the epithelial and mesenchymal proteins are altered or partial EMT which involves either loss of a few epithelial proteins or gain in mesenchymal proteins without loss of epithelial proteins. Some cells that undergo partial EMT morphologically still resemble the primary epithelial cells [181].

Signaling pathways involved in induction of EMT include, TGF- β , Wnt, NF- κ B, receptor tyrosine kinase (RTK), Notch and integrin mediated signaling [179]. All these pathways either result in transcriptional repression of E-cadherin or induction of EMT associated genes. Several extracellular signals can trigger these pathways to induce EMT. Presence of soluble growth factors, including TGF- β family members, fibroblast growth factor (FGF), epidermal growth factor (EGF) and hepatocyte growth factors (HGF); and changes in the components of the extracellular matrix (ECM), such as collagen and hyaluronic acid, have also been implicated in induction of EMT[179]. In response to these extracellular ligands several receptor mediated signaling pathways are triggered including activation of the Ras, Rho GTPase pathway, and activation of Src tyrosine-kinase family pathways. Activation of these pathways results in expression of transcriptional repressors (SNAIL, SLUG) which regulate epithelial protein expression, loss of junctional complexes, and changes in cytoskeletal organization.

Actin cytoskeleton remodeling and formation of focal adhesion complexes is a crucial step in EMT[182]. Cells undergoing EMT assemble actin into contractile stress fibers which are regulated by the Rho family GTPases [182]. Activation of the Rho pathway is crucial in maintaining fiber stability and inhibiting actin depolymerization. Actin stress fibers can be classified into four subtypes based on their intracellular location: ventral and dorsal stress fibers, perinuclear actin cap, and transverse arcs[182].

Ventral and dorsal stress fibers are organized as parallel stress fibers cross-linked via the α -actinin and myosin II proteins and associated with mesenchymal motility [183].

Other mechanisms which contribute to EMT in tumor cells include alterations in the extracellular matrix (ECM), hypoxia and components of the TME. EMT is associated with changes in ECM composition such as increased expression of Fibronectin or type I collagen. These changes can activate integrins resulting in outside-in signaling, and formation of focal adhesion complexes which can trigger cell migration. The integrin family of proteins are heterodimeric transmembrane proteins which are fundamental in conveying micro-environmental cues to the cell. They consist of one α - and one β -subunit and can form up to 24 combinations of the integrin heterodimers to interact with ECM proteins and alter cellular behavior[184]. During formation of focal adhesion and cell migration during EMT, there is extensive crosstalk between integrins and their ECM substrates (laminin, collagen, heparan sulfate proteoglycans, vitronectin, fibronectin, osteopontin, bone sialoprotein, thrombospondin, fibrinogen and tenascin) [184]. For instance, interaction and activation of $\alpha 1$ integrin is crucial for activation of p38 MAPK signaling and for Rho A and Rac1 activation [179]. Similarly, src dependent phosphorylation of focal adhesion kinase (FAK) and E-cadherin downregulation is dependent on $\alpha v 1$ integrin activation [179]. Thus, integrin mediated cell-matrix interactions play a key role in EMT.

3.1.1 EMT and Stemness

A significant body of research has also indicated that induction of EMT in epithelial tumor cells results in the acquisition of stem cell like characteristics in cancer cells, also designated as cancer stem cells (CSCs) [185]. CSCs are tumor initiating populations, which are capable of invading surrounding tissue and display therapeutic

resistance. Induction of EMT in human mammary epithelial cells results in the acquisition of stem cell markers and the formation of mammospheres, a property associated with mammary epithelial stem cells [186]. Conversely, stem cells isolated from endothelial cells express EMT markers [187]. There are several CSC markers that are expressed at different levels depending on the specific cancer. Some of the established stem cell markers include, CD133, CD44, DC24, Oct4, ALDH-1, Nestin, LGR5 and α 6 integrin [188].

3.1.2 TME and EMT

The TME also plays a vital role in induction of EMT. Cancer associated fibroblasts (CAFs), infiltrating inflammatory cells, CSCs, mesenchymal stem cells (MSCs) are all cells in the TME that can induce EMT in cancer cells [189]. Cancer-related inflammation induced by cytokines, leukocytes and Tumor Associated Macrophages (TAMs) are strong inducers of EMT. TAMs release TNF- α which upregulates TGF- β expression, a central signaling pathway in induction of EMT [190]. TNF- α also upregulates SNAIL-1 in breast cancer cells which represses E-cadherin expression in induction of EMT [191].

CAFs overexpress several MMPs such as MMP-2, MMP-9 and MT1-MMP during induction of EMT. Elevated levels of MMPs in TME can modify the ECM matrix, cleave substrates such as protease activated receptor-1 (PAR-1), IL-8, E-cadherin, α v integrin, and latent TGF- β to facilitate EMT in tumor cells. MMP-9 is particularly strongly implicated in EMT as it cleaves E-cadherin and enhances cell migration and invasion [109].

Apart from the cells of the TME, hypoxia and oxidative stress are the second most important factors in induction of EMT [189]. When cancer cells divide

uncontrollably to form larger tumors, there is limited availability of nutrients and oxygen in the microenvironment resulting in exposure to intermittent hypoxic conditions. Hypoxic conditions induce hypoxia-inducible factors (HIF) signaling in tumor cells. HIF signaling activates Snail and latent TGF- β 1 which are strong inducers of EMT [192, 193]. Hypoxia also induces increased production of reactive oxygen species (ROS) and activates ROS signaling. ROS activates nuclear factor kappa B (NF- κ B) signaling which is implicated in EMT in certain cell types [189].

sE-cad is a component of the TME and, via autocrine/paracrine signaling, upregulates MMP-9 levels both tumor cells and adjacent epithelial cells (see Results section of Chapter 2). Previous reports from our lab and others have shown that sE-cad can activate the EGFR pathway, which is also implicated in induction of EMT. However, the direct role of sE-cad in inducing EMT has not previously been investigated. I hypothesize that sE-cad plays a role in EMT and stemness in epithelial cells. sE-cad can itself act as growth factor by upregulating MMP expression in the TME to digest ECM to cause release of growth factors and remodel the ECM. This could result in activation of integrin and other signaling pathways to facilitate induction of EMT in the normal epithelial cells.

3.2 Materials and Methods

3.2.1 Cell lines

In this chapter, the same cell lines were used as described in Chapter 2.

3.2.2 Antibodies and Reagents

Primary antibodies used in this chapter for immunoblotting and immunostaining were as follows: E-cadherin antibody Decma-1 (Sigma-Aldrich), MMP-9 (Santa Cruz

Biotechnology) and N-cadherin (Abcam). Fibronectin and β -catenin antibodies were obtained from BD Transduction Laboratories, Smooth Muscle Actin (Santa Cruz Biotechnology). β 1 integrin and Oct 4 antibodies were purchased from Cell Signaling. The mouse, rabbit and rat horseradish peroxidase-conjugated secondary antibodies were obtained from Cell Signaling Technology. Anti-Mouse Alexa Fluor-488, Anti-Rabbit Alexa 633, Alexa-Fluor-546-conjugated phalloidin and TOPRO-3 were purchased from Molecular Probes (Eugene, OR). FITC- and Texas Red-labeled, affinity-purified secondary antibodies were obtained from Jackson ImmunoResearch Laboratories (West Grove, PA).

Growth factor-reduced MatrigelTM (Corning Discovery Labware) was used for three-dimensional culture. Protein-free, serum-free UltraDOMATM media (Lonza) was used for conditioned medium experiments. Corning cell recovery solution was used to harvest 3D cultures from the MatrigelTM matrix. EGFR Inhibitor CL-387,785 and MMP-9 Inhibitor I (CAS1177749-58-4) were purchased from EMD Millipore Chemicals.

3.2.3 Immunofluorescence of 3D MatrigelTM cultures

Cysts grown in MatrigelTM were immunostained as previously described in Chapter 2 of this dissertation.

3.2.4 Confocal microscopy and quantitation of 3D cysts

Images were captured using a *Leica* TCS SP5 scanning confocal microscope (Leica Microsystems Inc., Buffalo Grove, IL) using a 63X/1.4 NA oil immersion objective lens. The cysts were assessed for the presence of cells within the lumen and quantified as described in Chapter 2 of this dissertation.

3.2.5 Immunoblotting

SDS-PAGE was used to separate proteins in 3D cyst lysates. Separated proteins were transferred from the gel to a nitrocellulose membrane. For immunoblotting, the membranes were blocked in 5% non-fat milk in TBS/0.1% Tween 20 (TBS-T), and then probed with primary antibodies at a dilution of 1:1000 and incubated overnight at 4°C. The membranes were further probed with HRP-conjugated anti-rabbit, -mouse or -rat secondary antibodies diluted 1:2000 in 5% non-fat milk/TBS-T and incubated for 1 h at room temperature. For detection of Ki67 protein (Molecular weight 345-395 kDa) 3-8% Tris acetate (NuPage Novex) gradient gels were used. Antibody binding was visualized using Enhanced Chemiluminescence (ECL) and ECL prime (GE Healthcare). Image J software was utilized for immunoblot quantification and image analysis.

3.3 Results

3.3.1 Long term (96 h) sE-cad and CM treatment induces an EMT-like phenotype in MDCK cysts

Cysts in co-culture for more than 48 h showed striking morphological changes. At 96 h, control cysts remained spherical, whereas CM- and the sE-cad treated cysts showed more elongated cells emanating from the cysts, a fibroblastic mesenchymal phenotype (Figure 3.1). These cysts are much larger than the control cysts and appear to be motile and interacting with neighboring cysts via filopodia and lamellipodia like extensions. This observation led us to hypothesize that sE-cad and CM can induce EMT in the normal epithelial cysts.

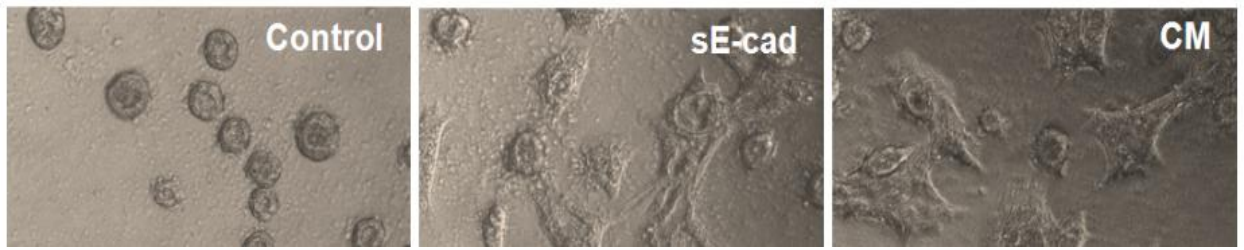


Figure 3.1: sE-cad and CM induces EMT like phenotype in MDCK cysts.

A, Phase contrast images of control MDCK cysts and cysts treated with CM and sE-cad for 96 h.

3.3.2 sE-cad and CM treatment induce actin stress fiber formation

Since the phase contrast images of sE-cad and CM treated cysts showed a mesenchymal phenotype, we analyzed these cysts for the presence of EMT markers. Actin cytoskeleton remodeling is a hallmark of EMT, and is crucial for mesenchymal cell motility through the ECM. Immunostaining of cysts with anti-phalloidin showed dorsal and ventral actin stress fibers in sE-cad and CM treated lumen filled cysts whereas control cysts showed presence of distinct cortical actin (Figure 3.2). Unlike control cells, lumens were filled in sE-cad and CM treated cysts.

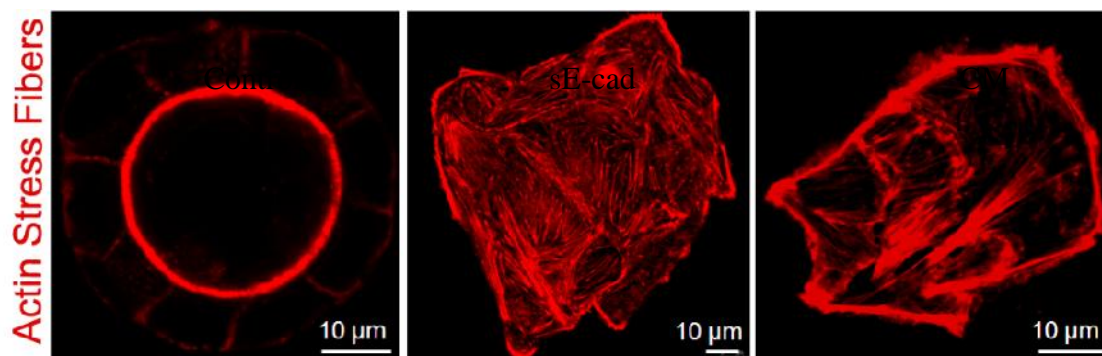


Figure 3.2: Presence of Actin stress fibers in Lumen filled cysts.

Immunofluorescence showing phalloidin actin staining (Red).

3.3.3 sE-cad and CM treatments upregulate expression of N-cadherin and Fibronectin

To confirm EMT, we examined expression of multiple EMT markers in the cysts using immunofluorescence and immunoblot analyses. N-cadherin is primarily expressed in neuronal cells and not in epithelial cells, however dedifferentiating epithelial tumor cells express N-cadherin and lose their E-cadherin [194]. N-cadherin activates the src kinase pathway and plays a key role in transendothelial migration which allows cancer cells to invade through the endothelial layer [195]. Expression of another marker of EMT, fibronectin, is also associated with carcinoma development, conferring tumor cells with chemotherapeutic resistance and promoting growth and survival. It induces EMT by activation of the src kinase and mitogen-activated protein (MAP) kinase signaling pathways. MMP-9 levels in the TME are upregulated during EMT [196]. Tumor cells undergoing EMT express high levels of MMP-9 [196]. MMP-9 is a gelatinase which can degrade type IV collagen, a major component of the basement membrane of epithelial tissues thereby facilitating invasion. MMP-9 can modulate the bioavailability of growth factors and influence signaling pathways from the ECM[197]. All three of these established EMT markers were increased in cysts treated with sE-cad or CM (Figure 3.3)

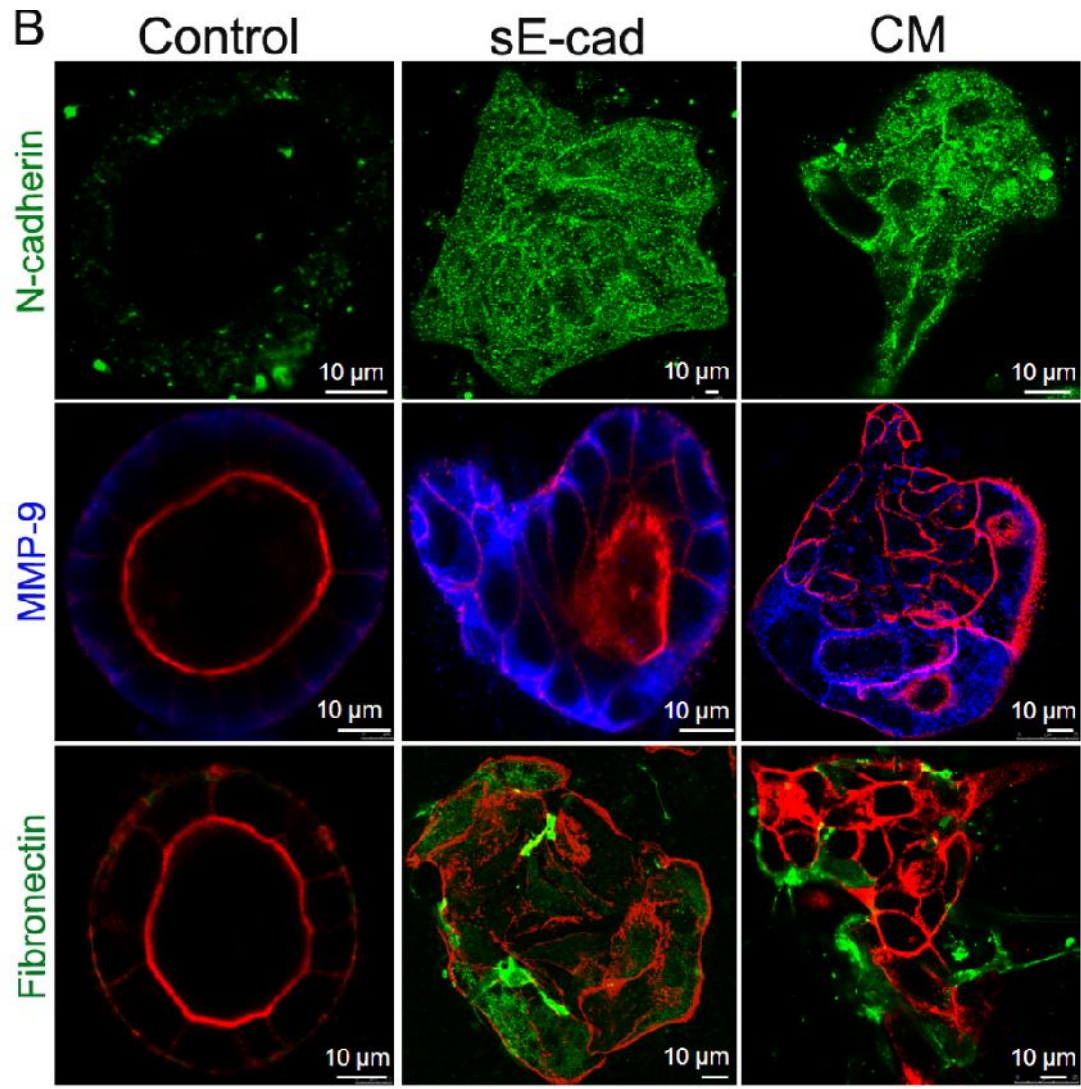


Figure 3.3: Upregulation of EMT markers in sE-cad and CM treated cysts
 Immunofluorescence staining with different EMT markers. Representative merged confocal images showing Actin (Red), Fibronectin (Green), N-cadherin (Green), MMP-9 (Blue).

3.3.4 Z-stacks showing EMT Markers in Lumen Filled Cysts

Z-stacks (2 -4 μ m) of control, sE-cad and CM treated MDCK cysts for 96 h also show lumen filling and expression of fibronectin, N-cadherin and actin stress fibers (Figure 3.4). Together, these results reveal that long-term sE-cad or tumor cell CM treatment induces EMT in MDCK cysts.

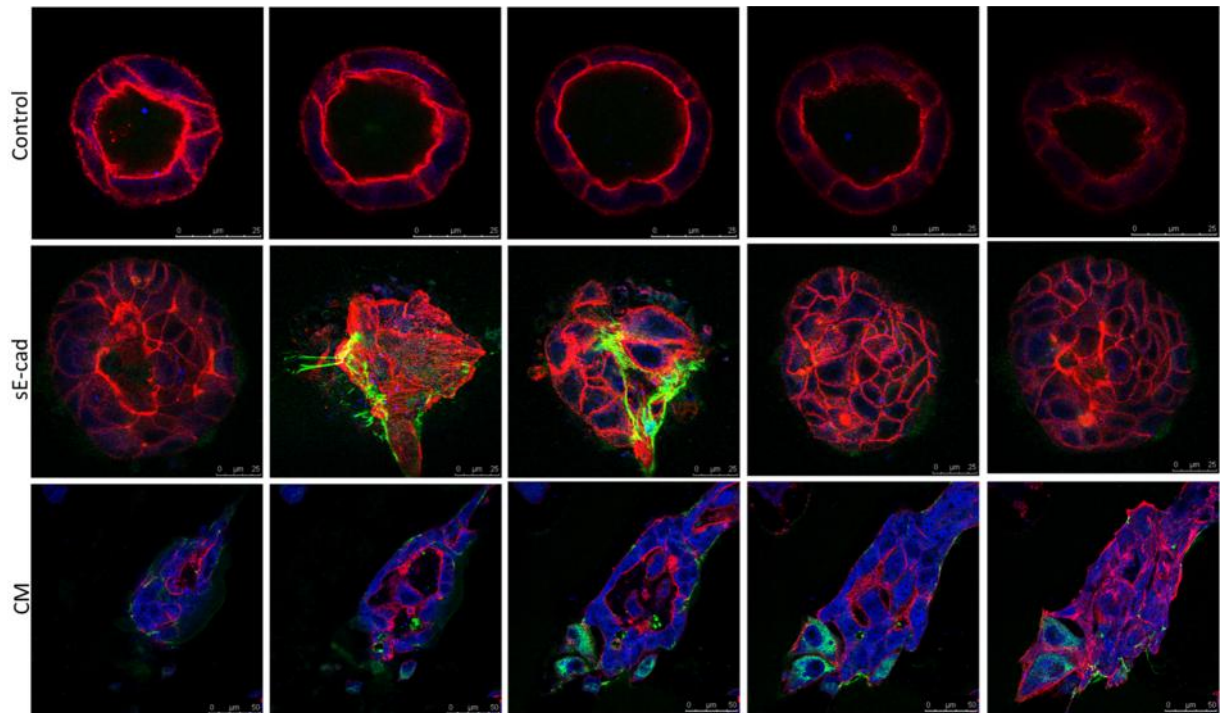


Figure 3.4: Lumen filling and EMT markers in Z-stacks gallery.

Z-stack images of control, sE-cad and CM treated cysts were stained for N-cadherin (blue), fibronectin (green) and Actin (red).

3.3.5 MSV-MDCK cells and MDCK cysts interact via Fibronectin fibrils

We observed that MSV-MDCK cells interact with MDCK cysts via a fibronectin fibril network. Immunofluorescence analysis shows that fibronectin fibrils from MSV-MDCK cells extend towards MDCK cysts and interact with their cell membrane, possibly by contact with surface receptors (Figure 3.5). MSV-MDCK cysts also clump with and surround the MDCK cysts. Additionally, MDCK cysts which are lumen filled and undergoing EMT interact with each other via fibronectin fibrils. Mechanical forces generated by cells are necessary for the process of fibrillogenesis, the transformation of the compact form of fibronectin to the extended fibrillar form [198]. Thus our results show that fibronectin is expressed as both a soluble form laid around the cells in the extracellular matrix as well as a fibrillar form that creates a network between the tumor cells and the lumen filled MDCK cysts.

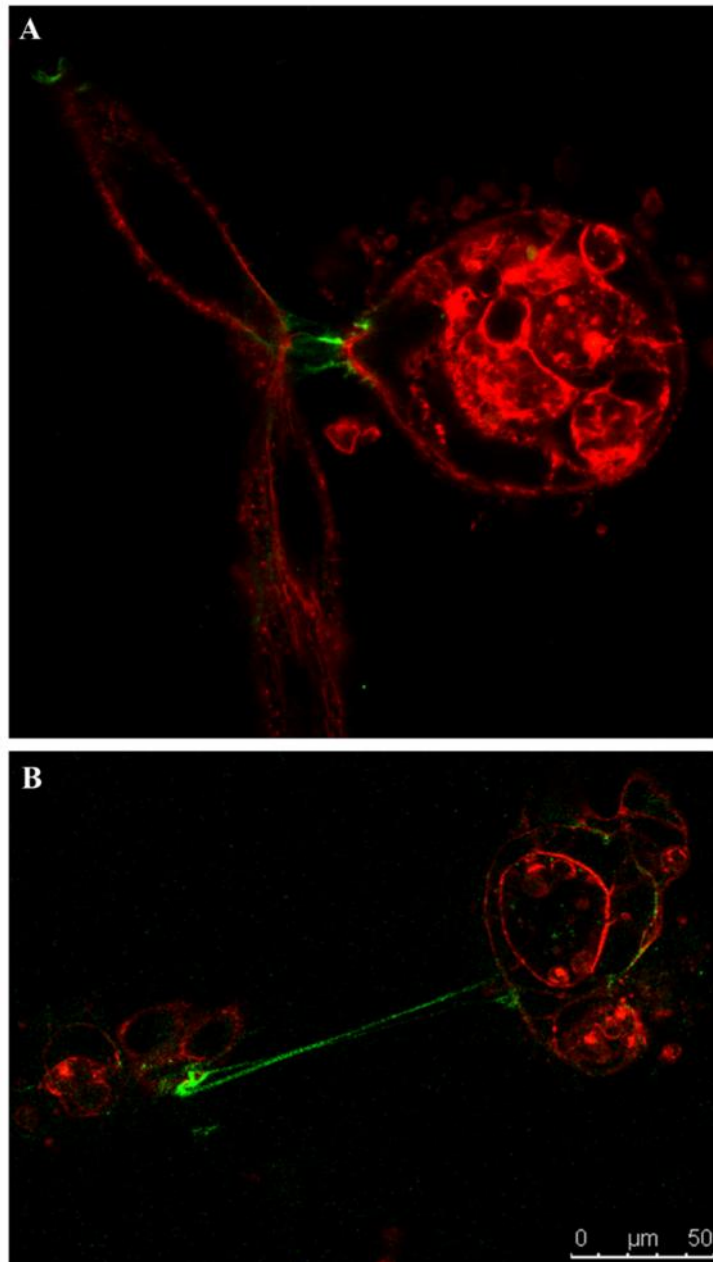


Figure 3.5: Fibrillar Fibronectin Network between MSV-MDCK and Lumen filled cysts.

Immunofluorescence showing Actin (red) and fibronectin (green) staining in (A) MSV-MDCK/MDCK co-culture (B) lumen filled MDCK cysts.

3.3.6 sE-cad increases $\alpha 1$ integrin levels

The increased fibronectin fibrillar network seen in lumen filled cysts with long-term sE-cad treatment is dependent on integrin activity [199]. The $\alpha v \beta 1$, and $\alpha 5 \beta 3$ integrins recognize and bind to fibronectin. Fibronectin ligand binding activates integrins resulting in intracellular signaling. To determine whether fibronectin expression by lumen filled cysts enhances expression of its integrin partners, we examined the expression of $\alpha 1$ and $\alpha 5$ integrins. sE-cad treated lumen filled cysts showed enhanced expression of $\alpha 1$ integrin (Figure 3.6).

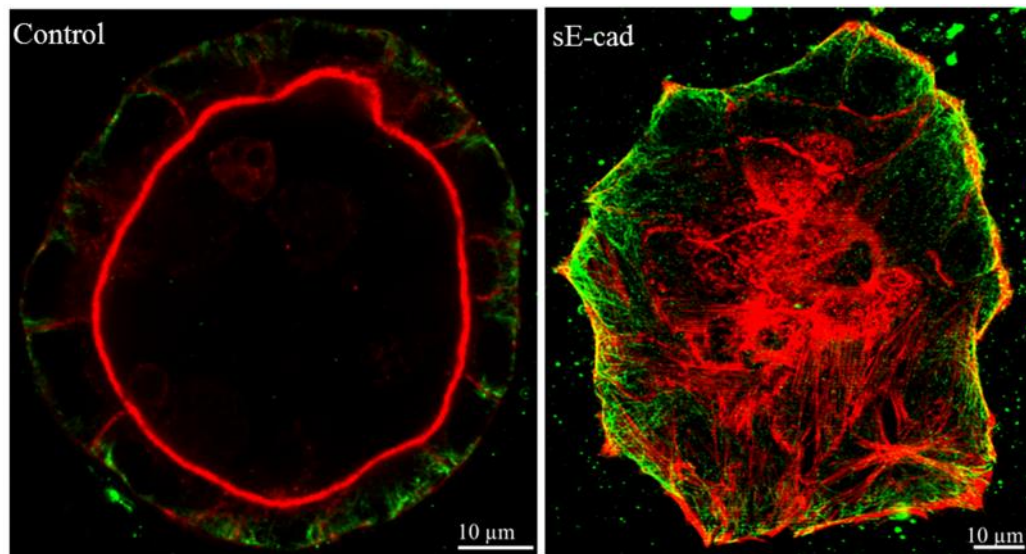


Figure 3.6: Upregulation of $\alpha 1$ integrin levels in sE-cad treated cysts.

Immunofluorescence showing integrin staining in control and sE-cad treated cysts. Representative merged confocal images showing Actin (Red), $\alpha 1$ integrin (Green).

3.3.7 Upregulation of the stem cell marker Oct4 in CM treated lumen filled cysts

EMT is also known to promote cancer stem cell properties. To determine whether lumen filled cysts undergoing EMT also upregulated expression of stem cell markers, we examined the expression of common cancer stem cell markers Aldehyde dehydrogenase (ALDH)-1 and Octamer-binding transcription factor 4 (Oct4) in the lumen filled cysts [200, 201]. Our results show that CM treated lumen filled cysts have increased Oct4 expression in comparison to the control cysts (Figure 3.7). Oct4 is a transcription factor critical for self-renewal and induction of pluripotent stem cells [202, 203]. Elevated Oct4 expression is also associated with several types of cancers including breast cancer, gastric cancer, non-small cell lung carcinomas, esophageal squamous cell carcinoma and glioma [204]. Oct4 promotes tumorigenicity and is also a biomarker for liver metastasis in colorectal cancers [204]. Our results thus indicate co-culturing MSV-MDCK tumor cells with epithelial MDCK cysts can upregulate EMT and stem cell-like properties in them. However, these results need to be validated by examining the mRNA levels and total protein levels of Oct 4 using qRT-PCR and immunoblotting respectively. ALDH-1 is a NAD(P)⁺ dependent enzyme which converts retinaldehyde to retinoic acid (RA) [205, 206]. RA is a ligand for the retinoid signaling pathways crucial in developmental processes [206]. ALDH-1 levels have been elevated in several solid tumors including colorectal, lung, liver, prostate and ovarian cancers as well as in acute myeloid leukemia [205]. We did not see any expression of ALDH-1 in the lumen filled cysts undergoing EMT.

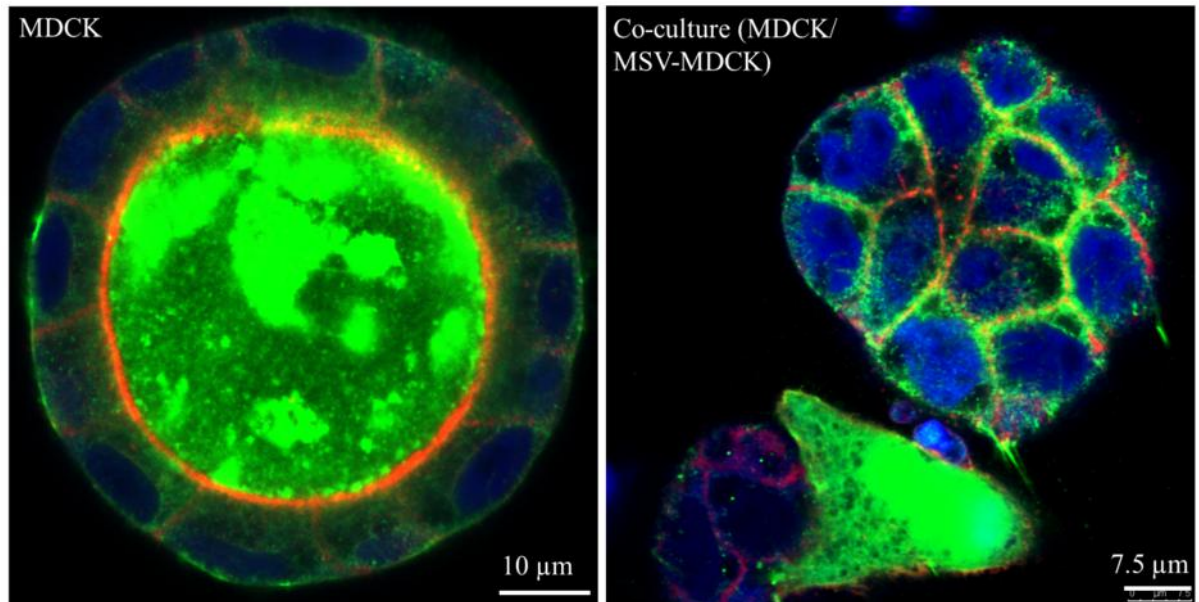


Figure 3.7: Upregulation of the stem cell marker Oct4 in lumen filled cysts.

Immunofluorescence showing stem cell marker Oct 4 (blue) and EMT marker Fibronectin (green) and Actin (red) staining in control and MSV-MDCK co-cultured cysts.

3.3.8 Epithelial Markers Retained in Lumen Filled Cysts Undergoing EMT

Even though MMP-9 cleaves cell surface E-cadherin from MDCK cysts, total E-cadherin protein levels and surface expression levels were not significantly reduced in the lumen filled cysts (Figure 3.8). Lumen filled cysts express the EMT marker N-cadherin but there was no concomitant loss of E-cadherin in these cysts (Figure 3.8 A). Immunoblot results further support this data and show that levels of another epithelial marker protein, Na,K 1, also did not change with sE-cad and CM treatment (Figure 3.8 B). This may be possibly due increased synthesis of E-cadherin and delivery to the cell surface and it indicates that the MDCK cysts likely undergo partial EMT where some of the epithelial markers are still retained.

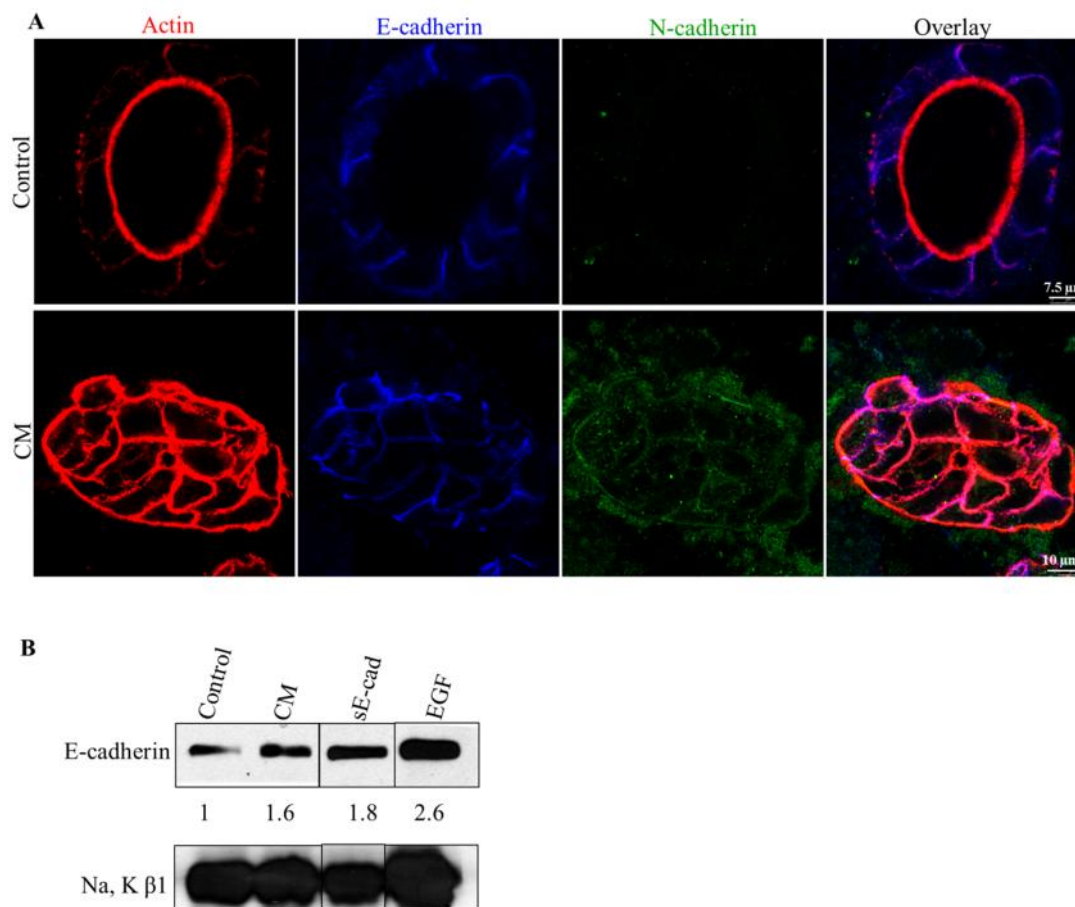


Figure 3.8: No change in epithelial protein in lumen filled cysts.

(A) Representative merged confocal images showing Actin (Red), E-cadherin (Blue) and N-cadherin (Green). (B) Immunoblot showing E-cadherin and Na,K 1 levels in CM and sE-cad treated cysts.

3.4 Discussion

In this chapter, using the 3D co-culture system comprising of MDCK and MSV-MDCK cells, I demonstrate that carcinoma cells sequentially induced pre-neoplastic lumen filling and EMT in the adjacent epithelial cysts. The occurrence of EMT in 2D cultures is well established. For example, TGF- β induces EMT [207, 208]. However, induction of EMT in 3D epithelial structures has not been shown previously. I

demonstrated that long-term treatment of MDCK cysts with sE-cad or CM induced transdifferentiation of the cysts into a disorganized motile mesenchymal phenotype. Cells with a mesenchymal morphology were observed emanating from the cysts with a consequent loss of cyst morphology. These mesenchymal cells were highly motile. Consistent with their morphology, mesenchymal markers N-cadherin, fibronectin and actin stress fibers were up-regulated. MMP-9 expression was also elevated in these cells. These results indicate that sE-cad produced either directly or indirectly by carcinoma cells can induce EMT in adjacent normal epithelial cells. The trigger that induces EMT following preneoplastic lumen filling is not known.

I discovered that lumen filled cysts undergo cytoskeletal remodeling to exhibit actin stress fibers. Assembly of these stress fibers is crucial for cell motility and invasiveness. Rho signaling pathway is central in actin cytoskeletal changes. Though I did not investigate the mechanism for the formation of these stress fibers, I hypothesize that the activation of RhoA and suppression of Rac1 may be critical in the expression of these stress fibers. I used a Rho-associated protein kinase inhibitor, Y-27632, to determine whether blocking the Rho A pathway could impact formation of stress fibers. Y-27632 (10 μ M) did not inhibit lumen filling or formation of stress fibers (data not shown) in the lumen filled cysts. This does not rule out the involvement of the RhoA pathway in stress fiber formation but suggests that blocking Rho-associated protein kinase is not sufficient to prevent lumen filling and stress fiber formation.

Expression of mesenchymal markers N-cadherin and fibronectin in the epithelial cysts can result in aberrant activation of several signaling pathways in these cells. N-cadherin is reported to enhance FGFR signaling pathway by preventing FGFR internalization resulting in sustained MAPK activation and MMP-9 expression [209].

Thus N-cadherin expression in epithelial cells can result in decreased cell-cell interactions and increased interaction with the stromal cells in the TME. Downregulation of N-cadherin in squamous carcinoma cells increases E-cadherin expression and cell adhesion. In prostate cancer cells, N-cadherin homophilic binding led to phosphatidylinositol 3-kinase (PI3-K)-dependent activation of Akt and increased stabilization of the anti-apoptotic protein Bcl-2 [210]. Thus, N-cadherin expression in epithelial cysts can promote cell survival by AKT activation.

I also showed increased expression of fibronectin and its integrin binding partner, α_1 , in sE-cad treated lumen filled cysts. Increased expression of α_1 integrin suggests integrin activation in response to fibronectin and outside in signaling in the epithelial cysts. Changes in signaling events will be examined in chapter 4 of this dissertation. Fibronectin and its integrin partner $\alpha_v \beta_1$ are strongly expressed in response to hypoxia in mice [211]. It is possible that hypoxia in the lumen filled cysts results in fibronectin expression at 96 h, though further investigation is necessary to examine this possibility.

Furthermore, I identified a novel mechanism by which tumor cells interact with the normal epithelial cells by formation of fibronectin fibrils. Binding of the $\alpha_v \beta_1$ integrin to the amino terminal of fibronectin is crucial for the assembly of a fibronectin fibrillar matrix [212]. Increased expression of α_1 integrin in lumen filled cysts may thus be involved in the formation of fibrillary fibronectin network, however further studies need to be done to validate this. This fibronectin fibrillar network between cells in TME can induce integrin activation and signaling in adjacent cells. It also results in changes in cell shape and aberrant cell signaling by exerting mechanical force on the cells.

We did not see a downregulation of epithelial markers E-cadherin and Na, K 1 levels in the lumen filled cysts. Even though E-cadherin is proteolytically cleaved and sE-cad levels are elevated in the CM, the total E-cadherin protein levels did not reduce. A possible explanation for this may be that the cells undergo rapid E-cadherin synthesis to sustain sE-cad shedding. Though further studies need to be done to explain this phenomenon. These findings, therefore suggest that the lumen filled cysts may be undergoing partial EMT where they express mesenchymal markers fibronectin and N-cadherin while retaining the epithelial proteins. The mechanism by which sE-cad induces lumen filling and disrupts epithelial architecture will be discussed in the next chapter.

My results showed that CM treated cysts undergoing EMT also had increased expression of stem cell marker Oct 4. Induction of EMT markers is associated with stemness and it is possible that the cysts undergoing EMT give rise to a stem cell like population. However, there is a lot of discrepancy in the field about CSC identification and the markers are not very reliable [188]. Multiple stem cell markers need to be expressed in the cells to conclusively identify CSCs population [188]. Moreover, expression of Oct 4 in lumen filled cysts needs to be validated at the mRNA and protein levels by alternate methods.

In summary, results from this chapter demonstrate that carcinoma cells induced shedding of cell bound E-cadherin from adjacent normal tissue and this might influence transdifferentiation of the compact epithelial tissue into a disorganized group of mesenchymal cells. Elevated sE-cad levels also has tumorigenic effects on normal epithelial cells and resulting in EMT. Thus, accumulation of sE-cad in the microenvironment may have additive or synergistic effects on the pro-oncogenic TME

since it can alter several components of the TME. Disruption of normal epithelial cell function could enhance basal extrusion of tumor cells [213], and thereby accelerate metastasis of the tumor cells.

Chapter 4

ANALYSIS OF SIGNALLING PATHWAYS ACTIVATED DURING SOLUBLE E-CADHERIN INDUCED LUMEN FILLING AND EPITHELIAL TO MESENCHYMAL TRANSITION IN NORMAL EPITHELIAL CYSTS

4.1 Introduction

Malignant transformation of epithelial cells by disruption of its architecture is one of the salient features of epithelial cancer progression. Signaling pathways and molecular mechanisms involved in the disruption of epithelial architecture are poorly understood. Epithelial cells grown in 3D cultures recapitulate numerous features of the glandular epithelium *in vivo* [145]. Apoptosis is fundamental in maintaining cell number and sculpting of organs during embryonic development [214] and akin to its *in vivo* function it is vital for cavitation and lumen formation in 3D epithelial structures *in vitro* [215, 216]. Filling up of the lumen is one of the hallmarks of cancer progression. *In vitro* studies have shown that both increased cell proliferation and antiapoptotic activity are necessary for filling up of the lumen [155]. For instance, oncogenes that only induce constitutive proliferation, such as cyclin D1 and c-myc, result in large epithelial cysts but they still have a hollow lumen [155]. Constitutive activation of ErbB2 (Her2) in breast epithelial cysts causes both constitutive proliferation and suppresses apoptosis by inhibiting caspase 3, leading to larger lumen filled cysts [217]. This ErbB2 induced lumen filling resembles lesions associated with carcinoma *in situ* in breast cancer. Other target genes known to disrupt the luminal architecture include prosurvival proteins such Bim and Bcl-XL, apico-basal polarity and tight junction assembly proteins such as the

Crumbs 3 and PAR complexes, $\alpha 1$ integrin, RhoA, and Na, K-ATPase β -subunit [171-176]. This chapter focuses on the mechanism by which adjacent tumor cells induce epithelial alterations and lumen filling in the epithelial MDCK cysts.

The EGFR (ErbB) family consists of four transmembrane tyrosine kinase receptors which include ErbB1 (EGFR), ErbB2 (Her2/neu), ErbB3 (Her3), ErbB4 (Her4) [218-222]. The EGFR pathway plays a critical role in several important cellular functions such as proliferation, differentiation, and tissue homeostasis [223]. EGFR has seven growth factor ligands: EGF, transforming growth factor- β (TGF β), heparin-binding EGF-like growth factor (HBEGF), amphiregulin, betacellulin, epiregulin, and epigen. ErbB3 and ErbB4 receptors bind to growth factor neureglins [224]. ErbB2 has no known ligand however it can heterodimerize with ErbB3 and ErbB4 receptors [224]. EGFR contains an extracellular ligand binding domain, a single transmembrane region, an intracellular domain and a C-terminal tail with multiple phosphorylation sites [223]. When a ligand binds to the extracellular domain, the receptors homodimerize or heterodimerize, activating their tyrosine kinase activity in the cytoplasmic tail leading to auto- and cross-phosphorylation of the tyrosine kinase residues [225-229]. The C-terminal tail of EGFR contains five autophosphorylation residues which link it to proteins that contain the SH2 or PTB (phospho-tyrosine binding) domains such as Grb2, Shc, phospholipase C-1 (PLC-1), the p85 subunit of PI3K (p85), p120 rasGAP, Src, Stats, and Cbl [227-229]. The binding of these signaling proteins to the receptor activates diverse downstream signaling pathways which modulate adhesion, migration, proliferation, differentiation and survival [229]. Figure 4.1 shows some of the signaling pathways activated by EGFR.

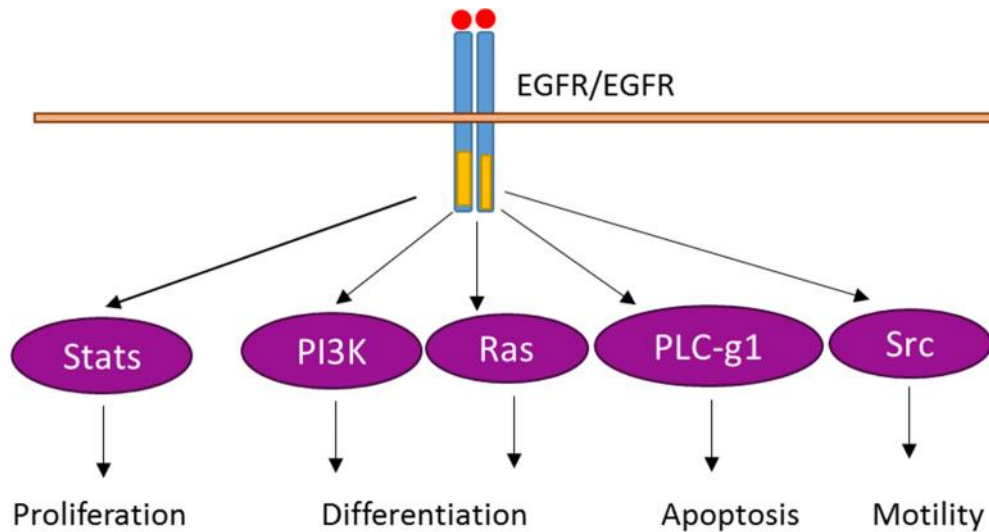


Figure 4.1: Signaling Pathways activated by EGFR.

Figure modified from open access book chapter Wang et al., Mutual Regulation of Receptor-Mediated Cell Signalling and Endocytosis: EGF Receptor System as an Example

Activated EGFR interacts with Shc and Grb2 to activate the Ras-Raf-Mek-ERK pathway which result in activation of several transcription factors such as c-fos, elk-1, c-myc which are important in mitosis and proliferation [228, 230-232] (Shown in Figure 4.1.2). Activated EGFR also activates the PI3K/AKT. AKT is a serine threonine kinase which phosphorylates several target proteins such as the BCL2-associated agonist of cell death (BAD), and the glycogen synthase kinase 3 (GSK3), forkhead box O transcription factors (FoxO) resulting in cell cycle entry, survival and suppression of pro-apoptotic pathways [233-235] (Figure 4.1.2). Activated EGFR also activates other signaling pathways including the PLC- , c-src and STATs [236-239].

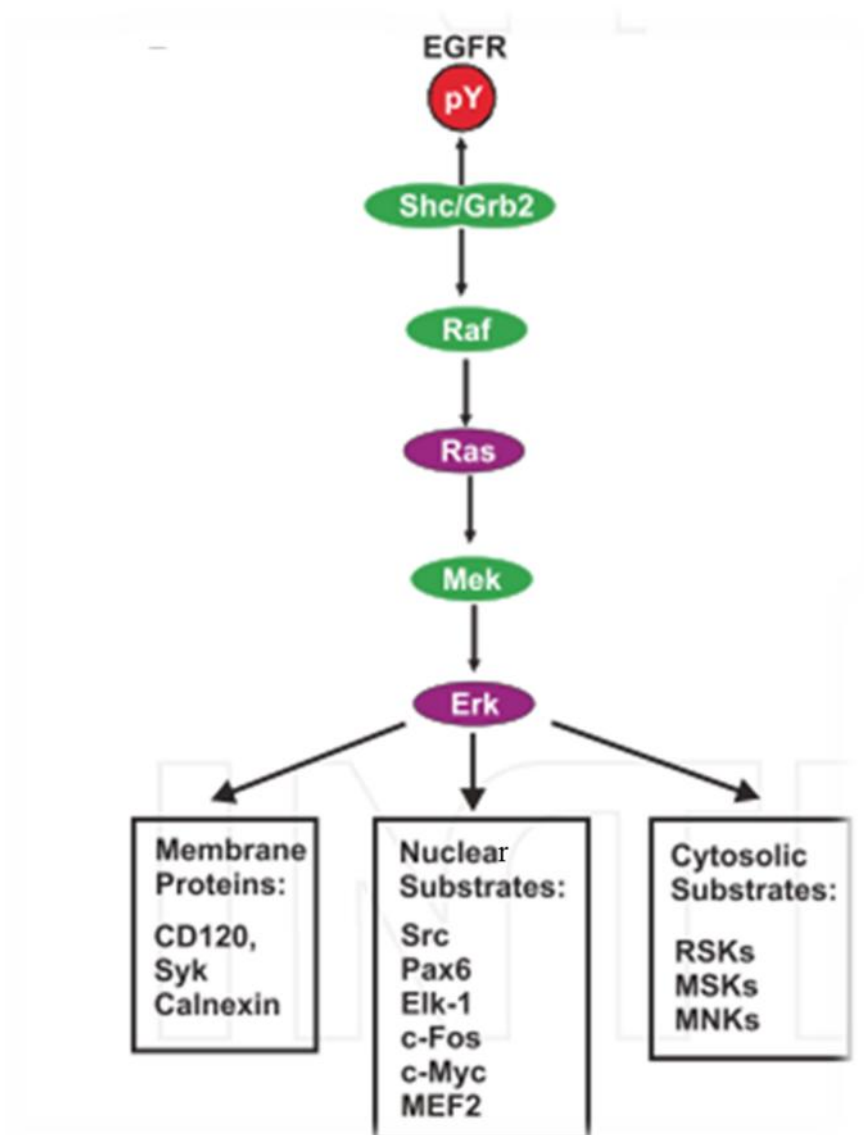


Figure 4.2: Activation of the downstream Ras-Raf-ERK pathway by EGFR and the downstream targets.

Figure modified from open access book chapter Wang et al., Mutual Regulation of Receptor-Mediated Cell Signalling and Endocytosis: EGF Receptor System as an Example

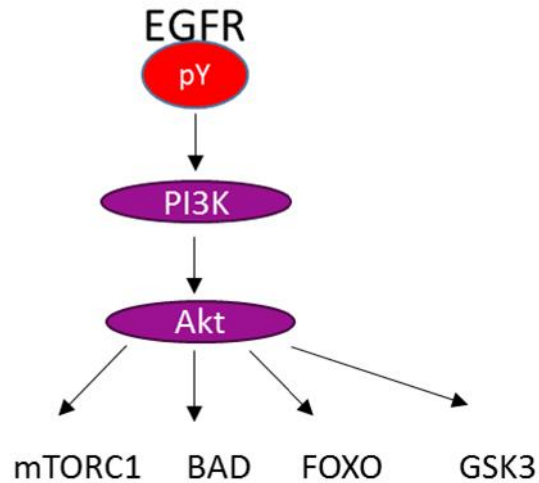


Figure 4.3: Activation of the PI3K/AKT pathway by EGFR and its downstream targets.

Figure modified from open access book chapter, Wang et al., Mutual Regulation of Receptor-Mediated Cell Signalling and Endocytosis: EGF Receptor System as an Example

Mutations that lead to overexpression, activation and misregulation of the EGFR family members are implicated in 30% of epithelial cancers. Activation of ErbB2 homodimers and ErbB1-ErbB2 heterodimers result in constitutive proliferation and filling of the luminal space in mammary epithelial cysts [217]. Aberrant hyperactivation of EGFR signaling is associated with early lumen-filling lesions, loss of epithelial polarity and disruption of adherens junctions in a renal cell carcinoma model in mice [240].

Activation of the EGFR pathway is also implicated in the induction of EMT. Results from the previous chapter show that conditioned media from carcinoma cells, and sE-cad can upregulate expression of EMT markers N-cadherin, fibronectin and actin stress fibers in MDCK cysts. However the mechanism by which this occurs is not

known. Fibronectin is a component of the extracellular matrix and is secreted by cancer associated fibroblasts and tumor cells in the TME [125]. Activation of the PI3K/AKT/mTOR and the NF- κ B pathway is implicated in excessive ECM production [241]. The PI3K/AKT pathway is also involved in fibronectin transcription and its alternative splicing resulting in the formation of plasma and cellular fibronectin [241]. It is also crucial in fibroblast activation, proliferation, and collagen production [242]. EGF also induces fibronectin expression in human dermal fibroblasts [243]. Fibronectin expression can in turn stimulate IL-18 expression and the Wnt7a signaling pathway [244, 245]. Fibronectin is involved in cell migration via its interaction with $\alpha_5\beta_1$ and activating integrin signaling [246]. The mechanism and role of fibronectin expression in lumen filled cysts is investigated in this chapter.

Our results also show increased N-cadherin expression in lumen filled epithelial cysts. N-cadherin is re-expressed in other cells of the TME including fibroblasts, endothelial cells and neurons [247]. Tumor cells interact with other cells in the TME via N-cadherin heterotypic ligation [247]. These interactions and N-cadherin mediated signaling is found to be crucial for receptor stability, invasion and metastasis [209]. In breast cancer cells, N-cadherin binds to the FGF receptor, stabilizing it at the cell surface and also enhancing its sensitivity to FGF-2 [209]. FGFR signaling is crucial in cancer cell invasion and MMP-9 activation. Additionally, N-cadherin can also undergo ectodomain shedding to release a 90 kDa soluble N-cadherin fragment into the extracellular milieu [248]. N-cadherin cleavage causes release of β -catenin from the cell surface, leading to activation of wnt signaling [249, 250]. Soluble N-cadherin also enhances cell migration, invasion and facilitates angiogenesis [249, 251, 252]. Thus, N-cadherin re-expression plays a vital role in tumor progression.

In tumor cells, sE-cad mediates its pro-oncogenic effects predominantly by activating the epidermal growth factor receptor (EGFR) pathway. *In vitro* and *in vivo* studies have shown that soluble E-cadherin (sE-cad) acts as a tumor promoting protein and these pro-oncogenic effects of sE-cad are mediated by activating several receptor tyrosine kinase (RTKs) pathways. Najy and colleagues were first to demonstrate that sE-cad complexes with the HER2 and HER3 receptors of the EGFR family in the MCF-7 breast cancer cells resulting in enhanced tumor cell migration and invasion[117]. In squamous cell carcinoma cells, sE-cad contributes to skin carcinogenesis via association with HER 1-3 and insulin-like growth factor-1 receptor (IGF-1R) resulting in activation of downstream mitogen-activated protein kinase (MAPK)-phosphatidylinositol 3-kinase (PI-3K)/AKT/mammalian target of rapamycin (mTOR) and inhibitor of apoptosis(IAP) signaling [118, 119]. Brouxhon and colleagues also demonstrated that sE-cad can act as a potential therapeutic target in squamous skin carcinogenesis as well as in Her2⁺ breast carcinoma. E-cadherin ectodomain specific monoclonal antibody Decma-1 was found to suppress tumor growth by downregulation of the HER family members and components of the MAPK-PI3K/AKT/mTOR pathways resulting in apoptosis [120, 253]. I hypothesize that sE-cad induced lumen filling and EMT in normal epithelial cysts is mediated by EGFR activation.

4.2 Materials and Methods

4.2.1 Cell lines

Madin-Darby canine kidney cells (MDCK) purchased from American Type Culture Collection (Manassas, VA) and Moloney Sarcoma virus-transformed MDCK cell line (MSV-MDCK) described previously were maintained in DMEM with 1 g/L

sodium bicarbonate, 10% fetal bovine serum, 1 mM L-glutamine, 100 U/ml penicillin, and 100 µg/ml streptomycin and were used for all the experiments described in this chapter.

4.2.2 Antibodies and Reagents

Primary antibodies used in this chapter 4 for immunoblotting and immunostaining were as follows: E-cadherin antibody Decma-1 (Sigma-Aldrich), MMP-9 (Santa Cruz Biotechnology), Ki67 and N-cadherin antibodies were purchased from Abcam, Fibronectin and β -catenin antibodies were obtained from BD Transduction Laboratories, Smooth Muscle Actin (Santa Cruz Biotechnology), Total EGFR (Fitzgerald Industries), Phospho-EGF Receptor (Tyr 1068), Phospho-AKT (Ser473), Phospho-p44/42 MAPK (Erk1/2), Grb2, Total AKT, Total MAPK, Cyclin D1, Ki67, Bcl2 antibodies were purchased from Cell Signaling Technology. The mouse, rabbit and rat horseradish peroxidase-conjugated secondary antibodies were obtained from Cell Signaling Technology. Anti-Mouse Alexa Fluor-488, Anti-Rabbit Alexa 633, Alexa-Fluor-546-conjugated phalloidin and TOPRO-3 were purchased from Molecular Probes (Eugene, OR). FITC- and Texas Red-labeled, affinity-purified secondary antibodies were obtained from Jackson ImmunoResearch Laboratories (West Grove, PA).

Growth factor-reduced MatrigelTM (Corning Discovery Labware) was used for three-dimensional culture. Protein-free, serum-free UltraDOMATM media (Lonza) was used for conditioned medium experiments. Corning cell recovery solution was used to harvest 3D cultures from the MatrigelTM matrix. Broad spectrum MMP inhibitor Marimastat, U0126 and LY294002 were purchased from Tocris (Minneapolis, MN).

Recombinant human EGF from Peptotech, EGFR Inhibitor CL-387,785 and MMP-9 Inhibitor I (CAS1177749-58-4) were purchased from EMD Millipore Chemicals.

4.2.3 Immunofluorescence of 3D Matrigel™ cultures

Cells grown in Matrigel™ were prepared and immunostained as follows: 3D MDCK cultures were fixed with 4% paraformaldehyde for 15 minutes at room temperature, washed three times with phosphate-buffered saline (PBS), then permeabilized and blocked with PBS, 0.7% fish skin gelatin and 10% saponin (PFS) for 30 minutes at room temperature. The fixed and permeabilized cysts were stained for the following proteins: β -catenin, actin, and phospho EGFR, Ki67, Bcl2, N-cadherin and Fibronectin by incubating the antibodies at 1:400 dilution in PFS overnight at 4°C. Staining was detected using Alexa-488, 546- and 633-conjugated secondary antibodies at 1:400 dilution in PFS and added to cultures for 2 h at room temperature. TOPRO-3 at 1:1000 dilution was used to stain nuclei. Cells and cysts were then washed with PBS three times and used for imaging.

4.2.4 Confocal microscopy and quantitation of 3D cysts

Images were captured using a Leica TCS SP5 scanning confocal microscope (Leica Microsystems Inc., Buffalo Grove, IL) using a 63X/1.4 NA oil immersion objective lens. The cysts were assessed for the presence of cells within the lumen. The number of cysts with clear or filled lumens were counted across at least ten different random fields and expressed as a percentage of total number of cysts. At least 100 cysts were examined per experimental group. All images were captured using the same laser intensity and gain/offset settings.

4.2.5 Generating 3D cell lysates and conditioned media from 3D cultures

3D cyst protein lysates were prepared by recovering cultured cells from the Matrigel™ basement matrix using a cell recovery solution (Corning Life Sciences Product#354253) following the manufacturer's instructions. The harvested cysts were then lysed as described previously [167]. Briefly, chilled RIPA buffer (50 mM Tris-HCl pH 7.4, 1% NP-40, 0.5 % Na-deoxycholate, 0.1% SDS, 150 mM NaCl, 2mM EDTA) supplemented with 1x protease inhibitor cocktail and 1% phenylmethylsulfonyl fluoride was added to the harvested cyst pellet. The cells in RIPA buffer were incubated on ice for 15 minutes followed by sonication for 15 minutes at 4°C. Lysates were cleared by centrifugation at 14,000 rpm for 15 minutes at 4°C. Supernatants were collected and the protein concentration was measured using Bio-Rad DC reagent (Bio-Rad Hercules, CA) as per manufacturer's instructions. For detection of proteins (shed sE-cad and MMP-9) in the CM, the cysts were grown in UltraDOMA-PF to prevent interference from albumin and other serum proteins present in the complete media. CM was collected and concentrated using Amicon ultracentrifugation filter devices (EMD, Millipore). Equal amounts of concentrated media were then loaded onto SDS-polyacrylamide gels and analyzed by immunoblotting or gelatin zymography.

4.2.6 Immunoblotting

SDS-PAGE was used to separate proteins in 3D cyst lysates which was then transferred on to a nitrocellulose membrane for immunoblotting as described in Chapter 3 of this dissertation.. For detection of Ki67 protein (Molecular weight 345-395 kDa) 3-8% Tris acetate (NuPage Novex) gradient gels were used. Antibody binding was visualized using Enhanced Chemiluminescence (ECL) and ECL prime (GE Healthcare). Image J software was utilized for immunoblot quantification and image analysis.

4.2.7 Co-Immunoprecipitation and Immunodepletion

Immunoprecipitation assays were carried out by harvesting cysts from Matrigel™ matrix using cell recovery solution (Corning Lifesciences) and preparing cell lysates using RIPA buffer as described above. pEGFR (Y-1068), Grb-2, E-cadherin and Myc-tag antibodies were pre-coupled to Protein G/A agarose beads with rabbit anti-mouse antibody (RAM) for 4 h and incubated overnight with 1000 µg of total protein lysate. The beads were washed and the samples eluted using 4x sample buffer. The samples were separated by SDS-PAGE and immunoblotted to visualize precipitated proteins.

4.3 Results

4.3.1 sE-cad and MSV-MDCK cells mediate lumen filling by activation of EGFR

Activation of the epidermal growth factor receptor (EGFR) has been implicated in sE-cad-mediated proliferation, migration and invasion effects [80, 83, 110, 115, 117, 118]. I hypothesized that induction of lumen filling in MDCK cysts by MSV-MDCK carcinoma cells and sE-cad is mediated by activation of EGFR signaling in MDCK cysts. Conditioned medium from MSV-MDCK also induces lumen filling therefore I examined EGFR activation in CM treated lumen filled cysts as well. The phosphorylation of EGFR in MDCK cysts following co-culture with MSV-MDCK cells or CM was visualized using immunofluorescence and confocal microscopy. As shown in Figure 4.4 A, co-culture of MDCK cysts with MSV-MDCK cells and CM disrupted luminal architecture and enhanced EGFR phosphorylation at the Tyr-1068. This phosphorylation could be blocked by the EGFR inhibitor CL-387,785. Stimulation with EGF also resulted in EGFR phosphorylation and disruption of the hollow luminal

architecture in MDCK cysts. Consistent with the immunofluorescence data, immunoblot analysis showed a 1.5- and 2-fold increase in the phosphorylation of EGFR in the co-culture and CM conditions, respectively (Figure 4.4 B). This phosphorylation was blocked by the EGFR inhibitor (Figure 4.4 B). Addition of purified sE-cad to MDCK cysts induced a 3-fold increase in EGFR phosphorylation, which was also inhibited by CL-387,785 (Figure 4.4 A and B). These results indicate that lumen filling induced by sE-cad or via MSV-MDCK carcinoma cells is mediated by EGFR activation.

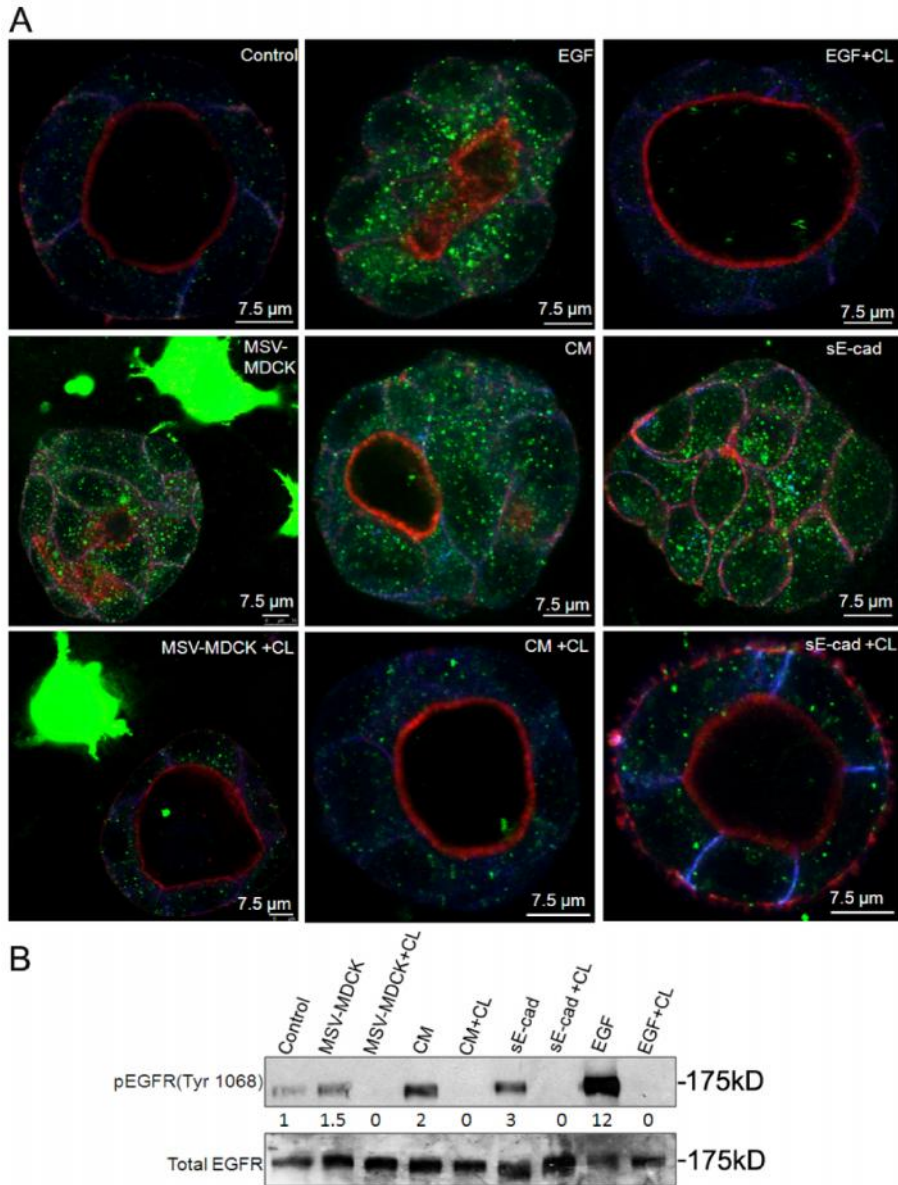


Figure 4.4: MSV-MDCK cells and sE-cad induce lumen filling in MDCK cells by EGFR activation.

A, Representative immunofluorescence images showing increased pEGFR expression in MDCK cysts treated with MSV-MDCK cells, CM sE-cad and EGF. Immunofluorescence showing actin (red), E-cadherin (blue), phospho EGFR (green). B, Immunoblot analysis showing phospho EGFR and total EGFR levels in MDCK 3D cyst lysates. 1 μ M CL-387,785 an EGFR kinase inhibitor was used to block EGFR activation for 4 h. EGF treatment is for 15 min.

4.3.2 Increased binding of Grb2 to pEGFR(Tyr-1068) with sE-cad Treatment

Depending on the phosphorylation pattern at the different tyrosine sites of EGFR, distinct downstream signaling pathways are activated [254-256]. We demonstrated that sE-cad, CM, and MSV-MDCK induced phosphorylation of EGFR at Tyr-1068. Tyr-1068 phosphorylation results in receptor dimerization, recruitment of Grb2 and subsequent activation of the AKT and ERK1/2 signaling pathway [257]. To determine whether the Grb2 adaptor protein binds EGFR Tyr-1068, CM or sE-cad-treated cyst lysates were immunoprecipitated with Grb2 antibody and blotted using an anti-phospho-EGFR-1068 antibody. Treatment with CM or purified sE-cad showed an enhanced association of phospho-EGFR with Grb2 in MDCK cells (Figure 4.5 A). At four h there was a 1.7 to 2-fold increase in association of phospho-EGFR with Grb2.

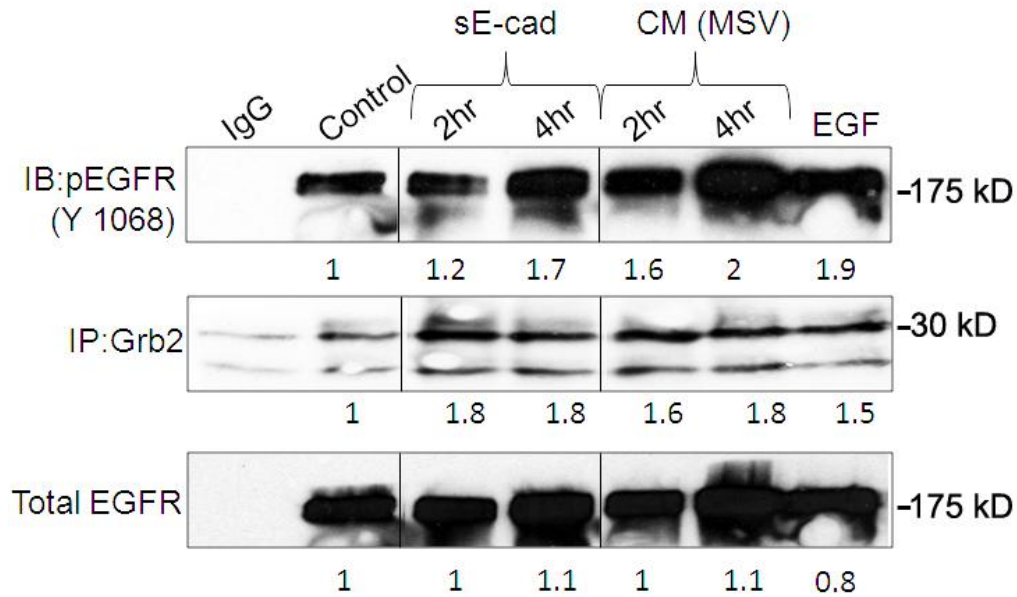


Figure 4.5: sE-cad induces phosphorylation of Tyr-1068 residue of EGFR resulting in Grb2 binding

A, Co-immunoprecipitation of phospho EGFR (Y-1068) with Grb2 in MDCK 3D cysts treated with CM or sE-cad at 2 h and 4 h.

4.3.3 Activation of the downstream ERK1/2 and AKT pathways during Lumen Filling

To determine whether increased Grb2 binding to phosphorylated EGFR (Y1068) activated the downstream signaling pathways, we examined the phosphorylation levels of ERK1/2 and AKT following co-culture and sE-cad treatment. Consistent with the activation of EGFR, immunoblotting data showed activation of downstream AKT and ERK1/2 signaling after co-culture or treatment with CM and sE-cad (Figure 4.6). Taken together, these results demonstrate that lumen filling induced by MSV-MDCK cells and sE-cad activates EGFR and subsequent downstream ERK1/2 and AKT signaling pathways in MDCK cysts.

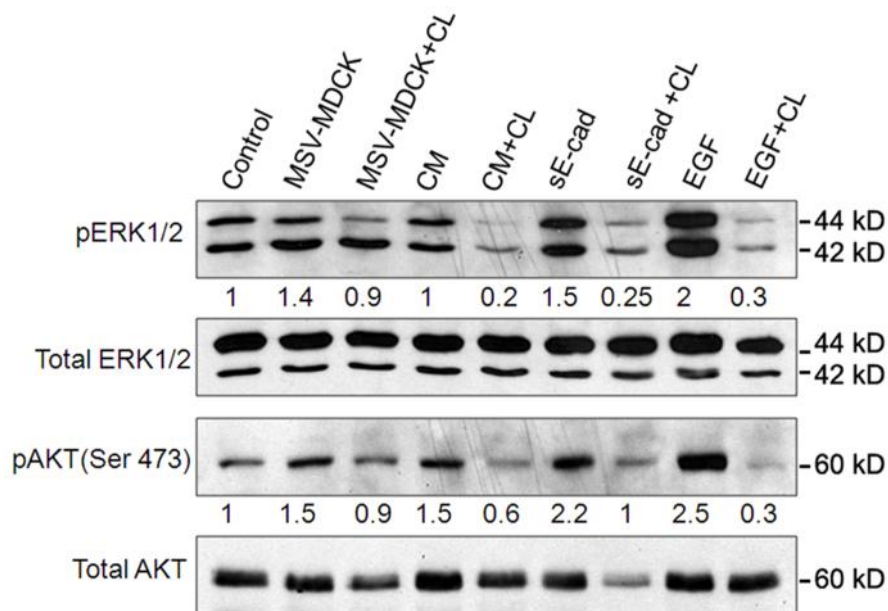


Figure 4.6: sE-cad and CM induce activation of downstream pERK1/2 and AKT pathways in MDCK cysts.

MDCK cysts were co-cultured with MSV-MDCK cells, CM, sE-cad and EGF for 4 h and phospho AKT, phospho ERK1/2 and total AKT and ERK1/2 levels were measured by immunoblot analysis. 1 μ M CL-387,785 EGFR inhibitor blocked AKT and ERK1/2 phosphorylation. . EGF treatment is for 15 min.

4.3.4 Mechanism of EGFR activation in CM treated cysts

To determine the mechanism of EGFR activation in CM treated cysts, we hypothesized that soluble factors present in the CM induce expression of EGF ligands in MDCK cysts resulting in activation of EGFR and downstream pathways in CM treated MDCK cysts. To examine the expression of EGF ligands in MDCK cysts we performed real time qPCR analysis. Our results show that mRNA levels of EGF ligand amphiregulin are 2.4 fold higher in CM treated cysts in comparison to the control MDCK cysts (Figure 4.7). Expression of ligands TGF- and EGF did not increase in CM treated cysts (Figure 4.7). These results indicate that EGFR activation by CM is by upregulating amphiregulin mRNA expression, but the significance of these changes are not clear.

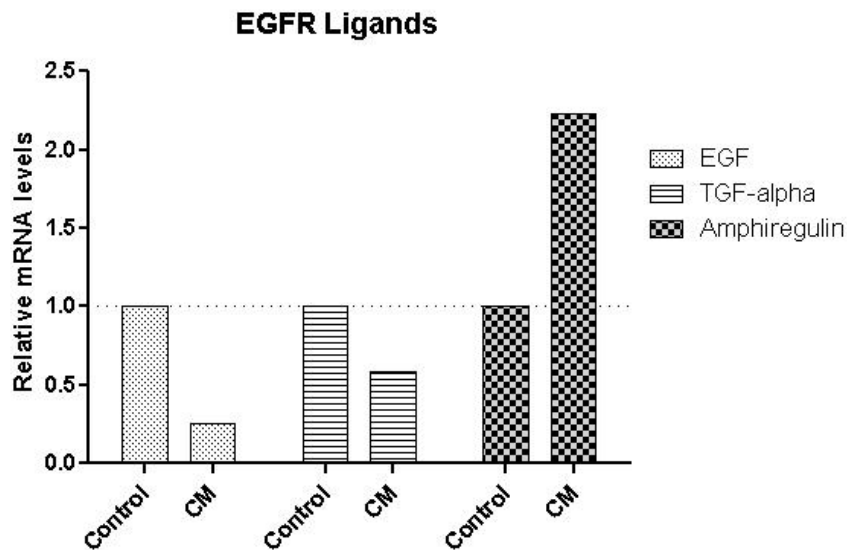


Figure 4.7: Amphiregulin mRNA levels increased in CM treated cysts.

RT-qPCR analysis showing fold change in mRNA levels of EGF, TGF- and Amphiregulin in CM treated MDCK cysts and control MDCK cysts.

4.3.5 Lumen filling is a consequence of increased survival and proliferation mediated by the MEK/ERK pathway

To determine whether activation of AKT and ERK1/2 signaling mediated by sE-cad results in an inhibition of apoptosis and/or increased cell proliferation which causes lumen filling, we analyzed expression levels of markers of cell proliferation and anti-apoptosis. Ki67 is a nuclear protein associated with cell proliferation [258]. Confocal microscopy showed that MDCK cysts treated with CM or sE-cad for 48 h have enhanced Ki67 nuclear staining, consistent with increased proliferation (Figure 4.8 A). Immunofluorescence analysis revealed enhanced expression of Bcl2, an anti-apoptotic marker in sE-cad- and CM-treated cysts compared to their respective controls (Figure 4.8 A). Immunoblot analysis of Ki67, cyclin D1, a second cell proliferation marker, and Bcl2 confirmed enhanced expression of these markers in sE-cad- or CM-treated cysts. Furthermore, the EGFR kinase inhibitor CL-387785 reduced the levels of cell proliferation and anti-apoptotic markers in the sE-cad- and CM-treated MDCK cysts (Figure 4.8 B). These results indicate that filling up of MDCK lumen by sE-cad and CM is caused by both increased cell proliferation and decreased apoptosis.

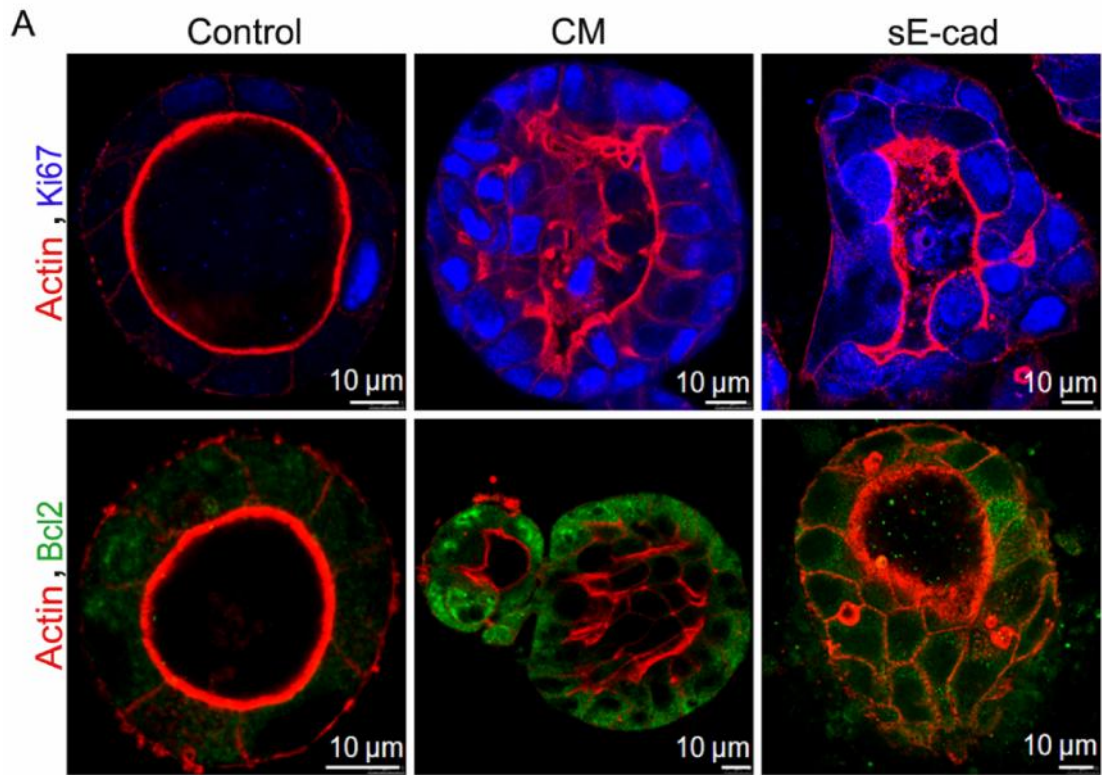


Figure 4.8 A: Lumen filling is a consequence of reduced apoptosis and increased proliferation.

Immunofluorescence images showing increased Ki67 and Bcl2 expression in MDCK cysts treated with CM and sE-cad for 48 h. Images were obtained from staining cysts with anti Bcl2 antibody (green), phalloidin-Alexa Fluor 546 (actin, red) and Ki67 (blue).

B

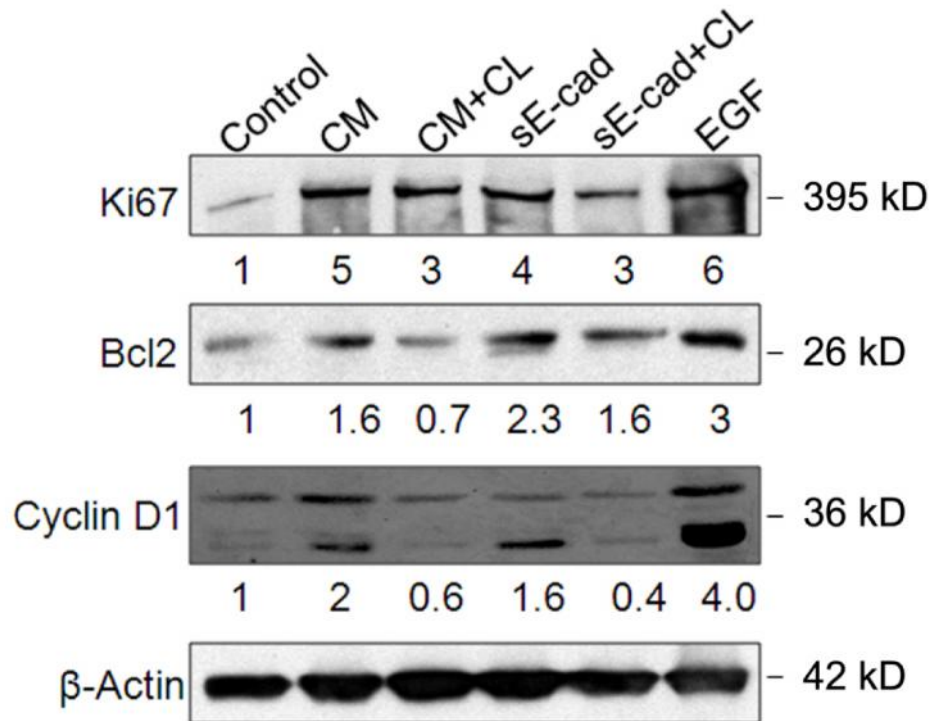


Figure 4.8 B: Lumen filling is a consequence of reduced apoptosis and increased proliferation.

Immunoblot showing Ki67, Bcl2 and cyclin D1 expression in MDCK cysts treated with sE-cad and CM. 1 μ M CL-387,785 was used to inhibit EGFR.

4.3.6 ERK1/2 is the primary pathway involved in lumen filling in MDCK cysts

In order to determine the role of downstream ERK1/2 and AKT pathways in lumen filling, CM or sE-cad treated cysts were treated with specific inhibitors of each pathway. Treatment with the MEK (upstream regulator of ERK) inhibitor U0126 suppressed the expression of both Ki67 and Bcl2 as revealed by immunofluorescence analysis (Figure 4.9 A-D). Further, lumen filling in CM or sE-cad treated cysts was reduced by 60-70% in presence of U0126. Inhibition of the AKT pathway with

LY294002 showed only a 25% reduction in lumen filling of CM and sE-cad treated cysts (Figure 4.9 B& D). Together, these results indicate that the MEK/ERK pathway predominantly drives lumen filling by increasing expression of Ki67 and Bcl2.

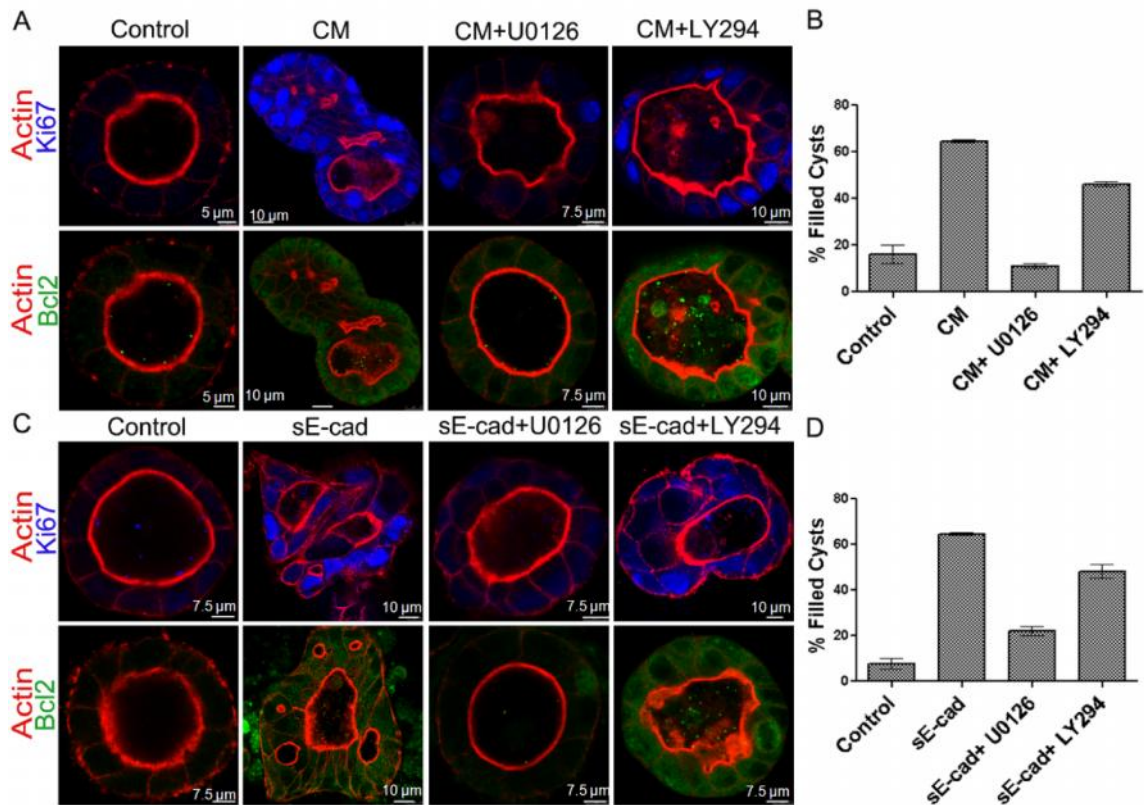


Figure 4.9: ERK1/2 is involved in lumen filling in MDCK cysts.

Immunofluorescence showing lumen filling in MDCK cysts treated with (A) CM or with sE-cad (C) in presence of 1 μ M U0126 to inhibit MEK/ERK pathway or 1 μ M LY294002 to block PI3K-AKT pathway at 48hr. Images were obtained from staining cysts with anti Bcl2 antibody (green), phalloidin-Alexa Fluor 546 (for actin, red) and Ki67 (blue). B & D, quantification showing percent lumen filled cysts with CM and sE-cad treatment in presence of inhibitors from three independent experiments. One hundred cysts under each condition were analyzed for the presence of hollow lumen and filled lumens.

We tested whether the concentration of U0126 and LY294002 (1 μ M) used in the immunofluorescence experiment effectively blocks the ERK1/2 and AKT pathways, respectively. Immunoblot analysis shows that 1 μ M concentration of U0126 selectively blocked ERK1/2 phosphorylation by over 80%. LY294002 (1 μ M) blocked AKT

phosphorylation by over 70% but also impaired ERK1/2 phosphorylation by 50% (Figure 4.10).

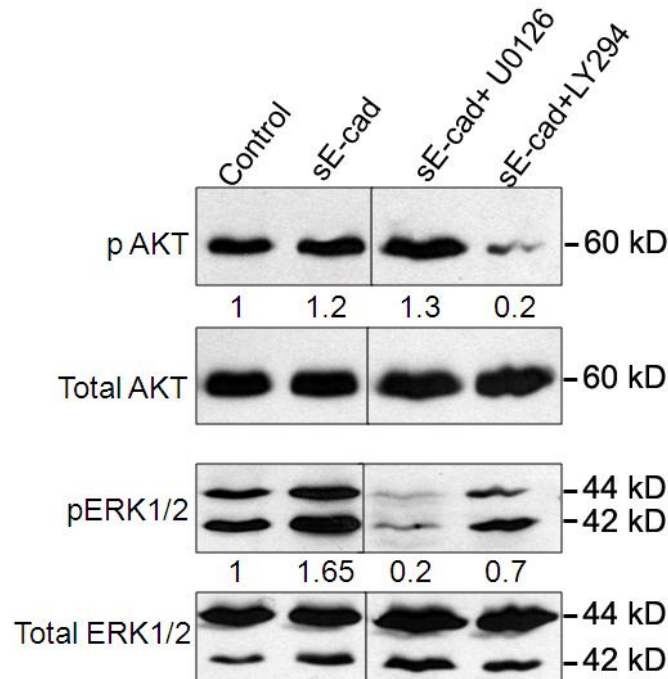


Figure 4.10: Immunoblot showing phospho ERK 1/2, phospho AKT and total ERK1/2 and total AKT levels in cysts treated with sE-cad in presence of inhibitors for 96h. (U0126 and LY294002 were used at 1 μ M concentration).

4.3.7 AKT is involved in the induction EMT in MDCK cysts

Results from the previous chapter demonstrated that long term treatment (96 h) with sE-cad and CM induced a mesenchymal phenotype in MDCK cysts. To determine the mechanisms involved in induction of EMT we analyzed the different signaling pathways implicated in EMT. PI3K/ AKT axis is frequently activated in human cancer and is known to be a key contributor in the induction of EMT [144]. To examine

whether the downstream ERK1/2 and AKT pathways are involved in induction of markers of EMT we used specific inhibitors of each pathway. Treatment with the PI3-kinase/AKT inhibitor LY294002 effectively blocked expression of EMT markers N-cadherin, fibronectin and actin stress fibers in MDCK cells in the sE-cad treated cysts (Figure 4.11). Also there was reduced lumen filling by sE-cad in presence of LY294002. By contrast, long-term sE-cad treated cysts in the presence of MEK/ERK inhibitor U0126 did not block expression of the EMT markers fibronectin, N-cadherin and stress fibers (Figure 4.11) Immunoblot analysis further validated these data, showing an increase in expression of EMT markers fibronectin, N-cadherin and MMP-9 after sE-cad treatment that was blocked in the presence of 1 μ M AKT inhibitor, LY294002, but not in the presence of 1 μ M MEK inhibitor levels (Figure 4.11). Interestingly, inhibition by U0126 enhanced expression of EMT markers in the lumen filled cysts (Figure 4.11 C), this is may be because MEK inhibition by U0126 is known to increase AKT activation [259], thereby further confirming the role of AKT in driving EMT in MDCK cysts.

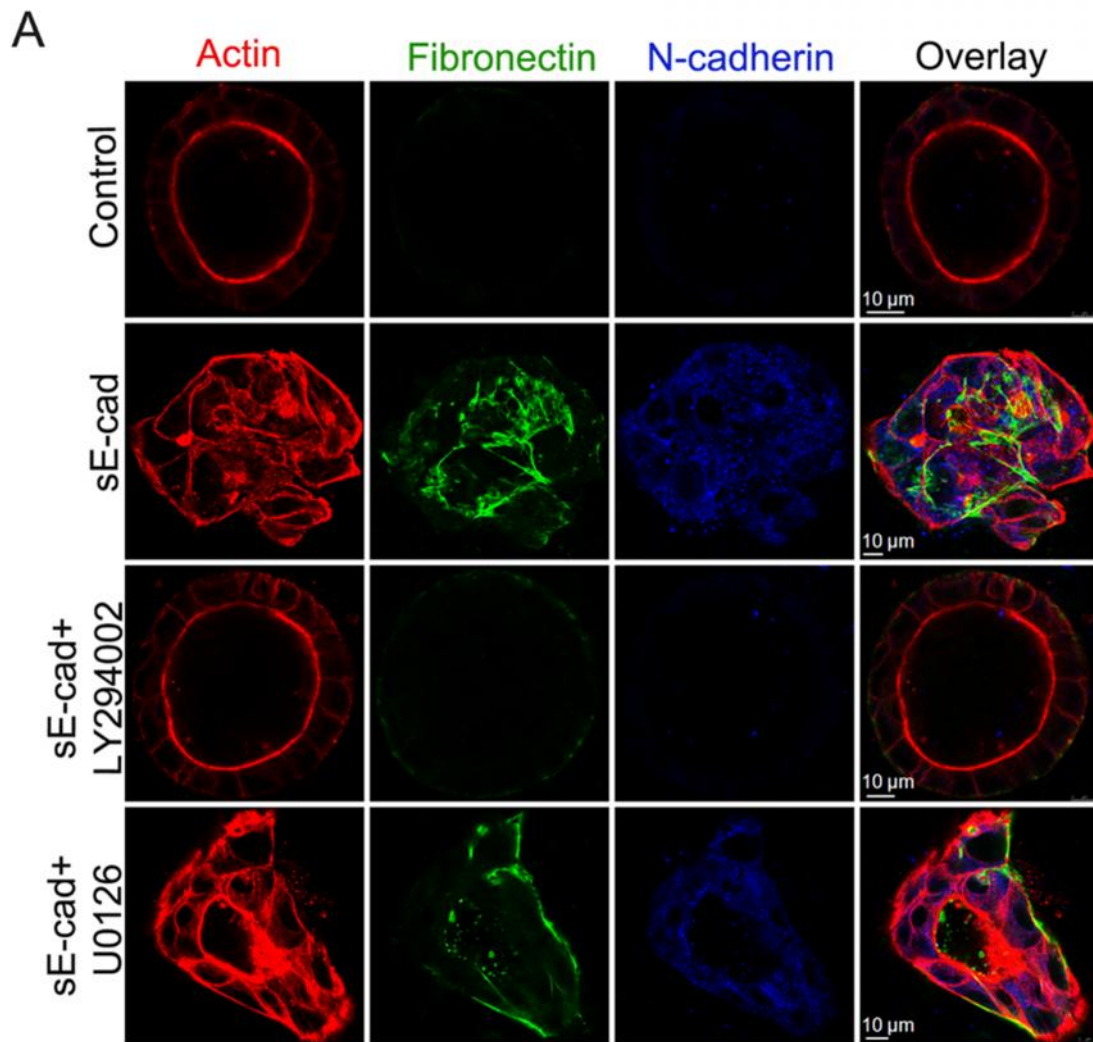


Figure 4.11 A: AKT is involved in the induction EMT in MDCK cysts. Immunofluorescence showing EMT expression in cysts treated with sE-cad in presence of inhibitors at 96 h. U0126 and LY294002 were used at 1 μ M each. Representative confocal images were obtained from staining cysts with anti-Fibronectin antibody (green), anti-N-cadherin antibody (blue), phalloidin-Alexa Fluor 546 (for actin, red).

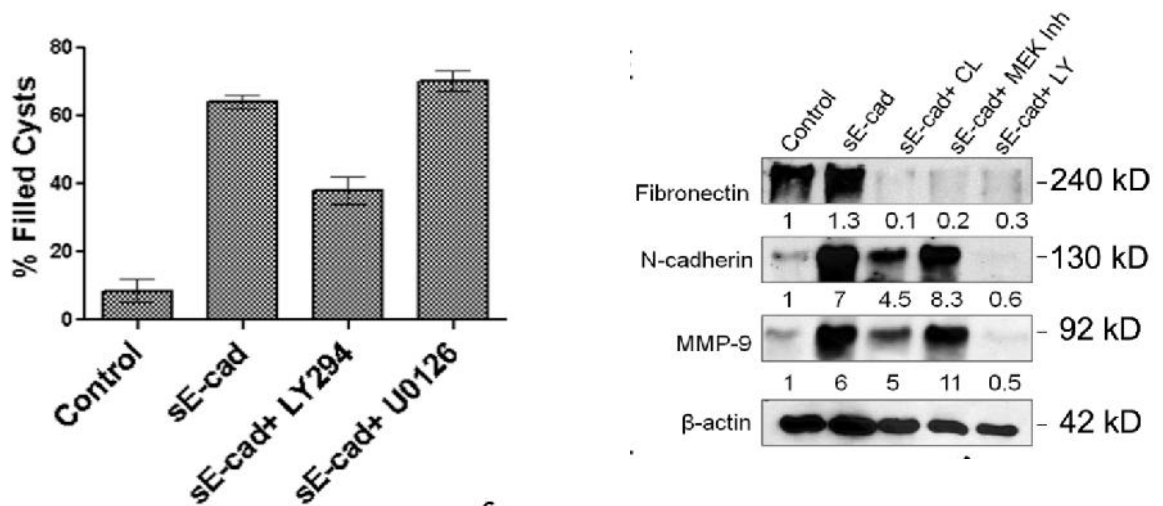


Figure 4.11 B: AKT is involved in the induction of EMT in MDCK cysts.

(B) Quantification of cysts undergoing EMT after 96 h treated with sE-cad in presence of inhibitors. (C) Immunoblot showing EMT markers Fibronectin, N-cadherin, MMP-9 in sE-cad treated cysts in presence of inhibitors. (U0126 and LY294002 were used at 1 μ M each). β -actin was used as a loading control.

Long term treatment with sE-cad revealed distinct activation patterns for ERK and AKT. While sE-cad-induced ERK activation diminished from 48 to 96 h the AKT phosphorylation was sustained over 96 h, as determined by immunoblot analysis (Figure 4.12). These results further authenticate sustained activation of AKT is involved in the induction of EMT in lumen filled MDCK cysts.

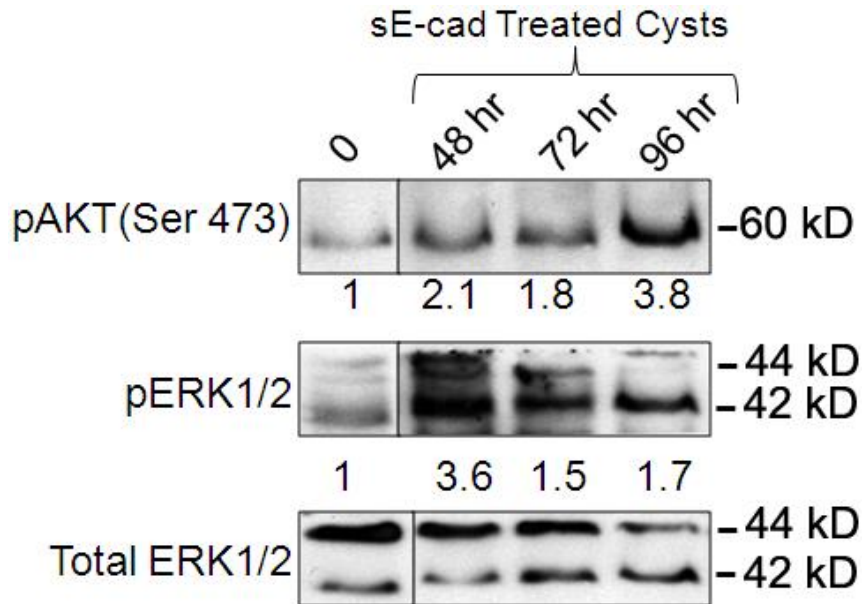


Figure 4.12: Immunoblot showing pAKT, pERK1/2 and total ERK1/2 in sE-cad treated cysts at 48, 72 and 96 h.

LY294002 also blocked EMT in CM treated cysts as observed previously in sE-cad treated cysts. Treatment with CM for 96 hr enhanced expression of Fibronectin, N-cadherin and actin stress fibers (Figure 4.13 A-C). This effect was blocked in the presence of 1 μ M AKT inhibitor, LY294002, but not in the presence of 1 μ M MEK inhibitor, U0126 (Figure 4.13 A-C). Immunoblot analysis also showed an increase in another EMT marker α -SMA however, α -SMA expression could not be detected with immunofluorescence analysis (Figure 4.13 C). Together, this data indicates that both sE-cad and CM induced EMT in epithelial cysts is driven by aberrant activation of AKT pathway.

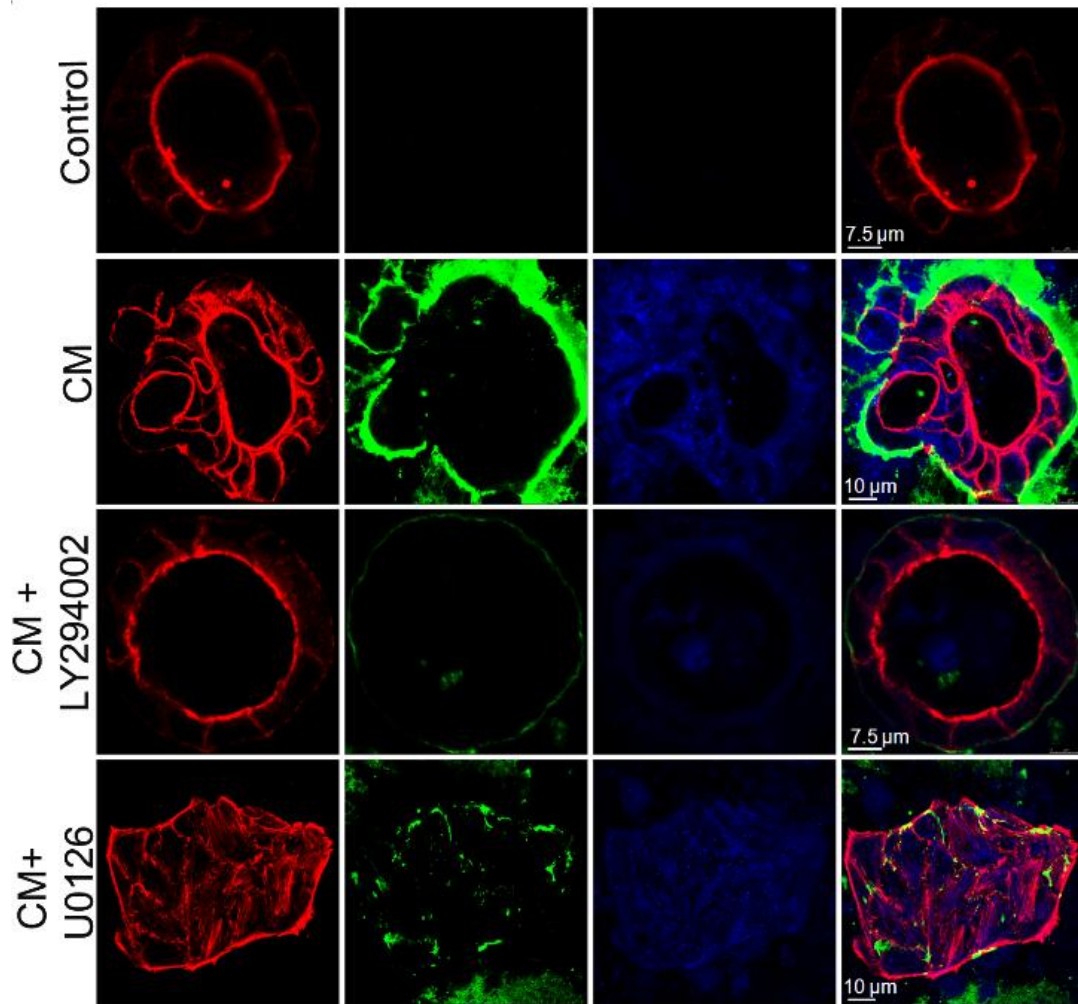


Figure 4.13 A: AKT is involved in the induction EMT in CM treated MDCK cysts. Immunofluorescence showing EMT expression in cysts treated CM in presence of inhibitors at 96 h. U0126 and LY294002 were used at 1 μ M each. Representative confocal images were obtained from staining cysts with anti-Fibronectin antibody (green), anti-N-cadherin antibody(blue), phalloidin-Alexa Fluor 546 (for actin, red) are shown.

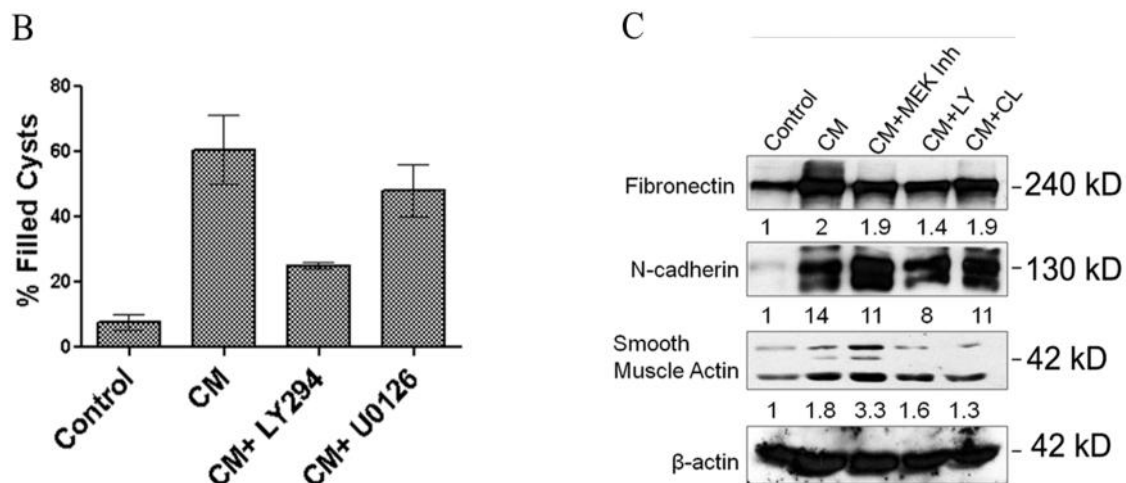


Figure 4.13 B: AKT is involved in the induction of EMT in CM treated MDCK cysts
 (B) Quantification of EMTed cysts after 96 h with CM treatment in presence of inhibitors. (C) Immunoblots showing EMT markers in CM treated cysts in presence of inhibitors.

4.3.8 Proposed Model for MSV-MDCK induced Lumen Filling and EMT in MDCK cysts

To summarize, our results demonstrate that carcinoma cells secrete MMP-9 which cleaves cellular E-cadherin from normal epithelial cells to generate sE-cad. We further demonstrated that sE-cad is a necessary and sufficient to induce lumen filling in epithelial cysts. Induction of lumen filling effect is mediated by the activation of EGFR and its downstream ERK1/2 and AKT pathways. Long-term sE-cad treatment induced EMT in epithelial cysts. Analysis of signaling pathways indicated that sE-cad induced activation of the ERK1/2 pathway is primarily involved in lumen filling, whereas, the AKT pathway plays a significant role in the induction of EMT (Figure 4.14). Our results also demonstrate that carcinoma cells utilize normal epithelial cells to generate the pro-oncogenic peptide sE-cad and release MMP-9 which facilitates normal cell

transdifferentiation. Thus, these studies indicate that carcinoma cells are capable of disrupting epithelial architecture and sequentially inducing lumen filling and EMT in adjacent normal epithelial cysts

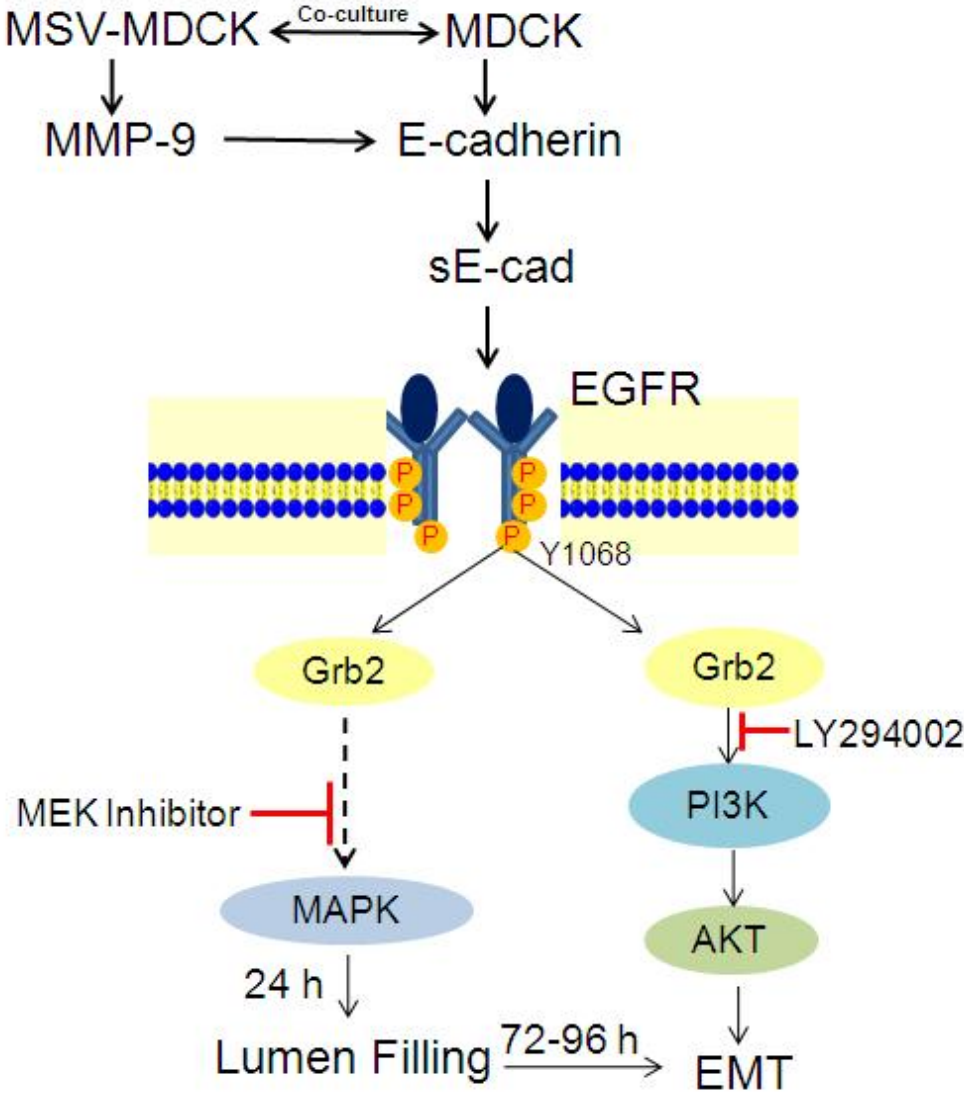


Figure 4.14: Proposed Model for sequential lumen filling and EMT induced by carcinoma cells in MDCK cysts.

4.4 Discussion

Our results demonstrate that carcinoma cells and sE-cad in the microenvironment can disrupt the epithelial architecture and sequentially induce lumen filling and EMT in the epithelial cysts. We demonstrated that the sE-cad-mediated loss of 3D architecture and lumen filling in MDCK cysts is driven by activation of the EGFR and its downstream ERK1/2 and AKT signaling pathways. We showed that co-culture with MSV-MDCK cells, CM or sE-cad-induced lumen filling in EGFR dependent manner. Activation of EGFR increased cell proliferation as well as reduced apoptosis thereby resulting in lumen filling, consistent with previous reports [154]. The mechanism by which sE-cad activates EGFR in our co-culture system is not known. Co-immunoprecipitation analysis did not detect an association between EGFR and sE-cad in MDCK cells, indicating that either this interaction is transient or too weak to be detected by immunoprecipitation. However, other groups have shown that sE-cad acts as a ligand to the EGFR family of receptors, leading to activation of oncogenic signaling in squamous cell carcinoma cells as well as breast cancer cells [117-119, 253]. It should be noted that the cell lines used in these studies were tumor derived cells. We speculate that, unlike in tumor cells where sE-cad activates the EGFR pathway by acting as its ligand, in normal epithelial cells EGFR may be transactivated by an interaction of sE-cad with cell bound E-cadherin as described below.

E-cadherin homophilic adhesion between adjacent cells transiently activates the EGFR and its downstream PI3K/AKT and ERK1/2 signaling cascades, thereby inducing cell survival and differentiation [260]. Previous reports from our laboratory have demonstrated that sE-cad retains the ability to interact with E-cadherin, and that E-cadherin is necessary for the anti-apoptotic effect of sE-cad in MDCK cells [115]. sE-cad binding to E-cadherin may mimic E-cadherin homophilic binding, resulting in the

activation of the EGFR signaling cascade. However, since sE-cad-E-cadherin interaction does not result in junction formation and cell adhesion, the subsequent EGFR transactivation may trigger atypical cellular pathways such as proliferation and survival.

Increased secretion of EGF ligands amphiregulin and TGF β in the CM is protective for the tumor cells and is associated with chemotherapeutic resistance to cetuximab in colorectal cancers [261]. We show that treatment with CM induced amphiregulin mRNA expression in the normal epithelial cells, it is possible that the tumor cells induce adjacent normal epithelial cells to increase amphiregulin secretion thereby providing resistance to tumor cells. Amphiregulin can also activate anti-apoptotic mechanisms by activating the Insulin Growth Factor (IGF)-1 pathway [262], however the role of IGF-1 pathway in lumen filling remains to be investigated.

We demonstrated that sE-cad produced either directly or indirectly by carcinoma cells can induce EMT in adjacent normal epithelial cells. The trigger that induces EMT following preneoplastic lumen filling is not known. Although both AKT and ERK1/2 pathways are activated, inhibition of AKT rather than ERK1/2 pathway abrogated EMT. Constitutively active AKT has been reported drive EMT within 72-96 h [263]. Here, we have shown the strength of the ERK1/2 signaling quelled after 48 h whereas AKT phosphorylation elevated at 72 and 96 h suggesting that sustained activation of AKT drives induction of EMT in MDCK cysts.

sE-cad blockade using a monoclonal antibody (mAb) has been shown to be an effective anti-tumor strategy in mouse models of breast carcinoma and squamous skin carcinoma. Anti sE-cad mAb treatment attenuates activation of multiple receptor tyrosine kinases such as HER1, HER2 and IGF-1R, and leads to activation of apoptotic pathways and inhibition of proliferative pathways, ultimately attenuating tumor growth

in mice [119, 120, 253]. Although a more detailed analysis examining the toxicity and specificity of anti sE-cad mAb therapy is necessary, antibody-mediated elimination of sE-cad could act synergistically with current EGFR-based therapies to improve efficacy in the treatment of a range of carcinomas.

Chapter 5

PERSPECTIVES AND FUTURE DIRECTIONS

The overall goal of this dissertation was to investigate the impact of tumor cells on adjacent epithelial cells using a 3D co-culture system and to determine whether sE-cad in the microenvironment exerts pro-oncogenic effects on normal epithelial cells (Figure 1). Carcinoma progression is no longer regarded as merely clonal expansion of tumor cells [264]. It is a multistep process wherein every component of the TME contributes in tumorigenesis [264]. In epithelial cancers, tumor cells interact with adjacent normal epithelial cells during the carcinoma *in situ* stages as well as during the homing of the metastatic cancer cells into the new secondary tumor site [149]. In this dissertation work, I investigated the impact of tumor cells on adjacent normal epithelial cells to gain insights into the host/tumor cell interaction during cancer progression. More specifically, I examined the role of sE-cad, a component of the TME, on carcinoma cell adjacent on normal epithelium.

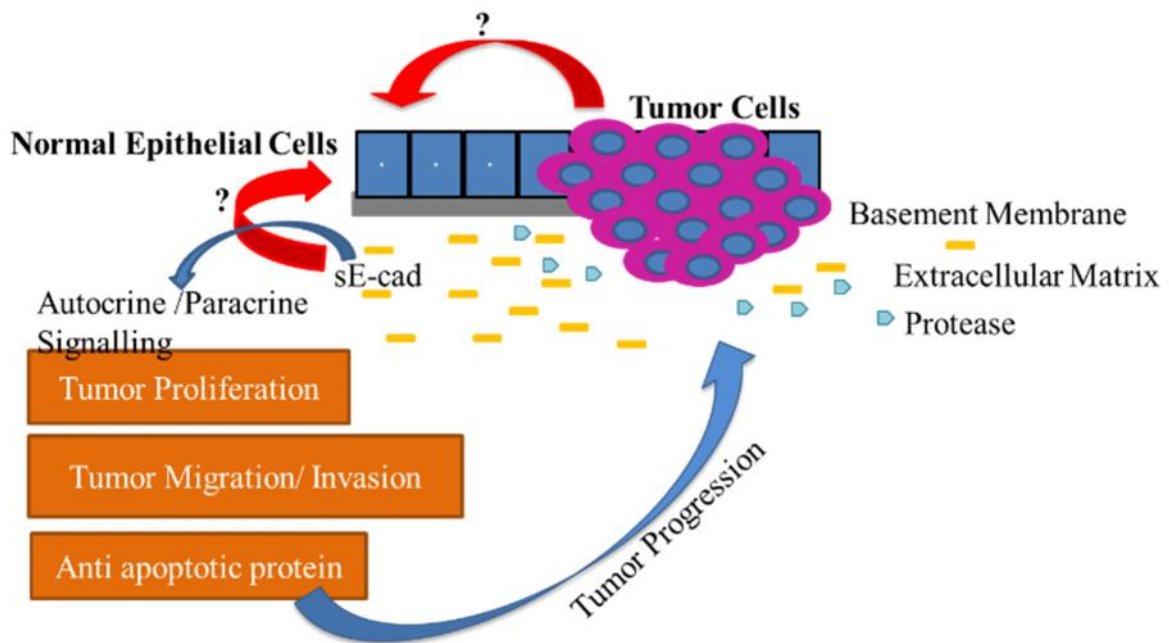


Figure 5.1: Pictorial representation of the overall goal of the dissertation work

This study reveals that adjacent normal epithelial cells are not innocent bystanders in the tumor microenvironment but are effectively modulated and possibly utilized by tumor cells to aid in tumor progression. This disruption of the epithelial cell phenotype and function by adjacent tumor cells can confer several advantages to tumor growth by facilitating oncogenic signaling and uncontrolled cell proliferation and anti-apoptotic survival mechanisms. The epithelial hollow lumen is a zone of strong apoptotic activity in which cells cannot proliferate. sE-cad and carcinoma cell induce lumen filling by blocking these normal apoptotic signals which suggests that these lumen filled epithelial cysts may be genetically damaged cells which fail to undergo apoptosis. However, further studies are needed to examine whether the tumor adjacent epithelial cells are genetically identical to the epithelial cells distant from the tumor site. This study shows that the lumen filled epithelial cysts on long term sE-cad and conditioned media treatment undergo EMT like changes via activation of aberrant AKT

signaling. Expression of EMT markers in these cells and atypical signaling events further make these cells more susceptible to genetic mutations. Thus, these tumor adjacent epithelial cells may not be ‘normal’ and are more likely to disseminate into the circulation.

Our results demonstrate tumor cells can induce increased secretion of MMP-9 in the transdifferentiated epithelial cells. MMP-9 degrades of the basement membrane and extracellular matrix components resulting in breakdown of the epithelial lining. Disruption of the epithelial cell lining by the tumor cells would allow easy access to endothelial cells, inflammatory cells and molecules across the epithelial barrier facilitating tumor vascularization and pro-tumor inflammation at the tumor site [265-267].

All the results in this dissertation work are demonstrated using MDCK cells as a source of epithelial cells. Although MDCK cells are canine kidney cells in origin they are an excellent model system for studying epithelial biology and they form acini like structures in 3D culture system replicating the *in vivo* epithelial tissues. MDCK is well-established cell line extensively used to study epithelial cell morphology and physiology and several findings from MDCK cells are pertinent in other human epithelial systems as well. Thus, we believe our findings on how transformed tumor cells impact the surrounding epithelial MDCK cells may be applicable to several epithelial cancers and not just kidney cancers.

This study establishes a novel platform to investigate tumor cells-epithelial cells dynamics in the 3D culture system. During the initial step of carcinogenesis, the epithelial cells are protective and eliminate tumor cells from their apical side by a mechanism known as apical extrusion [148]. Also, interaction with epithelial cells

inhibits tumor cells proliferation in cell culture systems [268]. This competitive interaction between normal epithelial cells and transformed cells is lost when epithelial cells transdifferentiate into a mesenchymal phenotype and are no longer be able to apically extrude tumor cells or secrete growth limiting factors. Investigating epithelial changes in response to tumor cell dynamics using 3D co-culture systems will help understand organ-specific affinity of different epithelial cancers during metastasis as well as help improve cellular response to drugs.

Additionally, this study also establishes a novel role of sE-cad in altering tumor adjacent epithelial morphology and inducing EMT like changes via aberrant EGFR activation in these cells. However, further studies need to be performed to investigate the mechanism of sE-cad mediated lumen filling in epithelial cysts. It is not known whether lumen filling occurs due to sE-cad-E-cad interaction or is a consequence of sE-cad induced signaling. We speculate that it is primarily the sE-cad induced cell signaling which results in lumen filling and EMT in MDCK cysts since *in vitro* studies have shown that sE-cad levels greater than 100 $\mu\text{g/ml}$ are necessary to disrupt the cell adhesion in MDCK cells [115]. Thus at 10 $\mu\text{g/ml}$ concentrations of sE-cad used in these experiments, it is unlikely that the disruption of cell adhesion by sE-cad –E-cad interaction causes disruption of the hollow lumen and this phenomenon chiefly may be a consequence atypical EGFR activation.

Further studies also need to be done to investigate the mechanism of sE-cad mediated EGFR activation. Colon cancer cells and breast cancer cells secrete EGF ligand amphiregulin in the conditioned media [269, 270], it needs to be investigated whether enhanced amphiregulin observed in the co-culture conditioned media in our system is responsible for activation of EGFR. Whether sE-cad induces ligand

production or transactivates EGFR by its interaction with E-cadherin during lumen filling needs to be further investigated.

This work indicates that elevated levels of sE-cad observed in the sera of cancer patients may be derived from both tumor cells as well as adjacent normal epithelial cells. Further these results suggest sE-cad in the microenvironment not only activates oncogenic signaling in tumor cells but also in the other cellular components of the TME such as the adjacent normal epithelial cells. Elevated sE-cad in tumor microenvironment can be indicative of aberrant EGFR activation in both tumor cells and normal cells. Thus, monitoring sE-cad in the sera of cancer patients can be an effective and inexpensive method to determine patient sensitivity to EGFR inhibitors. This work further validates the pro-oncogenic effects of sE-cad, therefore, effectively eliminating sE-cad from the blood or the tumor microenvironment using neutralizing antibody or peptides which bind specifically to sE-cad can contribute in slowing cancer progression as well as improve the current EGFR-based therapies targeted against various carcinomas. More research needs to be conducted for targeting sE-cad and development of specific sE-cad inhibitors.

5.1 Future Directions

While this dissertation has provided the proof of concept that tumor cells impact neighboring normal epithelial cells by inducing transdifferentiation, there are many unanswered questions that need to be addressed in the future as described below.

5.1.1 Does sE-cad binds to cellular E-cadherin as a monomer or an oligomer?

E-cadherin monomers form 'cis' and 'trans' homo dimers during cell adhesion and activate signaling events. It is not known whether sE-cad binds to cellular E-

cadherin as a monomer, dimer or oligomer in the media. Preliminary native gel electrophoresis result reveal that sE-cad can exist as a dimer (Figure 5.3), however these results need to be validated using size exclusion chromatography. Ever since elevated sE-cad levels have been reported in the sera of cancer patients, a wealth of information pertaining to its oncogenic role has been acquired. However, the oligomeric state of sE-cad is yet to be elucidated. Investigating the oligomeric state of sE-cad in the sera will help in understanding whether homodimerization is a prerequisite for sE-cad mediated signaling.

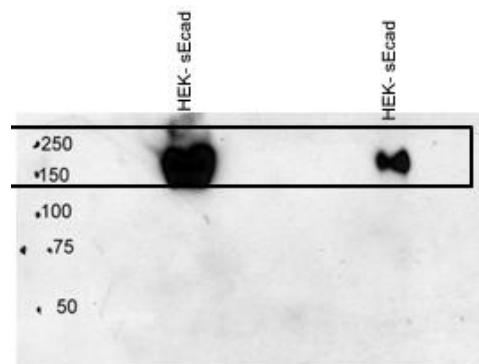


Figure 5.2: Purified sE-cad exists as 160 kDa dimer in the conditioned media

Immunoblot showing sE-cad at 160 kDa in presence of 1mM Ca^{2+} under native gel conditions. Two different loading concentrations of sE-cad from the sE-cad overexpressing HEK cells was loaded on the native gel.

5.1.2 Where does sE-cad bind cellular E-cadherin in polarized epithelial cells?

In polarized epithelial cells E-cadherin is localized to the AJs and also along the entire length of the basolateral plasma membrane. However, whether sE-cad displays preferential binding to a specific pool of E-cadherin (AJs or basolateral) is yet to be

elucidated. Recombinant sE-cad has a myc tag at its N-terminal and a myc antibody is used to differentiate it from the cellular E-cadherin. Preliminary immunofluorescence data reveal myc staining along the entire length of the basolateral membrane of MDCK cells indicating that sE-cad binds to basolaterally localized E-cadherin (Figure 5.4). Future studies using transmission electron microscopy and immunogold labeling are necessary to validate sE-cad interaction at the adherens junction. These findings will provide new insights into the cellular localization of sE-cad-E-cad interaction and help understand whether sE-cad interacts with the *cis* or *trans* E-cadherin dimers.

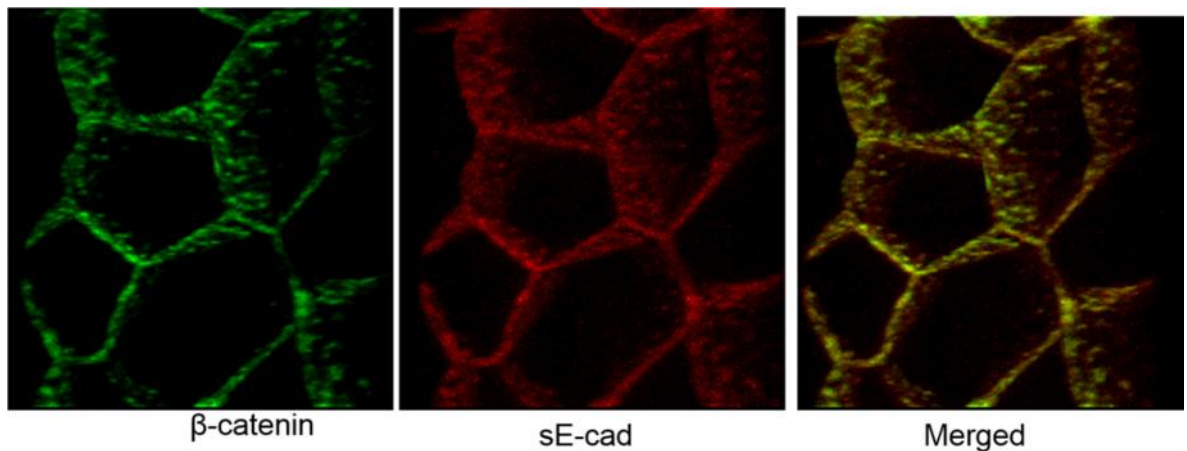


Figure 5.3: β -catenin and sE-cad show basolateral staining in MDCK cells.

Immunofluorescence showing β -catenin (green), sE-cad (anti-myc -Red) staining in MDCK cells treated with sE-cad. MDCK cells were grown on 0.4μ filters and treated with purified sE-cad for 4 h.

5.1.3 What is the mechanism of activation of EGFR leading to lumen filling and EMT?

We showed that EGFR pathway is involved in lumen filling, however the mechanism by which sE-cad activates the EGFR pathway and how this sequentially

induce lumen filling and EMT is not known. To determine the mechanism of EGFR activation, EGFR ligands in the extracellular media in sE-cad treated cells could be quantified using ELISA kits. If EGFR activation is not ligand mediated it could be transactivation of the receptor. Transactivation is much more complex involving multiple intracellular and extracellular events. For example altered cytoplasmic milieu inside the cells or ROS levels in the extracellular media are known to transactivate EGFR [271]. Experiments focused on blocking sE-cad-E-cad interaction by function blocking antibodies or EGTA to prevent abnormal activation of EGFR should be carried out in the future. The success of these experiments should help to develop novel therapeutic approaches to treat cancer.

5.1.4 Does sE-cad induces lumen filling and EMT in vivo preclinical models?

While I demonstrated proof-of-concept that sE-cad could induce sequentially lumen filling and EMT in 3D culture models, it is important to validate these findings in preclinical animal models. Future investigation on the validation of these findings in animal models should enable strategizing therapeutic approaches focused on attenuating sE-cad effects in patients. Also a better understanding of specific proteases involved in E-cadherin cleavage in different cancers will help designing inhibitors to prevent E-cadherin cleavage and generation of sE-cad. These protease inhibitors will help improve the efficacy of anti-cancer chemotherapeutics.

5.1.5 Utilizing the 3D culture system and lumen filling: Novel Assay Platform

Lumen filling and loss of apico-basal polarity are the hallmarks of epithelial cancer progression. 3D culture system can be used to study factors inducing preneoplastic lumen filling and provide insights into the pro-oncogenic effects of other

soluble factors. E-cadherin ectodomain shedding results in a shorter CTF2 fragment along with sE-cad. The shorter fragment has been implicated in wnt signaling however the direct role of the CTF2 fragment on tumor cells as well epithelial cells needs to be elucidated. An epithelial 3D culture system can be utilized to investigate the role of this CTF2 fragment.

Cellular interactions that occur during tumor progression such as invasion of cancer cells from the basal side of normal epithelial cells can only be investigated using a 3D co-culture setup. 3D co-culture model can also be utilized to investigate the role of sE-cad in facilitating homing of tumor cells to different types of 3D epithelial cells.

We demonstrate induction of EMT in epithelial structures. EMT can be examined in detail using time lapse confocal microscopy to reveal changes in cyst structure during the transitioning of epithelial cysts into mesenchymal structures. Long term treatment with sE-cad and CM upregulates EMT markers fibronectin, N-cadherin and actin stress fibres in the MDCK cysts. However the pathways and mechanisms implicated in induction of this EMT need to be further examined. Formation of actin stress fibers and cytoskeletal remodeling is regulated by the Rho signaling pathway. Understanding the involvement of Rho pathway in lumen filling would provide further insights into the mechanism of sE-cad and CM in inducing lumen filling. N-cadherin is known to activate the FGFR and the NF- κ B signaling pathway [209], however whether N-cadherin activates these pathways during EMT in epithelial cysts needs to be further investigated.

5.1.6 Investigating other possible pathological roles of sE-cad

E-cadherin is known to interact with KLRG1 receptor on T-lymphocytes and natural killer cells and suppress immune responses [42]. It is possible that sE-cad in the

microenvironment retains its ability to interact with T-lymphocytes and acts as an immunosuppressant. Thus elevated sE-cad shedding in normal epithelial cells can interfere with host immune response by serving as a dummy ligand to KLRG1 and conferring increased survival benefits to tumor cells. Additionally, elevated sE-cad levels in the sera are also prognostic of metastasis. sE-cad via its ability to interfere with cell adhesion and immune response can therefore act as a long range signaling molecule and aid in the preparation of secondary metastatic sites. More research needs to be conducted to explore sE-cad's function in protection of circulating tumor cells from immune cells as well as its ability in facilitating homing of tumor cells.

5.1.7 What is the impact of this study on cancer patients?

Results from this dissertation demonstrate that tumor cells can induce sE-cad shedding from adjacent normal epithelial cells via MMP production. This raises the possibility that elevated levels of sE-cad observed in the sera of cancer patients may be derived from both tumor cells as well as adjacent normal epithelial cells. Reducing the levels and inhibiting the activities of MMP or preventing sE-cad interaction with E-cadherin to block EGFR signaling may attenuate cancer progression and improve prognosis of cancer patients.

REFERENCES

1. Melo, S.A., et al., Cancer exosomes perform cell-independent microRNA biogenesis and promote tumorigenesis. *Cancer Cell*, 2014. **26**(5): p. 707-21.
2. Brouxhon, S.M., et al., Ectodomain-specific E-cadherin antibody suppresses skin SCC growth and reduces tumor grade: A multi-targeted therapy modulating RTKs and the PTEN-p53-MDM2 axis. *Mol Cancer Ther*, 2014.
3. Brouxhon, S.M., et al., Soluble E-cadherin: a critical oncogene modulating receptor tyrosine kinases, MAPK and PI3K/Akt/mTOR signaling. *Oncogene*, 2013.
4. Brouxhon, S.M., et al., Monoclonal Antibody against the Ectodomain of E-Cadherin (DECMA-1) Suppresses Breast Carcinogenesis: Involvement of the HER/PI3K/Akt/mTOR and IAP Pathways. *Clin Cancer Res*, 2013.
5. Gumbiner, B.M., Regulation of cadherin-mediated adhesion in morphogenesis. *Nat Rev Mol Cell Biol*, 2005. **6**(8): p. 622-34.
6. Takeichi, M., Cadherin cell adhesion receptors as a morphogenetic regulator. *Science*, 1991. **251**(5000): p. 1451-5.
7. Fagotto, F. and B.M. Gumbiner, Cell contact-dependent signaling. *Dev Biol*, 1996. **180**(2): p. 445-54.
8. Larue, L., et al., E-cadherin null mutant embryos fail to form a trophectoderm epithelium. *Proc Natl Acad Sci U S A*, 1994. **91**(17): p. 8263-7.
9. Takeichi, M., Morphogenetic roles of classic cadherins. *Curr Opin Cell Biol*, 1995. **7**(5): p. 619-27.
10. Overduin, M., et al., Solution structure of the epithelial cadherin domain responsible for selective cell adhesion. *Science*, 1995. **267**(5196): p. 386-9.
11. Shapiro, L., et al., Structural basis of cell-cell adhesion by cadherins. *Nature*, 1995. **374**(6520): p. 327-37.
12. Shapiro, L. and W.I. Weis, Structure and biochemistry of cadherins and catenins. *Cold Spring Harb Perspect Biol*, 2009. **1**(3): p. a003053.
13. Troyanovsky, R.B., O. Laur, and S.M. Troyanovsky, Stable and unstable cadherin dimers: mechanisms of formation and roles in cell adhesion. *Mol Biol Cell*, 2007. **18**(11): p. 4343-52.

14. Troyanovsky, R.B., E. Sokolov, and S.M. Troyanovsky, Adhesive and lateral E-cadherin dimers are mediated by the same interface. *Mol Cell Biol*, 2003. **23**(22): p. 7965-72.
15. Troyanovsky, R.B., E.P. Sokolov, and S.M. Troyanovsky, Endocytosis of cadherin from intracellular junctions is the driving force for cadherin adhesive dimer disassembly. *Mol Biol Cell*, 2006. **17**(8): p. 3484-93.
16. Pokutta, S., et al., Conformational changes of the recombinant extracellular domain of E-cadherin upon calcium binding. *Eur J Biochem*, 1994. **223**(3): p. 1019-26.
17. Nollet, F., P. Kools, and F. van Roy, Phylogenetic analysis of the cadherin superfamily allows identification of six major subfamilies besides several solitary members. *J Mol Biol*, 2000. **299**(3): p. 551-72.
18. Posy, S., L. Shapiro, and B. Honig, Sequence and structural determinants of strand swapping in cadherin domains: do all cadherins bind through the same adhesive interface? *J Mol Biol*, 2008. **378**(4): p. 954-68.
19. Nagar, B., et al., Structural basis of calcium-induced E-cadherin rigidification and dimerization. *Nature*, 1996. **380**(6572): p. 360-4.
20. Nose, A., K. Tsuji, and M. Takeichi, Localization of specificity determining sites in cadherin cell adhesion molecules. *Cell*, 1990. **61**(1): p. 147-55.
21. Shan, W.S., et al., The adhesive binding site of cadherins revisited. *Biophys Chem*, 1999. **82**(2-3): p. 157-63.
22. Zhang, Y., et al., Resolving cadherin interactions and binding cooperativity at the single-molecule level. *Proc Natl Acad Sci U S A*, 2009. **106**(1): p. 109-14.
23. Haussinger, D., et al., Calcium-dependent homoassociation of E-cadherin by NMR spectroscopy: changes in mobility, conformation and mapping of contact regions. *J Mol Biol*, 2002. **324**(4): p. 823-39.
24. Noe, V., et al., Inhibition of adhesion and induction of epithelial cell invasion by HA V-containing E-cadherin-specific peptides. *J Cell Sci*, 1999. **112** (Pt 1): p. 127-35.
25. Alattia, J.R., et al., Lateral self-assembly of E-cadherin directed by cooperative calcium binding. *FEBS Lett*, 1997. **417**(3): p. 405-8.

26. Yap, A.S., et al., Lateral clustering of the adhesive ectodomain: a fundamental determinant of cadherin function. *Curr Biol*, 1997. **7**(5): p. 308-15.
27. Hirokawa, N. and J.E. Heuser, Quick-freeze, deep-etch visualization of the cytoskeleton beneath surface differentiations of intestinal epithelial cells. *J Cell Biol*, 1981. **91**(2 Pt 1): p. 399-409.
28. Miyaguchi, K., Ultrastructure of the zonula adherens revealed by rapid-freeze deep-etching. *J Struct Biol*, 2000. **132**(3): p. 169-78.
29. Tepass, U., et al., Cadherins in embryonic and neural morphogenesis. *Nat Rev Mol Cell Biol*, 2000. **1**(2): p. 91-100.
30. Pecina-Slaus, N., Tumor suppressor gene E-cadherin and its role in normal and malignant cells. *Cancer Cell Int*, 2003. **3**(1): p. 17.
31. Riethmacher, D., V. Brinkmann, and C. Birchmeier, A targeted mutation in the mouse E-cadherin gene results in defective preimplantation development. *Proc Natl Acad Sci U S A*, 1995. **92**(3): p. 855-9.
32. Cavallaro, U. and G. Christofori, Cell adhesion and signalling by cadherins and Ig-CAMs in cancer. *Nat Rev Cancer*, 2004. **4**(2): p. 118-32.
33. Andl, C.D. and A.K. Rustgi, No one-way street: cross-talk between e-cadherin and receptor tyrosine kinase (RTK) signaling: a mechanism to regulate RTK activity. *Cancer Biol Ther*, 2005. **4**(1): p. 28-31.
34. McLachlan, R.W., et al., E-cadherin adhesion activates c-Src signaling at cell-cell contacts. *Mol Biol Cell*, 2007. **18**(8): p. 3214-23.
35. Clevers, H., Wnt/beta-catenin signaling in development and disease. *Cell*, 2006. **127**(3): p. 469-80.
36. Grigoryan, T., et al., Deciphering the function of canonical Wnt signals in development and disease: conditional loss- and gain-of-function mutations of beta-catenin in mice. *Genes Dev*, 2008. **22**(17): p. 2308-41.
37. Orsulic, S., et al., E-cadherin binding prevents beta-catenin nuclear localization and beta-catenin/LEF-1-mediated transactivation. *J Cell Sci*, 1999. **112** (Pt 8): p. 1237-45.
38. Gottardi, C.J., E. Wong, and B.M. Gumbiner, E-cadherin suppresses cellular transformation by inhibiting beta-catenin signaling in an adhesion-independent manner. *J Cell Biol*, 2001. **153**(5): p. 1049-60.

39. Priya, R., A.S. Yap, and G.A. Gomez, E-cadherin supports steady-state Rho signaling at the epithelial zonula adherens. *Differentiation*, 2013. **86**(3): p. 133-40.
40. Soto, E., et al., p120 catenin induces opposing effects on tumor cell growth depending on E-cadherin expression. *J Cell Biol*, 2008. **183**(4): p. 737-49.
41. Kuphal, S., et al., Loss of E-cadherin leads to upregulation of NFkappaB activity in malignant melanoma. *Oncogene*, 2004. **23**(52): p. 8509-19.
42. Solanas, G., et al., E-cadherin controls beta-catenin and NF-kappaB transcriptional activity in mesenchymal gene expression. *J Cell Sci*, 2008. **121**(Pt 13): p. 2224-34.
43. Karin, M. and F.R. Greten, NF-kappaB: linking inflammation and immunity to cancer development and progression. *Nat Rev Immunol*, 2005. **5**(10): p. 749-59.
44. Gumbiner, B.M. and N.G. Kim, The Hippo-YAP signaling pathway and contact inhibition of growth. *J Cell Sci*, 2014. **127**(Pt 4): p. 709-17.
45. Grundemann, C., et al., Cutting edge: identification of E-cadherin as a ligand for the murine killer cell lectin-like receptor G1. *J Immunol*, 2006. **176**(3): p. 1311-5.
46. Ito, M., et al., Killer cell lectin-like receptor G1 binds three members of the classical cadherin family to inhibit NK cell cytotoxicity. *J Exp Med*, 2006. **203**(2): p. 289-95.
47. Kilshaw, P.J., Alpha E beta 7. *Mol Pathol*, 1999. **52**(4): p. 203-7.
48. Nakamura, S., et al., Molecular basis for E-cadherin recognition by killer cell lectin-like receptor G1 (KLRG1). *J Biol Chem*, 2009. **284**(40): p. 27327-35.
49. Bickers, D.R. and D.R. Lowy, Carcinogenesis: a fifty-year historical perspective. *J Invest Dermatol*, 1989. **92**(4 Suppl): p. 121S-131S.
50. Birchmeier, W. and J. Behrens, Cadherin expression in carcinomas: role in the formation of cell junctions and the prevention of invasiveness. *Biochim Biophys Acta*, 1994. **1198**(1): p. 11-26.
51. Bracke, M.E., F.M. Van Roy, and M.M. Mareel, The E-cadherin/catenin complex in invasion and metastasis. *Curr Top Microbiol Immunol*, 1996. **213** (Pt 1): p. 123-61.

52. Efstathiou, J.A., et al., Mutated epithelial cadherin is associated with increased tumorigenicity and loss of adhesion and of responsiveness to the motogenic trefoil factor 2 in colon carcinoma cells. *Proc Natl Acad Sci U S A*, 1999. **96**(5): p. 2316-21.
53. Machado, J.C., et al., E-cadherin gene mutations provide a genetic basis for the phenotypic divergence of mixed gastric carcinomas. *Lab Invest*, 1999. **79**(4): p. 459-65.
54. Umbas, R., et al., Relation between aberrant alpha-catenin expression and loss of E-cadherin function in prostate cancer. *Int J Cancer*, 1997. **74**(4): p. 374-7.
55. Asnaghi, L., et al., E-cadherin negatively regulates neoplastic growth in non-small cell lung cancer: role of Rho GTPases. *Oncogene*, 2010. **29**(19): p. 2760-71.
56. Mateus, A.R., et al., EGFR regulates RhoA-GTP dependent cell motility in E-cadherin mutant cells. *Hum Mol Genet*, 2007. **16**(13): p. 1639-47.
57. Becker, K.F., et al., E-cadherin gene mutations provide clues to diffuse type gastric carcinomas. *Cancer Res*, 1994. **54**(14): p. 3845-52.
58. Berx, G., et al., E-cadherin is inactivated in a majority of invasive human lobular breast cancers by truncation mutations throughout its extracellular domain. *Oncogene*, 1996. **13**(9): p. 1919-25.
59. Huiping, C., et al., Chromosome alterations and E-cadherin gene mutations in human lobular breast cancer. *Br J Cancer*, 1999. **81**(7): p. 1103-10.
60. Risinger, J.I., et al., Mutations of the E-cadherin gene in human gynecologic cancers. *Nat Genet*, 1994. **7**(1): p. 98-102.
61. Perri, F., et al., Aberrant DNA methylation in non-neoplastic gastric mucosa of H. Pylori infected patients and effect of eradication. *Am J Gastroenterol*, 2007. **102**(7): p. 1361-71.
62. Cano, A., et al., The transcription factor snail controls epithelial-mesenchymal transitions by repressing E-cadherin expression. *Nat Cell Biol*, 2000. **2**(2): p. 76-83.
63. Perez-Moreno, M.A., et al., A new role for E12/E47 in the repression of E-cadherin expression and epithelial-mesenchymal transitions. *J Biol Chem*, 2001. **276**(29): p. 27424-31.

64. Comijn, J., et al., The two-handed E box binding zinc finger protein SIP1 downregulates E-cadherin and induces invasion. *Mol Cell*, 2001. **7**(6): p. 1267-78.
65. Blanco, M.J., et al., Correlation of Snail expression with histological grade and lymph node status in breast carcinomas. *Oncogene*, 2002. **21**(20): p. 3241-6.
66. Bolos, V., et al., The transcription factor Slug represses E-cadherin expression and induces epithelial to mesenchymal transitions: a comparison with Snail and E47 repressors. *J Cell Sci*, 2003. **116**(Pt 3): p. 499-511.
67. Elloul, S., et al., Snail, Slug, and Smad-interacting protein 1 as novel parameters of disease aggressiveness in metastatic ovarian and breast carcinoma. *Cancer*, 2005. **103**(8): p. 1631-43.
68. Rios-Doria, J., et al., The role of calpain in the proteolytic cleavage of E-cadherin in prostate and mammary epithelial cells. *J Biol Chem*, 2003. **278**(2): p. 1372-9.
69. Grabowska, M.M. and M.L. Day, Soluble E-cadherin: more than a symptom of disease. *Front Biosci (Landmark Ed)*, 2012. **17**: p. 1948-64.
70. Lawler, K., et al., Shear stress induces internalization of E-cadherin and invasiveness in metastatic oesophageal cancer cells by a Src-dependent pathway. *Cancer Sci*, 2009. **100**(6): p. 1082-7.
71. Xie, L.Q., et al., Altered expression of E-cadherin by hepatocyte growth factor and effect on the prognosis of nasopharyngeal carcinoma. *Ann Surg Oncol*, 2010. **17**(7): p. 1927-36.
72. Kleer, C.G., et al., Persistent E-cadherin expression in inflammatory breast cancer. *Mod Pathol*, 2001. **14**(5): p. 458-64.
73. Lewis-Tuffin, L.J., et al., Misregulated E-cadherin expression associated with an aggressive brain tumor phenotype. *PLoS One*, 2010. **5**(10): p. e13665.
74. Putzke, A.P., et al., Metastatic progression of prostate cancer and e-cadherin regulation by zeb1 and SRC family kinases. *Am J Pathol*, 2011. **179**(1): p. 400-10.
75. Reddy, P., et al., Formation of E-cadherin-mediated cell-cell adhesion activates AKT and mitogen activated protein kinase via phosphatidylinositol 3 kinase and ligand-independent activation of epidermal growth factor receptor in ovarian cancer cells. *Mol Endocrinol*, 2005. **19**(10): p. 2564-78.

76. Christiansen, J.J. and A.K. Rajasekaran, Reassessing epithelial to mesenchymal transition as a prerequisite for carcinoma invasion and metastasis. *Cancer Res*, 2006. **66**(17): p. 8319-26.
77. Rhodes, D.R., et al., Multiplex biomarker approach for determining risk of prostate-specific antigen-defined recurrence of prostate cancer. *J Natl Cancer Inst*, 2003. **95**(9): p. 661-8.
78. Saha, B., et al., Overexpression of E-cadherin protein in metastatic breast cancer cells in bone. *Anticancer Res*, 2007. **27**(6B): p. 3903-8.
79. Naora, H. and D.J. Montell, Ovarian cancer metastasis: integrating insights from disparate model organisms. *Nat Rev Cancer*, 2005. **5**(5): p. 355-66.
80. Tomlinson, J.S., M.L. Alpaugh, and S.H. Barsky, An intact overexpressed E-cadherin/alpha,beta-catenin axis characterizes the lymphovascular emboli of inflammatory breast carcinoma. *Cancer Res*, 2001. **61**(13): p. 5231-41.
81. Brouxhon, S., et al., Sequential down-regulation of E-cadherin with squamous cell carcinoma progression: loss of E-cadherin via a prostaglandin E2-EP2 dependent posttranslational mechanism. *Cancer Res*, 2007. **67**(16): p. 7654-64.
82. David, J.M. and A.K. Rajasekaran, Dishonorable discharge: the oncogenic roles of cleaved E-cadherin fragments. *Cancer Res*, 2012. **72**(12): p. 2917-23.
83. De Wever, O., et al., Soluble cadherins as cancer biomarkers. *Clin Exp Metastasis*, 2007. **24**(8): p. 685-97.
84. Maretzky, T., et al., ADAM10 mediates E-cadherin shedding and regulates epithelial cell-cell adhesion, migration, and beta-catenin translocation. *Proc Natl Acad Sci U S A*, 2005. **102**(26): p. 9182-7.
85. Steinhilber, U., et al., Cleavage and shedding of E-cadherin after induction of apoptosis. *J Biol Chem*, 2001. **276**(7): p. 4972-80.
86. Wheelock, M.J., et al., Soluble 80-kd fragment of cell-CAM 120/80 disrupts cell-cell adhesion. *J Cell Biochem*, 1987. **34**(3): p. 187-202.
87. Griffiths, T.R., et al., Cell adhesion molecules in bladder cancer: soluble serum E-cadherin correlates with predictors of recurrence. *Br J Cancer*, 1996. **74**(4): p. 579-84.

88. Protheroe, A.S., et al., Urinary concentrations of the soluble adhesion molecule E-cadherin and total protein in patients with bladder cancer. *Br J Cancer*, 1999. **80**(1-2): p. 273-8.
89. Shi, B., et al., E-cadherin tissue expression and urinary soluble forms of E-cadherin in patients with bladder transitional cell carcinoma. *Urol Int*, 2008. **81**(3): p. 320-4.
90. Gogali, A., et al., Soluble adhesion molecules E-cadherin, intercellular adhesion molecule-1, and E-selectin as lung cancer biomarkers. *Chest*, 2010. **138**(5): p. 1173-9.
91. Wilmanns, C., et al., Soluble serum E-cadherin as a marker of tumour progression in colorectal cancer patients. *Clin Exp Metastasis*, 2004. **21**(1): p. 75-8.
92. Chung, Y., et al., Serum soluble E-cadherin is a potential prognostic marker in esophageal squamous cell carcinoma. *Dis Esophagus*, 2011. **24**(1): p. 49-55.
93. Chan, A.O., et al., Early prediction of tumor recurrence after curative resection of gastric carcinoma by measuring soluble E-cadherin. *Cancer*, 2005. **104**(4): p. 740-6.
94. Soyama, A., et al., Significance of the serum level of soluble E-cadherin in patients with HCC. *Hepatogastroenterology*, 2008. **55**(85): p. 1390-3.
95. Darai, E., et al., Soluble adhesion molecules in serum and cyst fluid from patients with cystic tumours of the ovary. *Hum Reprod*, 1998. **13**(10): p. 2831-5.
96. Kuefer, R., et al., Assessment of a fragment of e-cadherin as a serum biomarker with predictive value for prostate cancer. *Br J Cancer*, 2005. **92**(11): p. 2018-23.
97. Billion, K., et al., Increased soluble E-cadherin in melanoma patients. *Skin Pharmacol Physiol*, 2006. **19**(2): p. 65-70.
98. Syrigos, K.N., et al., Circulating soluble E-cadherin levels are of prognostic significance in patients with multiple myeloma. *Anticancer Res*, 2004. **24**(3b): p. 2027-31.
99. Shirahama, S., et al., E- and P-cadherin expression in tumor tissues and soluble E-cadherin levels in sera of patients with skin cancer. *J Dermatol Sci*, 1996. **13**(1): p. 30-6.

100. Sewpaul, A., et al., Soluble E-cadherin: an early marker of severity in acute pancreatitis. *HPB Surg*, 2009. **2009**: p. 397375.
101. Jiang, H., et al., Identification of urinary soluble E-cadherin as a novel biomarker for diabetic nephropathy. *Diabetes Metab Res Rev*, 2009. **25**(3): p. 232-41.
102. Streeck, H., et al., Epithelial adhesion molecules can inhibit HIV-1-specific CD8 (+) T-cell functions. *Blood*, 2011. **117**(19): p. 5112-22.
103. Pittard, A.J., et al., Soluble E-cadherin concentrations in patients with systemic inflammatory response syndrome and multiorgan dysfunction syndrome. *Br J Anaesth*, 1996. **76**(5): p. 629-31.
104. Karayiannakis, A.J., et al., Serum E-cadherin concentrations and their response during laparoscopic and open cholecystectomy. *Surg Endosc*, 2002. **16**(11): p. 1551-4.
105. Lamont, R.J. and H.F. Jenkinson, Life below the gum line: pathogenic mechanisms of *Porphyromonas gingivalis*. *Microbiol Mol Biol Rev*, 1998. **62**(4): p. 1244-63.
106. Wu, S., et al., *Bacteroides fragilis* enterotoxin cleaves the zonula adherens protein, E-cadherin. *Proc Natl Acad Sci U S A*, 1998. **95**(25): p. 14979-84.
107. Katz, J., et al., Characterization of *Porphyromonas gingivalis*-induced degradation of epithelial cell junctional complexes. *Infect Immun*, 2000. **68**(3): p. 1441-9.
108. Dunsmore, S.E., et al., Matrilysin expression and function in airway epithelium. *J Clin Invest*, 1998. **102**(7): p. 1321-31.
109. Symowicz, J., et al., Engagement of collagen-binding integrins promotes matrix metalloproteinase-9-dependent E-cadherin ectodomain shedding in ovarian carcinoma cells. *Cancer Res*, 2007. **67**(5): p. 2030-9.
110. Zuo, J.H., et al., Activation of EGFR promotes squamous carcinoma SCC10A cell migration and invasion via inducing EMT-like phenotype change and MMP-9-mediated degradation of E-cadherin. *J Cell Biochem*, 2011. **112**(9): p. 2508-17.
111. Noe, V., et al., Release of an invasion promoter E-cadherin fragment by matrilysin and stromelysin-1. *J Cell Sci*, 2001. **114**(Pt 1): p. 111-118.

112. Nawrocki-Raby, B., et al., Upregulation of MMPs by soluble E-cadherin in human lung tumor cells. *Int J Cancer*, 2003. **105**(6): p. 790-5.
113. Lynch, C.C., et al., Cleavage of E-Cadherin by Matrix Metalloproteinase-7 Promotes Cellular Proliferation in Nontransformed Cell Lines via Activation of RhoA. *J Oncol*, 2010. **2010**: p. 530745.
114. Schirrmeyer, W., et al., Ectodomain shedding of E-cadherin and c-Met is induced by Helicobacter pylori infection. *Exp Cell Res*, 2009. **315**(20): p. 3500-8.
115. Lee, S.B., et al., ADAM10 is upregulated in melanoma metastasis compared with primary melanoma. *J Invest Dermatol*, 2010. **130**(3): p. 763-73.
116. Inge, L.J., et al., Soluble E-cadherin promotes cell survival by activating epidermal growth factor receptor. *Exp Cell Res*, 2011. **317**(6): p. 838-48.
117. Fedor-Chaiken, M., et al., E-cadherin binding modulates EGF receptor activation. *Cell Commun Adhes*, 2003. **10**(2): p. 105-18.
118. Najy, A.J., K.C. Day, and M.L. Day, The ectodomain shedding of E-cadherin by ADAM15 supports ErbB receptor activation. *J Biol Chem*, 2008. **283**(26): p. 18393-401.
119. Brouxhon, S.M., et al., Soluble-E-cadherin activates HER and IAP family members in HER2+ and TNBC human breast cancers. *Mol Carcinog*, 2013.
120. Ferber, E.C., et al., A role for the cleaved cytoplasmic domain of E-cadherin in the nucleus. *J Biol Chem*, 2008. **283**(19): p. 12691-700.
121. Agiostratidou, G., et al., The cytoplasmic sequence of E-cadherin promotes non-amyloidogenic degradation of A beta precursors. *J Neurochem*, 2006. **96**(4): p. 1182-8.
122. Hanahan, D. and L.M. Coussens, Accessories to the crime: functions of cells recruited to the tumor microenvironment. *Cancer Cell*, 2012. **21**(3): p. 309-22.
123. Paget, S., The distribution of secondary growths in cancer of the breast. 1889. *Cancer Metastasis Rev*, 1989. **8**(2): p. 98-101.
124. Hanahan, D. and R.A. Weinberg, Hallmarks of cancer: the next generation. *Cell*, 2011. **144**(5): p. 646-74.
125. Vong, S. and R. Kalluri, The role of stromal myofibroblast and extracellular matrix in tumor angiogenesis. *Genes Cancer*, 2011. **2**(12): p. 1139-45.

126. Duda, D.G., et al., Malignant cells facilitate lung metastasis by bringing their own soil. *Proc Natl Acad Sci U S A*, 2010. **107**(50): p. 21677-82.
127. Yang, L. and D.P. Carbone, Tumor-host immune interactions and dendritic cell dysfunction. *Adv Cancer Res*, 2004. **92**: p. 13-27.
128. Lu, P., et al., Extracellular matrix degradation and remodeling in development and disease. *Cold Spring Harb Perspect Biol*, 2011. **3**(12).
129. Chen, Q., X.H. Zhang, and J. Massague, Macrophage binding to receptor VCAM-1 transmits survival signals in breast cancer cells that invade the lungs. *Cancer Cell*, 2011. **20**(4): p. 538-49.
130. DeNardo, D.G., P. Andreu, and L.M. Coussens, Interactions between lymphocytes and myeloid cells regulate pro- versus anti-tumor immunity. *Cancer Metastasis Rev*, 2010. **29**(2): p. 309-16.
131. Rolny, C., et al., HRG inhibits tumor growth and metastasis by inducing macrophage polarization and vessel normalization through downregulation of PlGF. *Cancer Cell*, 2011. **19**(1): p. 31-44.
132. Pistone Creydt, V., et al., Human adipose tissue from normal and tumoral breast regulates the behavior of mammary epithelial cells. *Clin Transl Oncol*, 2013. **15**(2): p. 124-31.
133. Spink, B.C., et al., Inhibition of MCF-7 breast cancer cell proliferation by MCF-10A breast epithelial cells in coculture. *Cell Biol Int*, 2006. **30**(3): p. 227-38.
134. Bose, N. and A.M. Masellis, Secretory products of breast cancer cells upregulate hyaluronan production in a human osteoblast cell line. *Clin Exp Metastasis*, 2005. **22**(8): p. 629-42.
135. Sasahira, T., T. Sasaki, and H. Kuniyasu, Interleukin-15 and transforming growth factor alpha are associated with depletion of tumor-associated macrophages in colon cancer. *J Exp Clin Cancer Res*, 2005. **24**(1): p. 69-74.
136. Sen, M., et al., Blockade of Wnt-5A/frizzled 5 signaling inhibits rheumatoid synoviocyte activation. *Arthritis Rheum*, 2001. **44**(4): p. 772-81.
137. Tyryshkin, A., et al., Src kinase-mediated phosphorylation stabilizes inducible nitric-oxide synthase in normal cells and cancer cells. *J Biol Chem*, 2010. **285**(1): p. 784-92.

138. Hiratsuka, S., et al., The S100A8-serum amyloid A3-TLR4 paracrine cascade establishes a pre-metastatic phase. *Nat Cell Biol*, 2008. **10**(11): p. 1349-55.
139. Kaplan, R.N., B. Psaila, and D. Lyden, Bone marrow cells in the 'pre-metastatic niche': within bone and beyond. *Cancer Metastasis Rev*, 2006. **25**(4): p. 521-9.
140. Tsai, J.H. and J. Yang, Epithelial-mesenchymal plasticity in carcinoma metastasis. *Genes Dev*, 2013. **27**(20): p. 2192-206.
141. Yilmaz, M. and G. Christofori, EMT, the cytoskeleton, and cancer cell invasion. *Cancer Metastasis Rev*, 2009. **28**(1-2): p. 15-33.
142. Thiery, J.P., Epithelial-mesenchymal transitions in cancer onset and progression. *Bull Acad Natl Med*, 2009. **193**(9): p. 1969-78; discussion 1978-9.
143. Larue, L. and A. Bellacosa, Epithelial-mesenchymal transition in development and cancer: role of phosphatidylinositol 3' kinase/AKT pathways. *Oncogene*, 2005. **24**(50): p. 7443-54.
144. Debnath, J., S.K. Muthuswamy, and J.S. Brugge, Morphogenesis and oncogenesis of MCF-10A mammary epithelial acini grown in three-dimensional basement membrane cultures. *Methods*, 2003. **30**(3): p. 256-68.
145. Lin, R.Z. and H.Y. Chang, Recent advances in three-dimensional multicellular spheroid culture for biomedical research. *Biotechnol J*, 2008. **3**(9-10): p. 1172-84.
146. Chitcholtan, K., et al., Differences in growth properties of endometrial cancer in three dimensional (3D) culture and 2D cell monolayer. *Exp Cell Res*, 2013. **319**(1): p. 75-87.
147. Hogan, C., et al., Interactions between normal and transformed epithelial cells: Their contributions to tumourigenesis. *Int J Biochem Cell Biol*, 2011. **43**(4): p. 496-503.
148. Kajita, M., et al., Interaction with surrounding normal epithelial cells influences signalling pathways and behaviour of Src-transformed cells. *J Cell Sci*, 2010. **123**(Pt 2): p. 171-80.
149. Toillon, R.A., et al., Normal breast epithelial cells induce p53-dependent apoptosis and p53-independent cell cycle arrest of breast cancer cells. *Breast Cancer Res Treat*, 2002. **71**(3): p. 269-80.

150. Ivers, L.P., et al., Dynamic and influential interaction of cancer cells with normal epithelial cells in 3D culture. *Cancer Cell Int*, 2014. **14**(1): p. 108.
151. Olumi, A.F., et al., Carcinoma-associated fibroblasts direct tumor progression of initiated human prostatic epithelium. *Cancer Res*, 1999. **59**(19): p. 5002-11.
152. Orimo, A., et al., Stromal fibroblasts present in invasive human breast carcinomas promote tumor growth and angiogenesis through elevated SDF-1/CXCL12 secretion. *Cell*, 2005. **121**(3): p. 335-48.
153. Reginato, M.J., et al., Bim regulation of lumen formation in cultured mammary epithelial acini is targeted by oncogenes. *Mol Cell Biol*, 2005. **25**(11): p. 4591-601.
154. Debnath, J., et al., The role of apoptosis in creating and maintaining luminal space within normal and oncogene-expressing mammary acini. *Cell*, 2002. **111**(1): p. 29-40.
155. Debnath, J. and J.S. Brugge, Modelling glandular epithelial cancers in three-dimensional cultures. *Nat Rev Cancer*, 2005. **5**(9): p. 675-88.
156. Gumbiner, B., B. Stevenson, and A. Grimaldi, The role of the cell adhesion molecule uvomorulin in the formation and maintenance of the epithelial junctional complex. *J Cell Biol*, 1988. **107**(4): p. 1575-87.
157. Farina, A.R. and A.R. Mackay, Gelatinase B/MMP-9 in Tumour Pathogenesis and Progression. *Cancers (Basel)*, 2014. **6**(1): p. 240-96.
158. Hibbs, M.S., et al., Biochemical and immunological characterization of the secreted forms of human neutrophil gelatinase. *J Biol Chem*, 1985. **260**(4): p. 2493-500.
159. Murphy, G., et al., Matrix metalloproteinase degradation of elastin, type IV collagen and proteoglycan. A quantitative comparison of the activities of 95 kDa and 72 kDa gelatinases, stromelysins-1 and -2 and punctuated metalloproteinase (PUMP). *Biochem J*, 1991. **277 (Pt 1)**: p. 277-9.
160. Chan, A.O., et al., Soluble E-cadherin is an independent pretherapeutic factor for long-term survival in gastric cancer. *J Clin Oncol*, 2003. **21**(12): p. 2288-93.
161. Katayama, M., et al., Soluble E-cadherin fragments increased in circulation of cancer patients. *Br J Cancer*, 1994. **69**(3): p. 580-5.

162. Rajasekaran, S.A., et al., Na,K-ATPase beta-subunit is required for epithelial polarization, suppression of invasion, and cell motility. *Mol Biol Cell*, 2001. **12**(2): p. 279-95.
163. Barwe, S.P., et al., Novel role for Na,K-ATPase in phosphatidylinositol 3-kinase signaling and suppression of cell motility. *Mol Biol Cell*, 2005. **16**(3): p. 1082-94.
164. O'Brien, L.E., et al., Rac1 orientates epithelial apical polarity through effects on basolateral laminin assembly. *Nat Cell Biol*, 2001. **3**(9): p. 831-8.
165. O'Brien, L.E., et al., Morphological and biochemical analysis of Rac1 in three-dimensional epithelial cell cultures. *Methods Enzymol*, 2006. **406**: p. 676-91.
166. Tushir, J.S. and C. D'Souza-Schorey, ARF6-dependent activation of ERK and Rac1 modulates epithelial tubule development. *EMBO J*, 2007. **26**(7): p. 1806-19.
167. Lu, K.V., et al., Upregulation of tissue inhibitor of metalloproteinases (TIMP)-2 promotes matrix metalloproteinase (MMP)-2 activation and cell invasion in a human glioblastoma cell line. *Lab Invest*, 2004. **84**(1): p. 8-20.
168. Behrens, J., et al., Dissecting tumor cell invasion: epithelial cells acquire invasive properties after the loss of uvomorulin-mediated cell-cell adhesion. *J Cell Biol*, 1989. **108**(6): p. 2435-47.
169. Taylor, D.P., et al., Hepatic nonparenchymal cells drive metastatic breast cancer outgrowth and partial epithelial to mesenchymal transition. *Breast Cancer Res Treat*, 2014. **144**(3): p. 551-60.
170. Barwe, S.P., et al., Na,K-ATPase beta-subunit cis homo-oligomerization is necessary for epithelial lumen formation in mammalian cells. *J Cell Sci*, 2012. **125**(Pt 23): p. 5711-20.
171. Martin-Belmonte, F., et al., PTEN-mediated apical segregation of phosphoinositides controls epithelial morphogenesis through Cdc42. *Cell*, 2007. **128**(2): p. 383-97.
172. Schluter, M.A., et al., Trafficking of Crumbs3 during cytokinesis is crucial for lumen formation. *Mol Biol Cell*, 2009. **20**(22): p. 4652-63.
173. Shin, K., S. Straight, and B. Margolis, PATJ regulates tight junction formation and polarity in mammalian epithelial cells. *J Cell Biol*, 2005. **168**(5): p. 705-11.

174. Straight, S.W., et al., Loss of PALS1 expression leads to tight junction and polarity defects. *Mol Biol Cell*, 2004. **15**(4): p. 1981-90.
175. Yu, W., et al., Involvement of RhoA, ROCK I and myosin II in inverted orientation of epithelial polarity. *EMBO Rep*, 2008. **9**(9): p. 923-9.
176. Tiwari, N., et al., EMT as the ultimate survival mechanism of cancer cells. *Semin Cancer Biol*, 2012. **22**(3): p. 194-207.
177. Thiery, J.P. and J.P. Sleeman, Complex networks orchestrate epithelial-mesenchymal transitions. *Nat Rev Mol Cell Biol*, 2006. **7**(2): p. 131-42.
178. Yang, J. and R.A. Weinberg, Epithelial-mesenchymal transition: at the crossroads of development and tumor metastasis. *Dev Cell*, 2008. **14**(6): p. 818-29.
179. Brabletz, T., et al., Variable beta-catenin expression in colorectal cancers indicates tumor progression driven by the tumor environment. *Proc Natl Acad Sci U S A*, 2001. **98**(18): p. 10356-61.
180. Shankar, J. and I.R. Nabi, Actin cytoskeleton regulation of epithelial mesenchymal transition in metastatic cancer cells. *PLoS One*, 2015. **10**(3): p. e0119954.
181. Tojkander, S., G. Gateva, and P. Lappalainen, Actin stress fibers-assembly, dynamics and biological roles. *J Cell Sci*, 2012. **125**(Pt 8): p. 1855-64.
182. Mamuya, F.A. and M.K. Duncan, aV integrins and TGF-beta-induced EMT: a circle of regulation. *J Cell Mol Med*, 2012. **16**(3): p. 445-55.
183. Polyak, K. and R.A. Weinberg, Transitions between epithelial and mesenchymal states: acquisition of malignant and stem cell traits. *Nat Rev Cancer*, 2009. **9**(4): p. 265-73.
184. Mani, S.A., et al., The epithelial-mesenchymal transition generates cells with properties of stem cells. *Cell*, 2008. **133**(4): p. 704-15.
185. Bussolati, B., C. Grange, and G. Camussi, Tumor exploits alternative strategies to achieve vascularization. *FASEB J*, 2011. **25**(9): p. 2874-82.
186. Medema, J.P., Cancer stem cells: the challenges ahead. *Nat Cell Biol*, 2013. **15**(4): p. 338-44.
187. Jing, Y., et al., Epithelial-Mesenchymal Transition in tumor microenvironment. *Cell Biosci*, 2011. **1**: p. 29.

188. Sullivan, D.E., et al., TNF-alpha induces TGF-beta1 expression in lung fibroblasts at the transcriptional level via AP-1 activation. *J Cell Mol Med*, 2009. **13**(8B): p. 1866-76.
189. Dong, R., et al., Role of nuclear factor kappa B and reactive oxygen species in the tumor necrosis factor-alpha-induced epithelial-mesenchymal transition of MCF-7 cells. *Braz J Med Biol Res*, 2007. **40**(8): p. 1071-8.
190. Luo, D., et al., Mouse snail is a target gene for HIF. *Mol Cancer Res*, 2011. **9**(2): p. 234-45.
191. Zhou, G., et al., Hypoxia-induced alveolar epithelial-mesenchymal transition requires mitochondrial ROS and hypoxia-inducible factor 1. *Am J Physiol Lung Cell Mol Physiol*, 2009. **297**(6): p. L1120-30.
192. Nakajima, S., et al., N-cadherin expression and epithelial-mesenchymal transition in pancreatic carcinoma. *Clin Cancer Res*, 2004. **10**(12 Pt 1): p. 4125-33.
193. Ramis-Conde, I., et al., Multi-scale modelling of cancer cell intravasation: the role of cadherins in metastasis. *Phys Biol*, 2009. **6**(1): p. 016008.
194. Gavrilovic, J., et al., Expression of transfected transforming growth factor alpha induces a motile fibroblast-like phenotype with extracellular matrix-degrading potential in a rat bladder carcinoma cell line. *Cell Regul*, 1990. **1**(13): p. 1003-14.
195. Sternlicht, M.D. and Z. Werb, How matrix metalloproteinases regulate cell behavior. *Annu Rev Cell Dev Biol*, 2001. **17**: p. 463-516.
196. Hynes, R.O., The dynamic dialogue between cells and matrices: implications of fibronectin's elasticity. *Proc Natl Acad Sci U S A*, 1999. **96**(6): p. 2588-90.
197. Mao, Y. and J.E. Schwarzbauer, Fibronectin fibrillogenesis, a cell-mediated matrix assembly process. *Matrix Biol*, 2005. **24**(6): p. 389-99.
198. Hu, T., et al., Octamer 4 small interfering RNA results in cancer stem cell-like cell apoptosis. *Cancer Res*, 2008. **68**(16): p. 6533-40.
199. Marcato, P., et al., Aldehyde dehydrogenase: its role as a cancer stem cell marker comes down to the specific isoform. *Cell Cycle*, 2011. **10**(9): p. 1378-84.

200. Takahashi, K., et al., Induction of pluripotent stem cells from adult human fibroblasts by defined factors. *Cell*, 2007. **131**(5): p. 861-72.
201. Takahashi, K. and S. Yamanaka, Induction of pluripotent stem cells from mouse embryonic and adult fibroblast cultures by defined factors. *Cell*, 2006. **126**(4): p. 663-76.
202. Dai, X., et al., OCT4 regulates epithelial-mesenchymal transition and its knockdown inhibits colorectal cancer cell migration and invasion. *Oncol Rep*, 2014. **29**(1): p. 155-60.
203. Moreb, J.S., Aldehyde dehydrogenase as a marker for stem cells. *Curr Stem Cell Res Ther*, 2008. **3**(4): p. 237-46.
204. Vasiliou, V., A. Pappa, and T. Estey, Role of human aldehyde dehydrogenases in endobiotic and xenobiotic metabolism. *Drug Metab Rev*, 2004. **36**(2): p. 279-99.
205. Heldin, C.H., M. Landstrom, and A. Moustakas, Mechanism of TGF-beta signaling to growth arrest, apoptosis, and epithelial-mesenchymal transition. *Curr Opin Cell Biol*, 2009. **21**(2): p. 166-76.
206. Kim, E.S., M.S. Kim, and A. Moon, TGF-beta-induced upregulation of MMP-2 and MMP-9 depends on p38 MAPK, but not ERK signaling in MCF10A human breast epithelial cells. *Int J Oncol*, 2004. **25**(5): p. 1375-82.
207. Suyama, K., et al., A signaling pathway leading to metastasis is controlled by N-cadherin and the FGF receptor. *Cancer Cell*, 2002. **2**(4): p. 301-14.
208. Tran, N.L., et al., Signal transduction from N-cadherin increases Bcl-2. Regulation of the phosphatidylinositol 3-kinase/Akt pathway by homophilic adhesion and actin cytoskeletal organization. *J Biol Chem*, 2002. **277**(36): p. 32905-14.
209. Milner, R., et al., Increased expression of fibronectin and the alpha 5 beta 1 integrin in angiogenic cerebral blood vessels of mice subject to hypobaric hypoxia. *Mol Cell Neurosci*, 2008. **38**(1): p. 43-52.
210. Wu, C., et al., The alpha 5 beta 1 integrin fibronectin receptor, but not the alpha 5 cytoplasmic domain, functions in an early and essential step in fibronectin matrix assembly. *J Biol Chem*, 1993. **268**(29): p. 21883-8.
211. Slattum, G.M. and J. Rosenblatt, Tumour cell invasion: an emerging role for basal epithelial cell extrusion. *Nat Rev Cancer*, 2014. **14**(7): p. 495-501.

212. Danial, N.N. and S.J. Korsmeyer, Cell death: critical control points. *Cell*, 2004. **116**(2): p. 205-19.
213. Blatchford, D.R., et al., Influence of microenvironment on mammary epithelial cell survival in primary culture. *J Cell Physiol*, 1999. **181**(2): p. 304-11.
214. Coucouvanis, E. and G.R. Martin, Signals for death and survival: a two-step mechanism for cavitation in the vertebrate embryo. *Cell*, 1995. **83**(2): p. 279-87.
215. Muthuswamy, S.K., et al., ErbB2, but not ErbB1, reinitiates proliferation and induces luminal repopulation in epithelial acini. *Nat Cell Biol*, 2001. **3**(9): p. 785-92.
216. Bargmann, C.I., M.C. Hung, and R.A. Weinberg, The neu oncogene encodes an epidermal growth factor receptor-related protein. *Nature*, 1986. **319**(6050): p. 226-30.
217. Kraus, M.H., et al., Isolation and characterization of ERBB3, a third member of the ERBB/epidermal growth factor receptor family: evidence for overexpression in a subset of human mammary tumors. *Proc Natl Acad Sci U S A*, 1989. **86**(23): p. 9193-7.
218. Plowman, G.D., et al., Ligand-specific activation of HER4/p180erbB4, a fourth member of the epidermal growth factor receptor family. *Proc Natl Acad Sci U S A*, 1993. **90**(5): p. 1746-50.
219. Plowman, G.D., et al., Molecular cloning and expression of an additional epidermal growth factor receptor-related gene. *Proc Natl Acad Sci U S A*, 1990. **87**(13): p. 4905-9.
220. Ullrich, A., et al., Human epidermal growth factor receptor cDNA sequence and aberrant expression of the amplified gene in A431 epidermoid carcinoma cells. *Nature*, 1984. **309**(5967): p. 418-25.
221. Singh, A.B. and R.C. Harris, Autocrine, paracrine and juxtacrine signaling by EGFR ligands. *Cell Signal*, 2005. **17**(10): p. 1183-93.
222. Schneider, M.R. and E. Wolf, The epidermal growth factor receptor ligands at a glance. *J Cell Physiol*, 2009. **218**(3): p. 460-6.
223. Carpenter, G., Receptors for epidermal growth factor and other polypeptide mitogens. *Annu Rev Biochem*, 1987. **56**: p. 881-914.

224. Schlessinger, J. and A. Ullrich, Growth factor signaling by receptor tyrosine kinases. *Neuron*, 1992. **9**(3): p. 383-91.
225. Olayioye, M.A., et al., ErbB receptor-induced activation of stat transcription factors is mediated by Src tyrosine kinases. *J Biol Chem*, 1999. **274**(24): p. 17209-18.
226. Pawson, T., Protein modules and signalling networks. *Nature*, 1995. **373**(6515): p. 573-80.
227. Yarden, Y. and M.X. Sliwkowski, Untangling the ErbB signalling network. *Nat Rev Mol Cell Biol*, 2001. **2**(2): p. 127-37.
228. Avruch, J., MAP kinase pathways: the first twenty years. *Biochim Biophys Acta*, 2007. **1773**(8): p. 1150-60.
229. Marshall, C.J., Cell signalling. Raf gets it together. *Nature*, 1996. **383**(6596): p. 127-8.
230. Pearson, G., et al., Mitogen-activated protein (MAP) kinase pathways: regulation and physiological functions. *Endocr Rev*, 2001. **22**(2): p. 153-83.
231. Burgering, B.M. and P.J. Coffer, Protein kinase B (c-Akt) in phosphatidylinositol-3-OH kinase signal transduction. *Nature*, 1995. **376**(6541): p. 599-602.
232. Downward, J., Mechanisms and consequences of activation of protein kinase B/Akt. *Curr Opin Cell Biol*, 1998. **10**(2): p. 262-7.
233. Okano, J., et al., Akt/protein kinase B isoforms are differentially regulated by epidermal growth factor stimulation. *J Biol Chem*, 2000. **275**(40): p. 30934-42.
234. Kim, H.K., et al., PDGF stimulation of inositol phospholipid hydrolysis requires PLC-gamma 1 phosphorylation on tyrosine residues 783 and 1254. *Cell*, 1991. **65**(3): p. 435-41.
235. Maa, M.C., et al., Potentiation of epidermal growth factor receptor-mediated oncogenesis by c-Src: implications for the etiology of multiple human cancers. *Proc Natl Acad Sci U S A*, 1995. **92**(15): p. 6981-5.
236. Rotin, D., et al., SH2 domains prevent tyrosine dephosphorylation of the EGF receptor: identification of Tyr992 as the high-affinity binding site for SH2 domains of phospholipase C gamma. *EMBO J*, 1992. **11**(2): p. 559-67.

237. Tice, D.A., et al., Mechanism of biological synergy between cellular Src and epidermal growth factor receptor. *Proc Natl Acad Sci U S A*, 1999. **96**(4): p. 1415-20.
238. Morris, Z.S. and A.I. McClatchey, Aberrant epithelial morphology and persistent epidermal growth factor receptor signaling in a mouse model of renal carcinoma. *Proc Natl Acad Sci U S A*, 2009. **106**(24): p. 9767-72.
239. White, E.S., et al., Control of fibroblast fibronectin expression and alternative splicing via the PI3K/Akt/mTOR pathway. *Exp Cell Res*, 2010. **316**(16): p. 2644-53.
240. Han, S., F.R. Khuri, and J. Roman, Fibronectin stimulates non-small cell lung carcinoma cell growth through activation of Akt/mammalian target of rapamycin/S6 kinase and inactivation of LKB1/AMP-activated protein kinase signal pathways. *Cancer Res*, 2006. **66**(1): p. 315-23.
241. Mimura, Y., et al., Epidermal growth factor induces fibronectin expression in human dermal fibroblasts via protein kinase C delta signaling pathway. *J Invest Dermatol*, 2004. **122**(6): p. 1390-8.
242. Reddy, V.S., et al., Interleukin-18 stimulates fibronectin expression in primary human cardiac fibroblasts via PI3K-Akt-dependent NF-kappaB activation. *J Cell Physiol*, 2008. **215**(3): p. 697-707.
243. Bentzinger, C.F., et al., Fibronectin regulates Wnt7a signaling and satellite cell expansion. *Cell Stem Cell*, 2013. **12**(1): p. 75-87.
244. Zhang, Z., et al., The alpha v beta 1 integrin functions as a fibronectin receptor but does not support fibronectin matrix assembly and cell migration on fibronectin. *J Cell Biol*, 1993. **122**(1): p. 235-42.
245. Hult, J., et al., N-cadherin signaling potentiates mammary tumor metastasis via enhanced extracellular signal-regulated kinase activation. *Cancer Res*, 2007. **67**(7): p. 3106-16.
246. De Wever, O. and M. Mareel, Role of tissue stroma in cancer cell invasion. *J Pathol*, 2003. **200**(4): p. 429-47.
247. Reiss, K., et al., ADAM10 cleavage of N-cadherin and regulation of cell-cell adhesion and beta-catenin nuclear signalling. *EMBO J*, 2005. **24**(4): p. 742-52.

248. Zi, X., et al., Expression of Frzb/secreted Frizzled-related protein 3, a secreted Wnt antagonist, in human androgen-independent prostate cancer PC-3 cells suppresses tumor growth and cellular invasiveness. *Cancer Res*, 2005. **65**(21): p. 9762-70.
249. Derycke, L., et al., Soluble N-cadherin fragment promotes angiogenesis. *Clin Exp Metastasis*, 2006. **23**(3-4): p. 187-201.
250. Theisen, C.S., et al., NHERF links the N-cadherin/catenin complex to the platelet-derived growth factor receptor to modulate the actin cytoskeleton and regulate cell motility. *Mol Biol Cell*, 2007. **18**(4): p. 1220-32.
251. Chattopadhyay, A., et al., The role of individual SH2 domains in mediating association of phospholipase C-gamma1 with the activated EGF receptor. *J Biol Chem*, 1999. **274**(37): p. 26091-7.
252. Sturla, L.M., et al., Requirement of Tyr-992 and Tyr-1173 in phosphorylation of the epidermal growth factor receptor by ionizing radiation and modulation by SHP2. *J Biol Chem*, 2005. **280**(15): p. 14597-604.
253. Yarden, Y., The EGFR family and its ligands in human cancer. signalling mechanisms and therapeutic opportunities. *Eur J Cancer*, 2001. **37 Suppl 4**: p. S3-8.
254. Rojas, M., S. Yao, and Y.Z. Lin, Controlling epidermal growth factor (EGF)-stimulated Ras activation in intact cells by a cell-permeable peptide mimicking phosphorylated EGF receptor. *J Biol Chem*, 1996. **271**(44): p. 27456-61.
255. Scholzen, T. and J. Gerdes, The Ki-67 protein: from the known and the unknown. *J Cell Physiol*, 2000. **182**(3): p. 311-22.
256. Aksamitiene, E., et al., PI3K/Akt-sensitive MEK-independent compensatory circuit of ERK activation in ER-positive PI3K-mutant T47D breast cancer cells. *Cell Signal*, 2010. **22**(9): p. 1369-78.
257. Pece, S. and J.S. Gutkind, Signaling from E-cadherins to the MAPK pathway by the recruitment and activation of epidermal growth factor receptors upon cell-cell contact formation. *J Biol Chem*, 2000. **275**(52): p. 41227-33.
258. Hobor, S., et al., TGFalpha and amphiregulin paracrine network promotes resistance to EGFR blockade in colorectal cancer cells. *Clin Cancer Res*, 2014. **20**(24): p. 6429-38.

259. Hurbin, A., et al., Inhibition of apoptosis by amphiregulin via an insulin-like growth factor-1 receptor-dependent pathway in non-small cell lung cancer cell lines. *J Biol Chem*, 2002. **277**(51): p. 49127-33.
260. Grille, S.J., et al., The protein kinase Akt induces epithelial mesenchymal transition and promotes enhanced motility and invasiveness of squamous cell carcinoma lines. *Cancer Res*, 2003. **63**(9): p. 2172-8.
261. Rasanen, K. and M. Herlyn, Paracrine signaling between carcinoma cells and mesenchymal stem cells generates cancer stem cell niche via epithelial-mesenchymal transition. *Cancer Discov*, 2012. **2**(9): p. 775-7.
262. Johnson, G.R., et al., Autocrine action of amphiregulin in a colon carcinoma cell line and immunocytochemical localization of amphiregulin in human colon. *J Cell Biol*, 1992. **118**(3): p. 741-51.
263. Shoyab, M., et al., Amphiregulin: a bifunctional growth-modulating glycoprotein produced by the phorbol 12-myristate 13-acetate-treated human breast adenocarcinoma cell line MCF-7. *Proc Natl Acad Sci U S A*, 1988. **85**(17): p. 6528-32.
264. Martin, T.A. and W.G. Jiang, Loss of tight junction barrier function and its role in cancer metastasis. *Biochim Biophys Acta*, 2009. **1788**(4): p. 872-91.
265. Martin, T.A., R.E. Mansel, and W.G. Jiang, Antagonistic effect of NK4 on HGF/SF induced changes in the transendothelial resistance (TER) and paracellular permeability of human vascular endothelial cells. *J Cell Physiol*, 2002. **192**(3): p. 268-75.
266. Ren, J., et al., Ultrastructural differences in junctional intercellular communication between highly and weakly metastatic clones derived from rat mammary carcinoma. *Cancer Res*, 1990. **50**(2): p. 358-62.
267. Bignami, M., et al., Differential influence of adjacent normal cells on the proliferation of mammalian cells transformed by the viral oncogenes myc, ras and src. *Oncogene*, 1988. **2**(5): p. 509-14.

Appendix A

IMAGE REPRINT APPROVALS

Journal of Cancer Publishing Team <publish@jcancer.org>

Dear Dr. Pratima Patil,

Thanks for your email. Permission is granted to reproduce/use the figure as requested, with citation and credit of the original source in our journal.

Kind regards,
Publishing Team
Journal of Cancer
<http://www.jcancer.org>

-----Original Message-----

Sent: Tuesday, 14 July 2015 6:48 AM

To: publish@jcancer.org

Subject: [JCA Inquiry] Permission to Reprint Figure

Hi,

I am writing to request for permission to reprint the Figure 2 of an article (PMID: 23386906) for my PhD dissertation. Please see the details of the article I am seeking permission for.

Title: The tumor microenvironment contribution to development, growth, invasion and metastasis of head and neck squamous cell carcinomas.

J Cancer. 2013;4(1):66-83. doi: 10.7150/jca.5112. Epub 2013 Jan 1.

Figure 2

PMID: 23386906

PMCID: PMC3564248

Thank you.

Regards,

Pratima Patil